The mode of action of the synthetic peptides Os and Os-C derived from the soft tick *Ornithodoris savignyi*

By

Helena Taute

Submitted in fulfilment of the requirements for the degree

Doctor of Philosophy

in

Anatomy

Faculty of Health Sciences

University of Pretoria

South Africa

Supervisor: Prof MJ Bester (Dept. Anatomy)

Co-supervisor: Prof ARM Gaspar (Dept. Biochemistry)

2017

Declaration

I, Helena Taute, hereby declare that this thesis entitled: “The mode of action of the synthetic peptides Os and Os-C derived from the soft tick *Ornithodoris savignyi*” which I hereby submit for the degree at the University of Pretoria, is my own work and has not previously been submitted by me for a degree at this or any other tertiary institution. I understand what plagiarism is and am aware of the University’s policy in this regard. Where other people’s work has been used (either from a printed source, Internet or any other source), this has been properly acknowledged and referenced in accordance with departmental requirements. I have not used work previously produced by another student or any other person to hand in as my own.

Ethics statement: The author, Helena Taute, has obtained, for the research described in this work, the applicable research ethics approval. The author declares that she has observed the ethical standards required in terms of the University of Pretoria’s Code of ethics for researchers and the Policy guidelines for responsible research.

....

SIGNATURE **DATE**

Summary

Antimicrobial peptides (AMPs) have been identified as important therapeutic agents that can be developed as new multifunctional antibiotic compounds, which may address antibiotic resistance. AMPs have a wide range of bioactivities, including antimicrobial, antioxidant, anti-inflammatory and anticancer properties. Os and Os-C (a derivative of Os, lacking cysteine residues) are two synthetic AMPs derived from the tick defensin OsDef2 which have been shown to have antibacterial, antioxidant and anti-inflammatory activity. Differences in bacterial killing times between these peptides indicate differences in the modes of bacterial killing.

For the further development of Os and Os-C for therapeutic application, the aim of this study was to establish the mode of bacterial killing, to determine if these peptides are cytotoxic to human erythrocytes and leukocytes. Lastly, to determine if these peptides have additional beneficial cellular effects such as antioxidant activity.

Ultrastructural analysis with electron microscopy techniques revealed that both peptides adversely affected the membranes and intracellular structures of both Gram-negative *Escherichia coli* and Gram-positive *Bacillus subtilis* bacteria. Effects included membrane ruffling, cytoplasmic retraction, intracellular granulation and the formation of dense fibres. At the minimum bactericidal concentrations (MBCs) of 0.77 µM for Os and 1.74 µM for Os-C membrane permeabilisation measured with the SYTOX green assay was found not to be the principle mode of action. In stationary phase bacteria, fluorescent triple staining showed that both peptides caused permeabilisation. Studies using fluorescently labelled peptides revealed that the membrane penetrating activities of Os and Os-C were similar to buforin II, a cell-penetrating peptide. Os was able to enter stationary phase *E. coli* and *B. subtilis* while Os-C was unable to enter *E. coli* cells and accumulated on *B. subtilis* septa. Using plasmid binding and fluorescence displacement assays both peptides could bind DNA, while a dosage effect was only observed for Os.

Evaluation of cytotoxicity revealed that Os and Os-C caused no erythrocyte haemolysis or changes to erythrocyte morphology. Only the highest concentration of Os (100 µM), which is 130 fold greater than the MBC for *E. coli* and *B. subtilis,* caused cellular damage to peripheral mononuclear (MN) and polymorphonuclear (PMN) cells. In contrast, Os-C caused

leukocyte activation identified by associated morphological features and reactive oxygen species (ROS) formation.

Chemical and erythrocyte antioxidant assays indicated that both Os and Os-C had antioxidant activity. Both peptides provided extracellular protection of erythrocytes against 2,2'-azobis(2-amidinopropane) dihydrochloride induced oxidative damage. In MN and PMN cells Os showed low levels of antioxidant activity while Os-C had minimal activity.

In conclusion, both peptides showed a dual mechanism of bacterial killing, targeting both the membrane and intracellular elements. Os had a predominant membrane effect while Os-C targeted the septa of *B. subtilis* and had a higher affinity for DNA. Cytotoxicity in erythrocytes and leukocytes was minimal. In addition, Os exhibited antioxidant properties while Os-C caused leukocyte activation. Both peptides have been identified as promising therapeutic agents although activity in plasma and the effect on coagulation must still be determined.

Keywords: Antimicrobial peptide, defensin, mechanism of action, antioxidant, leukocyte activation, ultrastructure

Acknowledgements

"Science is not about building a body of known 'facts'. It is a method for asking awkward questions and subjecting them to a reality-check, thus avoiding the human tendency to believe whatever makes us feel good." (Pratchett *et al.*, 2003)

Firstly, I want to thank the Lord for bestowing on me the abilities necessary to conduct a PhD study. It has been a big learning experience which I could not have done without the help of various people whom I want to thank.

My supervisors, Prof Megan Bester and Prof Anabella Gaspar as well as Prof Albert Neitz for their continual help, support, insights and massive amounts of knowledge made available to me.

My colleagues, June Serem and Nanette Oberholzer, who were always ready to help and to give advice.

The personnel at the Unit for Microscopy and Microanalysis at the University of Pretoria for their knowledge and assistance with microscopy.

A big thank you to all my friends and family who supported me, especially emotionally, during these years.

My everlasting gratefulness to my husband, Leon, who encouraged me all the way. He spent countless weekends and nights with me in the laboratory. Thank you for your never-ending love, patience and support.

The project was funded by the National Research Foundation and the Medical Research Council of South Africa.

Table of contents

List of tables

List of figures

List of abbreviations

µm	Micrometer
3D	Three dimensional
5FAM	5-Carboxyfluorescein
$A_{0\%}$	Absorbance of isoPBS exposed cells
$A_{100\%}$	Absorbance of SDS exposed cells
AAPH	2,2'-Azobis(2-amidinopropane) dihydrochloride
AB	Alamar blue
ABTS	2,2'-Azo-bis (3-ethylbenzothiazoline-6-sulfuric acid) diamonium salt
ACE	Angiotensin-converting-enzyme
AFM	Atomic Force Microscopy
AMP	Antimicrobial peptide
ANOVA	Analysis of variance
APD	Antimicrobial peptide database
$A_{peptide}$	Absorbance of peptide exposed cells
Arg	Arginine
Asn	Asparagine
ATCC	American Type Culture Collection
CAP-e	Cell-based antioxidant protection in an erythrocyte model
CFU	Colony forming units
CM-NP	Cecropin-melittin- gold nanoparticle
CTC	5-Cyano-2,3-ditolyl tetrazolium chloride
Cys	Cysteine
DAPI	4',6-Diamidino-2-phenylindole
DCFH-DA	2',7'-Dichlorofluorescin diacetate
ddH_2O	Double distilled water
$dddH_2O$	Double distilled deionised water
DMEM	Dulbecco's modified eagle medium
DNA	Deoxyribonucleic acid
DPPH	1,1-Diphenyl-2-picrylhydrazyl
EDTA	Ethylenediaminetetraacetic acid
E. coli	*Escherichia coli*
EM	Electron microscopy
FBS	Foetal bovine serum

FDA	Fluorescein diacetate
FEG	Field emission gun
FID	Fluorescence intercalator displacement
FITC	Fluorescein 5(6)-isothiocyanate
$Fl_{control}$	Fluorescence of control
$Fl_{treated}$	Fluorescence of treated sample
FS	Freeze substitution
g	Gravity
GFP	Green fluorescent protein
Gly	Glycine
GM-CSF	Granulocyte-macrophage colony-stimulating factor
$\Delta g'O_2$	Singlet oxygen
GSH	Glutathione
HBD	Human β-defensin
His	Histidine
HMDS	Hexamethyldisilazane
HNP	Human neutrophil peptide
HPF	High pressure freezing
HPLC	High-performance liquid chromatography
H_2O_2	Hydrogen peroxide
IDSA	Infectious Diseases Society of America
IL	Interleukin
Ile	Isoleucine
isoPBS	Isotonic phosphate buffered saline
Leu	Leucine
LB	Luria-Bertani
LPS	Lipopolysaccharides
Lys	Lysine
MBC	Minimum bactericidal concentration
Mel	Melittin
Met	Methionine
MN	Mononuclear
MRSA	Methicillin-resistant *Staphylococcus aureus*
MTT	3-(4,5-Dimethylthiazol-2-yl)-2,5-diphenyltetrazolium bromide
MW	Molecular weight
NADPH	Nicotinamide adenine dinucleotide phosphate

NaP	Sodium phosphate buffer
NO	Nitric oxide
nm	Nanometer
NPN	1-N-phenylnaphthylamine
NR	Neutral red
$^{\bullet}O_2^-$	Superoxide anion
•OH	Hydroxyl radicals
ORAC	Oxygen Radical Absorbance Capacity
PBS[a]	Phosphate buffered saline used for DAPI
PBS[b]	Phosphate buffered saline
Phe	Phenylalanine
PMA	Phorbol 12-myristate 13-acetate
PMN	Polymorphonuclear
Pro	Proline
RER	Rough endoplasmic reticulum
RNA	Ribonucleic acid
RNS	Reactive nitrogen species
ROS	Reactive oxygen species
RPMI	Roswell Park Memorial Institute medium 1640
RTD	Rhesus θ-defensin
SDS	Sodium dodecyl sulphate
SEM	Scanning electron microscopy
SE	Standard error of the mean
SRB	Sulforhodamine B
TAE	Tris acetate EDTA buffer
TE	Trolox equivalent
TEAC	Trolox equivalent antioxidant capacity
TEM	Transmission electron microscopy
TLR4	Toll-like receptor 4
TNF	Tumour necrosis factor
Trp	Tryptophan
TUNEL	Terminal deoxynucleotidyl transferase dUTP nick end labelling
Tyr	Tyrosine
Val	Valine

Chapter 1: Introduction

After the discovery of penicillin, a multitude of infectious diseases that previously often led to death could easily be treated. Penicillin was first clinically administered by a team of doctors led by Dr Howard Florey in 1941 to a patient suffering from septicaemia. Although the patient showed improvement, he unfortunately did not survive because of the shortage of penicillin available at the time (Fletcher, 1984). The same team later treated various patients with localised infections successfully with penicillin. Mass production of penicillin started around 1943, but bacteria resistant to this antibiotic were already a significant problem in health care facilities by the 1950s (Chambers and Deleo, 2009). As with penicillin, bacteria developed resistance against other antibiotics, and some bacterial strains have even developed resistance to multiple antibiotics.

Drug resistance is a global problem and the South African population is particularly at risk to various antibiotic resistant strains of bacteria such as *Streptococcus pneumoniae*, *Neisseria meningitidis*, *Haemophilus influenzae*, *Salmonella enterica*, *Shigella*, *E. coli*, and *Neisseria gonorrhoeae* (Crowther-Gibson *et al.*, 2011). Due to bacteria becoming resistant to frequently used drugs, the development of new antibiotics and treatment strategies is essential. One possibility is the development of antimicrobial peptides (AMPs) into antibacterial agents.

AMPs are found in all forms of life including plants and animals, and form part of the innate immune system (Wang, 2010). These peptides have been isolated and characterised, and have been found to be active against a wide range of microbes and bacteria. AMPs of natural origin have served as lead compounds for the development of new synthetic antimicrobial agents. The development of resistance against AMPs is less frequent than the occurrence of resistance against traditional antibiotics, and various AMPs have entered clinical trials (Lazarev and Govorun, 2010). For example, pexiganan led to a 90% improvement of patients in combination with the antibiotic ofloxacin in a phase 3 clinical-efficacy trial (Hancock and Sahl, 2006).

At physiological concentrations, AMPs have been shown to be effective against a vast range of microbes including bacteria, viruses and fungi (Ganz, 2003, Izadpanah and Gallo, 2005). The amphipathic structure of AMPs allows these molecules to be soluble in an aqueous environment, but also to penetrate lipid-rich membranes. The primary target of AMPs is the

bacterial membrane. AMPs kill cells by causing membrane permeabilisation or through a wide range of intracellular mechanisms (Izadpanah and Gallo, 2005). Several AMPs have been identified as multifunctional molecules and have shown antioxidant, anti-inflammatory or antiproliferative activity in addition to the antimicrobial activity (Boman, 2003, Finlay and Hancock, 2004, Lehmann *et al.*, 2006, Marta Guarna *et al.*, 2006).

Defensins are one of the major groups of AMPs that have been extensively studied. These peptides are cationic peptides, and all defensins of natural origin contain six to eight cysteine (Cys) amino acid residues (Stotz *et al.*, 2009). Three disulphide bonds form between three pairs of Cys and play a role in the three-dimensional (3D) structure of these peptides. Although invertebrate defensins are active mainly against Gram-positive bacteria, peptides derived from their C-terminal ends show a wider spectrum of antimicrobial activity (Varkey *et al.*, 2006, Tsuji *et al.*, 2007). Similarly, OsDef2 a tick defensin has been shown to be active only against Gram-positive bacteria. A synthetic peptide, Os, was derived from the C-terminal end of a tick defensin (OsDef2). A derivative of this peptide, Os-C that lacks cysteine residues found in Os was synthesised (Prinsloo *et al.*, 2013). In a collaborative study between the Departments of Biochemistry and the Division of Cell Biology, Histology and Embryology, Department of Anatomy, it has been shown that both peptides have activity against Gram-negative *E. coli* and *Pseudomonas aeruginosa*, and Gram-positive *Staphylococcus aureus* and *B. subtilis*. Cell culture studies have found that both peptides are not cytotoxic to mammalian cells and in addition have antioxidant activity significantly higher than that of glutathione (GSH), a physiologically active antioxidant tripeptide. These results have been published in the Journal of Peptide Science (Prinsloo *et al.*, 2013). However, little was known about the mode of antibacterial activity as well as cytotoxic and antioxidant effects on physiologically relevant cell types such as human erythrocytes and leukocytes. Therefore, the aim of this study was to further elucidate the mode of action of synthetic peptides Os and Os-C. The research objectives addressed in this thesis are summarised as follows:

1. To identify the cellular targets of Os and Os-C on selected bacterial strains.
2. To evaluate the effects of the peptides on physiologically relevant human cell types such as erythrocytes and leukocytes.
3. To investigate the antioxidant properties of Os and Os-C.

The thesis concludes with a summary of the results obtained in all experiments and possible future studies.

1.1) Outputs

The results of this study have been published in the following articles:

Prinsloo L, Naidoo A, Serem J, **Taute H**, Sayed Y, Bester M, Neitz A & Gaspar A, 2013. Structural and functional characterization of peptides derived from the carboxy-terminal region of a defensin from the tick *Ornithodoros savignyi*. *J Pept Sci,* 19: 325-332.

Taute H, Bester MJ, Neitz AWH & Gaspar ARM, 2015. Investigation into the mechanism of action of the AMPs Os and Os-C derived from a tick defensin. *Peptides*, 71: 179-187.

A third manuscript on the effects of the peptides on peripheral leukocyte viability and ROS production is being prepared.

The results have also been presented at the following conferences:

51st Microscopy Society of Southern Africa meeting: University of Kwa-Zulu Natal, South Africa, April 2013. *Oral presentation*: Evaluation of the antimicrobial, cellular and antioxidant effects of synthetic peptides Os and Os-C. L Prinsloo, J Serem, **H Taute**, MJ Bester, AWH Neitz, ARM Gaspar.

18th International Microscopy Congress: Prague, Czech Republic, September 2014. *Poster presentation:* Investigation of the membrane effects and mode of action of the synthetic peptides Os and Os-C. **H Taute**, MJ Bester, AWH Neitz, ARM Gaspar.

43rd Anatomical Society of Southern Africa meeting: Parys, Free State, South Africa, May 2015. *Oral presentation:* Investigating the mode of bacterial killing of the synthetic peptides Os and Os-C derived from the C-terminus of OsDef2. **H Taute**, MJ Bester, AWH Neitz, ARM Gaspar.

53rd Microscopy Society of Southern Africa meeting: Centurion, Gauteng, South Africa, December 2015. *Oral presentation:* Investigation into the mode of action of the antimicrobial peptides Os and Os-C. **H Taute**, MJ Bester, AWH Neitz, ARM Gaspar. Award: Best presentation in confocal microscopy.

Chapter 2: Review of the literature

In the early 1900s Fleming discovered lysozyme, and some believe this to be the first report of a eukaryotic AMP (Phoenix *et al.*, 2013). Research on AMPs started with the identification of gramicidin and tyrocidine from the prokaryote, *Bacillus brevis* (Hotchkiss and Dubos, 1941). Its therapeutic use was demonstrated when it was successfully used to treat infected skin wounds in guinea pigs. Gramicidin was also the first commercially produced AMP antibiotic. It was only later found that besides lysozyme, eukaryotic organisms also possess AMPs. In 1969, Zeya and Spitznagel reported the identification of five cationic AMPs isolated from rabbit leukocytes. Later in 1980, Hultmark *et al.* reported the discovery of cecropins and other AMPs in the haemolymph of the silk moth pupae after exposure to bacterial debris. Since then thousands of AMPs have been identified in other animals including mammals (Sarmasik, 2002). The AMP database (APD) has information of more than 2696 peptides of natural origin as of May 2016 (Wang *et al.*, 2009).

AMPs are an essential component of the innate immune system protecting organisms against infection and associated consequences of inflammation. Several of these AMPs and derivatives have been developed and are being tested in clinical trials. Low rates of success in clinical trials requires continuous research and development of new AMPs and in this endeavour invertebrates provide an underutilized source of novel bioactive peptides such as tick defensins. The focus of this study is the development of derivatives of a defensin (OsDef2) from the tick *Ornithodoris savignyi* as antimicrobial agents.

In this chapter the literature related to the role of AMPs in innate immunity, the development of peptides as therapeutic agents, their structures and the modes of action will be reviewed.

2.1) Immunity

Immunity is the system by which an organism is protected against pathogens or foreign microbes. The ancient Chinese promoted resistance to smallpox in their children by giving them powder made from the skin lesions of recovering patients to inhale. This indicates that the idea of immunity has been around for millennia (Abbas *et al.*, 2015). Immunology, which is the study of the body's immune defence system, is said to have originated in 1796 when the English physician Edward Jenner observed that dairy workers who had recovered from cowpox never fell victim to smallpox again. He decided to inject an eight-year-old boy with

cowpox, or “vaccinia”. After some time, the boy was deliberately exposed to smallpox but did not develop the disease. Jenner called this procedure vaccination, and this term is still used today. After Jenner published his results, it still took two centuries to eliminate smallpox entirely with vaccination. In 1979, the World Health Organization announced that smallpox had been eradicated worldwide (Murphy *et al.*, 2012, Abbas *et al.*, 2015). Concurrent with the development of vaccines, knowledge related to the biochemistry and cellular mechanisms involved in immunity has increased. The immune system is comprised of the innate and adaptive immune responses. The adaptive immune response is specific to a pathogen, on exposure to a pathogen this immune response is stimulated and antibodies against this particular pathogen are produced by lymphocytes such as observed for smallpox. Once an organism has been exposed to a specific pathogen, the immune response will be more vigorous following future exposures to the same pathogen. The innate immune response, on the other hand, is the first defence of an organism against invading microbes and the mode of action against the microbe is not specific. From the time of infection, the innate immune response provides initial protection within the first few hours, and the adaptive immune response develops later over several days as the lymphocytes are stimulated (Murphy *et al.*, 2012, Abbas *et al.*, 2015). As AMPs are an integral component of the innate immune system, this system will be described in greater detail.

2.1.1) Innate immunity

The concept of innate immunity has arisen from botanical and entomological studies undertaken in recent decades (Izadpanah and Gallo, 2005). It includes all physical entities that offer protection against infection without prior exposure to a pathogen (Izadpanah and Gallo, 2005). As microbes and multicellular organisms evolved, the innate immune system developed to protect against infection. Due to common ancestral paths, there are many similarities between mammalian, plant and invertebrate innate immunity. Defensins, which are part of the innate immune system, are peptides that have antibacterial and antifungal properties that are present in both plants and mammals. Defensins from plants and mammals have basically the same tertiary structure (Murphy *et al.*, 2012, Abbas *et al.*, 2015).

2.1.2) Vertebrate innate immunity

There are four components of the vertebrate innate immunity which are both cellular and biochemical in nature. The first component is physical and chemical barriers, for example

epithelium (that forms a physical barrier) and antimicrobial chemicals produced on the surfaces including AMPs. The second component is cellular, which includes phagocytic cells (neutrophils and macrophages), dendritic cells and natural killer cells. The third component is blood proteins that include the complement system and other mediators of inflammation. The last component of the innate immune response is cytokines, which are proteins that modulate the actions of the cells of innate immunity. The components of innate immunity are present in their functional state before contact with microbes and are more rapidly activated than the adaptive immune response components (Murphy *et al.*, 2012, Abbas *et al.*, 2015). All multicellular organisms have an innate immune system, and AMPs are a major part of this innate immunity (Boman, 2003, Izadpanah and Gallo, 2005).

2.1.3) Invertebrate innate immunity

Invertebrates lack an adaptive immune system, and rely solely on innate immunity for protection from all invading microorganisms. Since 1930, it has been known that the immune system of invertebrates consists of cellular and humoral components. Cellular based immunity includes phagocytosis, cell aggregation, nodule formation and large-scale encapsulation (Hoffmann, 1995). Humoral immunity includes humoral encapsulation, haem-agglutination and the production of AMPs by the fat body and some blood cells (Taylor, 2006).

2.2) Antimicrobial peptides

AMPs are polypeptides with low molecular weight consisting of fewer than 100 amino acids. At low concentrations AMPs show activity against a vast range of microbes including bacteria, viruses and fungi (Ganz, 2003, Izadpanah and Gallo, 2005). Most AMPs are cationic with a net charge between +2 and +9, due to a high content of positively charged amino acid residues and contain between 30-50% hydrophobic residues. The amphipathic structures adopted by AMPs allow these molecules to interact with bacterial membranes. Modification of the net charge or hydrophobicity of an AMP can alter its effectiveness and the range of microorganisms it is effective against (Laverty *et al.*, 2011).

Even though most AMPs are cationic, some anionic AMPs occur and these also form a part of the eukaryotic innate immunity. These peptides are made up of between 5 to 70 amino acid residues and have a net charge of usually -1 or -2. Anionic peptides are also amphipathic and thus able to interact with membranes. Anionic peptides often need to

associate with a cation such as zinc (Zn^{2+}) to enable them to cross the cell membrane and intracellularly inhibit ribonuclease activity that results in cell death (Laverty *et al.*, 2011).

2.2.1) Therapeutic potential

Traditional antibiotics enter microorganisms without damaging the membrane, and the mode of action is to target and disrupt specific internal cellular functions leading to the death of the microorganism. The microorganism can adapt these cellular pathways to avoid this onslaught, thereby developing drug resistance. Bacteria develop resistance most frequently through changes in the DNA, which results in a specific type of resistance. Genetic changes associated with resistance can be either natural or acquired (Alanis, 2005). Natural resistance happens when a spontaneous mutation occurs, that results in resistance. The bacteria with the mutation survive and the gene is inherited by the next generations of bacteria. Acquired resistance takes place either when the antibiotic stimulates gene mutation, or the bacterium exchanges resistant genes with other cells. Genetic material may be exchanged among bacteria through conjugation, transformation or transduction. Development of resistance occurs when genomic changes alters biochemical processes that prevents the antibiotic form reaching its specific cellular target. These effects can be generally divided into three groups. The first mechanism is antibiotic destruction or transformation through enzymatic activity. Secondly, bacteria may develop active transport mechanisms to expel drugs that have intracellular targets. Lastly, the bacteria may modify the receptor so the antibiotic is unable to bind to its target (Alanis, 2005). Exposure to several drugs leads to the development of multidrug resistance and consequently, this will compromise the health of the host.

In contrast to conventional antibiotics, the primary target of AMPs is the cell membrane of microorganisms. Killing is rapid and non-specific and this is believed to be a reason why drug resistance is less likely to occur (Laverty *et al.*, 2011, Flamm *et al.*, 2015). Due to their membrane targeting effects several AMPs have been found also to have antitumor, antiparasitic and antiviral properties (Sarmasik, 2002). Various AMPs have also been shown to have antimicrobial and antifungal properties. An example is the rabbit defensin NP-2 that causes *Candida albicans* membrane permeabilisation (Yeung *et al.*, 2011).

Besides killing of pathogens, AMPS often have additional benefical properties. The peptide derived from the α_{s2}-casein fragment has antimicrobial activity as well as antioxidant and angiotensin-converting-enzyme (ACE)-inhibition (López-Expósito, *et al.* 2007). A defensin derived from sweet potato was shown to have antioxidant activity with various assays

including the 2,2'-azo-bis (3-ethylbenzothiazoline-6-sulfuric acid) diamonium salt (ABTS), 1,1-diphenyl-2-picrylhydrazyl (DPPH) radical scavenging and intracellular dichlorofluorescein diacetate (DCFH-DA) assays (Huang *et al.*, 2012). Another AMP, plantaricin A, was shown to protect keratinocytes against oxidative damage (Marzani *et al.*, 2012). This antioxidant activity in peptides may be attributed to specific amino acid residues contained in the peptide as well as their specific placement in the sequence (Sarmadi and Ismail, 2010). Antioxidant amino acid residues include cysteine (Cys), methionine (Met), tryptophan (Trp), tyrosine (Tyr), phenylalanine (Phe), histidine (His) and proline (Pro) as well as the sequences Pro-His-His, Trp-Asn-Ile, Ile-Arg and Leu-His (Elias *et al.*, 2008, Minkiewicz *et al*., 2008, Yang *et al.*, 2009, Sarmadi and Ismail, 2010, Shen *et al.*, 2010).

Many AMPs have been subjected to preclinical testing and clinical trials for various applications, and this includes the treatment of microbial infections, organ failure, wound healing, diabetes and cancers (Yeung *et al.*, 2011). The first commercially available AMP was tyrocidine, which can only be used as a topical antibiotic because of its haemolytic activity and toxicity toward reproductive cells. Neosporin® is a topical infection treatment currently in use that contains the polypeptide bacitracin. Daptomycin, polymixin B, polymixin E and caspofungin are lipopeptides which are also currently used commercially (Laverty *et al.*, 2011). Up to 2011, only three synthetic cationic peptides have entered phase III clinical trials, and none of these have been approved for clinical use. Although several cationic AMPs showed efficiency in clinical trials, these AMPs were found to be less efficient than existing therapies and therefore were not approved (Yeung *et al.*, 2011). An example is the peptide, pexiganan, which showed a 90% improvement in patients when administered topically for the treatment of diabetic foot ulcers. It was, however, not approved by the US Food and Drug Administration at that stage as it did not prove to be more effective than the oral antibiotic, ofloxacin (Boman, 2003, Hancock and Sahl, 2006). However, pexiganan is undergoing further clinical trials as reported by Flamm *et al.* (2015). AMPs in the process of development as antibiotics are listed in Table 2.1.

Most clinical trials are limited to the use of AMPs in topical treatments based on reported antimicrobial, antioxidant and anti-inflammatory activities. Factors that need to be considered are the high cost of production, susceptibility to proteases, limited knowledge on toxicity profiles and unknown systemic effects (Yeung *et al.*, 2011). Cost of production can be reduced by using more efficient recombinant DNA expression strategies or developing shorter peptides that contain the essential sequences required for activity. The effects of digestion, salts and serum on AMP derivatives need to be investigated if oral or intravenous administration is to be considered.

Table 2.1. AMPs in clinical trials or in development (adapted from Fox, 2013 and US National Institutes of Health, 2015).

Drug name	Company	Indication	Trial phase
Magainin peptide/ pexiganan acetate	Dipexium Pharma (New York, USA) / MacroChem (Wittenberg, Germany)	Diabetic foot ulcers	3
Omiganan	BioWest Therapeutics (Vancouver, USA) / Maruho (Osaka, Japan)	Rosacea	2
OP-145	OctoPlus (Leiden, The Netherlands)	Chronic bacterial middle-ear infection	2
Novexatin	NovaBiotics (Aberdeen, UK)	Fungal infections of the toenail	1/2
Lytixar (LTX-109)	Lytix Biopharma (Oslo, Norway)	Nasally colonized Methicillin-resistant *Staphylococcus aureus* (MRSA)	1/2
NVB302	Novacta (Welwyn Garden City, UK)	Gram-negative bacteria *C. difficile*	1
MU1140	Oragenics (Florida, USA)	Gram-positive bacteria (MRSA, *C. difficile*)	Preclinical
Arenicin	Adenium Biotech (Copenhagen, Denmark)	Multiresistant Gram-positive bacteria	Preclinical
Avidocin and purocin	AvidBiotics (California, USA)	Narrow spectrum antibiotic for human health and food safety	Preclinical
IMX924	Iminex (British Columbia, Canada)	Gram-negative and Gram-positive bacteria	Preclinical

The question is raised why continue research into the development of new AMPs for clinical application? Compared with existing antibiotics, AMPs show activity against a wide range of bacteria, and some also show activity against viruses or fungi. Furthermore, the low possibility for the development of resistance still makes AMPs worthy molecules for further research and development. In the last decade, few new antibiotics with a novel mechanism of action with low risk of developing resistance have been approved for use (Wright, 2013). The Infectious Diseases Society of America (IDSA) realised the great demand for novel antibiotics. To address the lack of progress in the development of new antibiotics the IDSA launched the 10 x '20 initiative in 2010. The initiative was set up to promote antibiotic research with the aim to have ten novel systemic antibiotics approved by 2020. However, by early 2013 only two new antibiotics have been approved (Boucher *et al.*, 2013). Therefore, all avenues of potential novel antibiotic development should be explored.

AMPs have also been shown to have multifunctional properties, and could potentially be used as more than just an antibiotic. It is interesting to note that some AMPs that entered clinical trials for their antimicrobial activity, have since been found to have immunomodulatory effects, for example MX-226 (Yeung *et al.*, 2011). These

immunomodulatory AMPs can be used in conjunction with other antibiotics as adjuvants to regulate the inflammatory reaction against pathogens (Yeung *et al.*, 2011). Most AMPs are evaluated as topical treatments. However, AMPs can also be evaluated as aerosol treatments, for example, the treatment of persistent airway infections in cystic fibrosis. AMPs may also be administered intravenously or transcutaneously, thereby bypassing the proteolytic effects of the digestive system, however, these peptides may still be subjected to systemic proteolytic degradation.

2.2.2) Types of antimicrobial peptides

AMPs have been isolated from all phyla of life and can be classified by various criteria. For instance, AMPs can be classified into the taxonomic group it originates from, for example animal or plant, and animal peptides can then also be further divided into insect, reptile, amphibian and mammalian. AMPs can also be classified according to biological function (antibacterial, antiviral and/or antifungal), amino acid sequences (linear, loops or circular), 3D structure (α-helical, β-sheets, combination or random) and mechanism of action (membrane or non-membrane targeting) (Wang, 2010).

Based on the 3D structure of peptides, Laverty and colleagues (2011) divide AMPs into four groups. The first group is composed of AMPs that form amphipathic β-sheet structures in solution with two or three disulphide bonds between Cys residues. These AMPs could also have a short α-helix and have between 2-4 β-strands. This group includes the α- and β-mammalian defensins. The second group is linear peptides that have no defined structure in hydrophilic solution, but form amphipathic α-helices in a hydrophobic environment. Structurally, one end of this α-helix contains most of the hydrophobic residues, whereas the opposite end contains most of the hydrophilic residues. These peptides have no Cys residues, and thus cannot form disulphide bonds. Examples include melittin (Mel), magainin and cecropins. Cyclic peptides containing a β-turn and one disulphide bond make up the third group. These are uncommon peptides, and an example is a dodecapeptide from bovine neutrophils. The last group is AMPs with no defining structure that contains a high amount of a certain amino acid residue such as Pro, Gly, His or Trp for example tritrpticin and indolicidin (Laverty *et al.*, 2011).

2.2.3) Defensins

The family of AMPs known as defensins are grouped together by structure as these AMPs all contain six Cys that are bound by three disulphide bonds with characteristic β-sheet hairpin folds (White *et al.*, 1995, Ganz, 2003). Vertebrate defensins are α- and β-defensins which are similar in 3D structure and function. These AMPs are rich in Cys residues and have a flat triple-sheet structure stabilised with three disulphide bonds (Van Wetering *et al.*, 1999). The two groups of defensins differ in the manner in which the Cys residues are linked and the length of peptide sequences between Cys residues. Generally, β-defensins are larger and may have modified termini.

The six Cys residues in α-defensins are linked in a 1-6, 2-4, 3-5 pattern, whereas with the β-defensins the Cys residues are linked in a 1-5, 2-4, 3-6 pattern (Figure 2.1). This difference does not cause a significant variation in the structure between α- and β-defensins, because Cys 5 and 6 are adjacent in these two types (Ganz, 2003). More recently a third group of defensins have been discovered, the θ-defensins that are formed from two hemi-α-defensins that each contribute three Cys residues. The two precursor α-defensins are spliced into a circular θ-defensin without a free N- or C-terminus (Figure 2.1). The θ-defensins were first discovered in the rhesus macaque monkey, and evidence suggested that it evolved in primates, but it is inactivated in humans due to genetic mutations that encode for premature stop-codons (Cole *et al.*, 2002, Ganz, 2003).

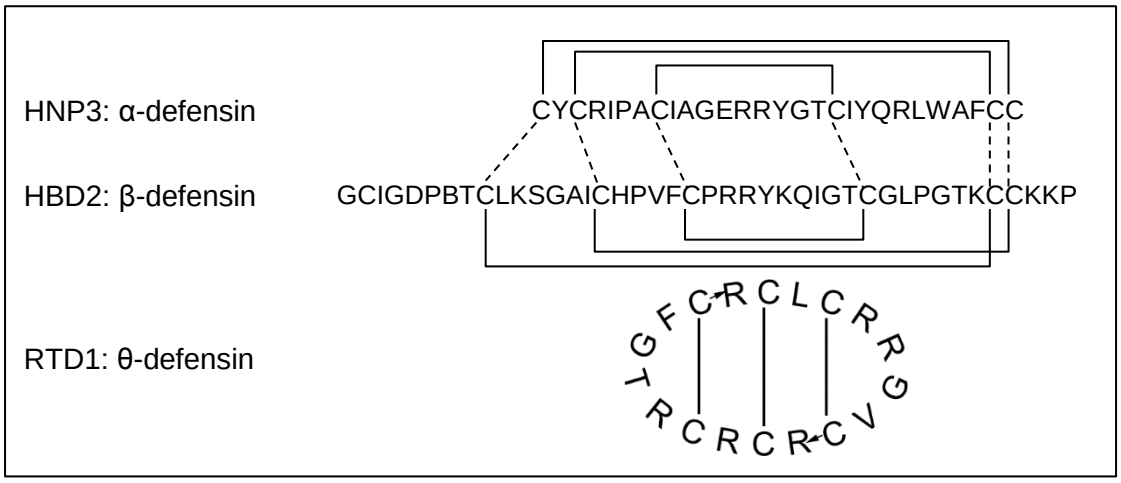

Figure 2.1. Sequences and disulphide pairing of α-, β-, and θ-defensins (Ganz, 2003). Solid lines indicate disulphide bonds between Cys pairs, and broken lines indicate corresponding Cys residues in the α- and β-defensin peptides. The peptide bonds between the two hemi-α-defensins of the θ-defensin are shown as arrows. Human neutrophil peptide (α-defensin) (HNP); human β-defensin (HBD); rhesus θ-defensin (RTD).

Defensins have also been found in invertebrates and plants. Structural differences exist between plant and invertebrate peptides when compared with vertebrate peptides. For example, insect defensins contain an α-helix linked with disulphide bonds to a β-sheet (Figure 2.2), and the Cys linkage pattern is 1-4, 2-5, 3-6 (Ganz, 2003).

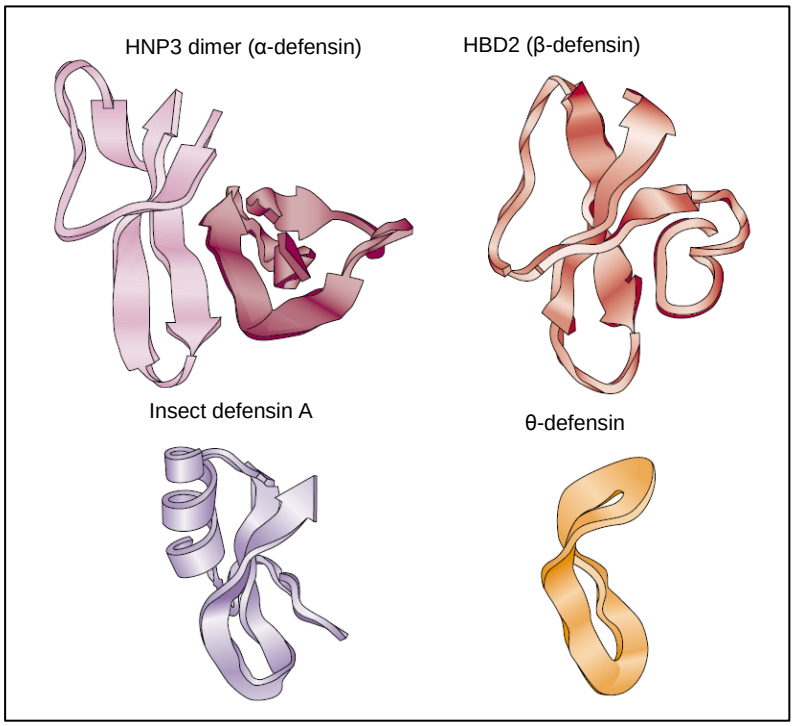

Figure 2.2. Ribbon diagrams of the major classes of mammalian and insect defensins (Ganz, 2003). Human neutrophil peptide 3 (HNP3) is an α-defensin with a dimer structure containing abundant β-sheets (indicated by flat ribbons with arrows). The monomer, human β-defensin 2(HBD2) also contains β-sheets with a short α-helical segment at the N-terminus. The insect defensin has a prominent α-helical segment making up the C-terminal β-sheet with two disulphide bonds. The θ-defensin consists of a simple β-sheet in a cyclic structure.

2.2.4) Insect defensins

Insect defensins are synthesised in the fat body, which is the functional equivalent of the liver in insects, and in some blood cells and form part of the innate immunity of insects. Insect defensins conform to the defensin prerogative by possessing six Cys residues linked by three disulphide bonds. However, the structure differs markedly from vertebrate defensins. The structure of insect defensin A includes an amino-terminal loop, a prominent α-helix and an anti-parallel β-sheet as shown in Figure 2.3. The amino-terminal loop is linked to the first strand of the β-sheet by a single disulphide bond, the other two disulphide bonds link the α-helix to the second β-sheet strand. In insect defensins a Cys-stabilised α-helix pattern exists, where the Cys pairs involved in the disulphide bonds between the α-helix and β-sheet are separated by three residues on the α-helix (which forms one turn) and one

residue on the β-sheet, resulting in a CXXXC/CXC pattern, where C is Cys, and X is any other amino acid (Hoffmann and Hetru, 1992). This secondary structure is present in most insect defensins and was described by Cornet *et al.* in 1995 as a Cys-stabilised αβ (CSαβ) motif. In contrast, the N-terminal loop shows variability between peptides which may play a role in the mechanism of action, level of activity and antibiotic specificity of each different peptide (Cornet *et al.*, 1995). The disulphide bonds create a hinge-like structure whereby the N-terminal loop can assume different orientations in space relative to the CSαβ structure (Figure 2.3).

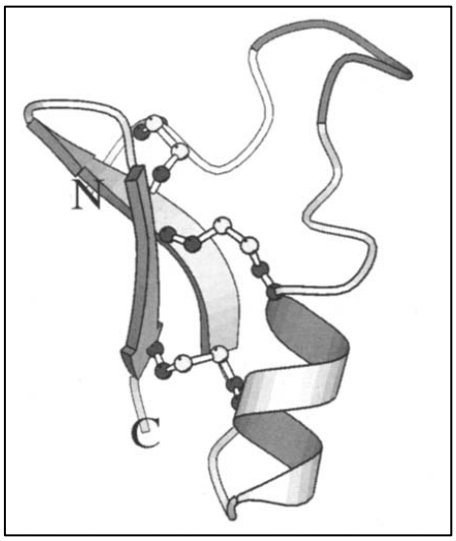

Figure 2.3. Simplified representation of insect defensin A (Cornet *et al.*, 1995). This insect defensin contains an amino-terminal loop bound to one β-sheet by a disulphide bond, and an α-helix bound to the second β-sheet by two disulphide bonds.

2.2.5) Bacteria and antibacterial peptides

Bacteria are prokaryotic single cell organisms that lack a nucleus or other membranous organelles. Three basic shapes of bacteria exist namely, spherical (coccus), rod (bacillus) and spiral (vibrio, spirillum or spirochete). In culture, depending on the amount of nutrition, the same type of bacteria may have differing sizes and shapes (Black and Black, 2008).

The bacterial envelope consists of a cell wall and cell membrane. The cell wall is comprised mainly of peptidoglycans while the main component of the cell membrane is phospholipids (Harvey *et al.*, 2013). The phospholipids of the cell membrane form a bilayer, with the polar phosphate groups on the outside and the nonpolar lipid chains on the inside. There are distinct differences in the cell wall and membrane structures of Gram-positive and Gram-negative bacterial strains (Figure 2.4). The cell wall of Gram-positive bacteria is on the

outside of the membrane and consists of multiple layers of peptidoglycan. Most Gram-positive bacteria have teichoic acids covalently linked to the peptidoglycans that act as cell surface antigens (Harvey *et al.*, 2013). The composition and structure of the peptidoglycan layer of Gram-positive bacteria can vary widely. However, the most prominent difference is the peptide cross-links between glycan strands. The glycan peptides of various Gram-positive bacteria are linked by a pentaglycine bridge attached to one of the stem peptides. Other Gram-positive bacteria such as *B. subtilis* do not contain bridged stem peptides (Silhavy *et al.*, 2010).

Gram-negative bacteria, on the other hand, have three layers. These three layers are an outer and inner membrane with a thin peptidoglycan layer in the periplasmic space between the two. The thin peptidoglycan layer in Gram-negative bacteria makes these bacteria more vulnerable to physical damage. The Gram-negative outer membrane contains lipopolysaccharides (LPS) embedded in the phospholipid bilayer (Harvey *et al.*, 2013). Gram-negative bacteria are generally more resistant to antibiotics because of their selectively permeable outer membrane and secondary protective mechanisms, including active antibiotic efflux and the periplasmic enzyme β-lactamase. Nevertheless, these bacteria are susceptible to cationic AMPs, which can cross the outer membrane via a self-promoted uptake pathway (Hancock and Rozek, 2002).

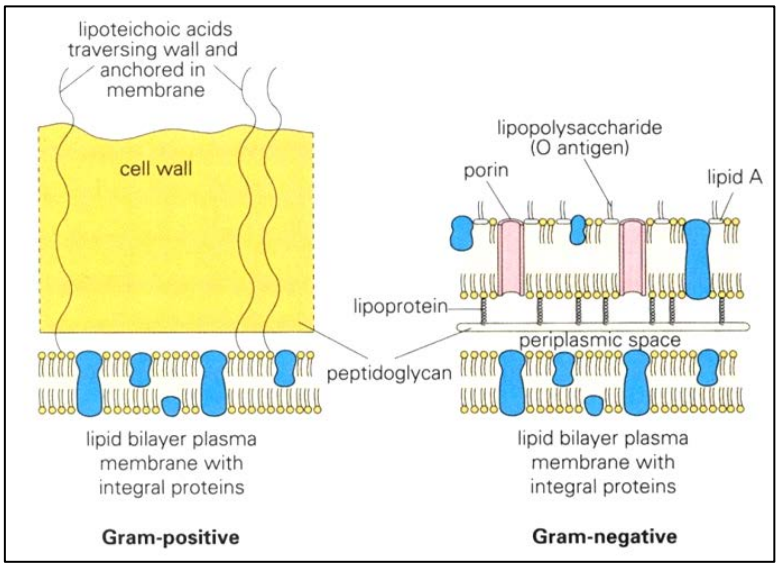

Figure 2.4. Structure of Gram-positive and Gram-negative cell envelopes (Goering and Mims, 2013). Gram-positive bacteria typically have a thick outer peptidoglycan cell wall and inner phospholipid bilayer membrane. Gram-negative bacteria have three layers, an outer and inner membrane separated by a thin layer of peptidoglycan.

AMPs are amphipathic, with both cationic and hydrophilic components. The cationic characteristics of AMPs allow them to interact with negatively charged lipids of bacterial membranes, whereas the hydrophilic constituents allow them to insert into the membrane. This interaction may lead to membrane destabilisation and permeabilisation which causes leakage of the cell content. There are four classical theories of how AMPs interact with the bacterial cell membrane (Figure 2.5), namely the toroidal pore, aggregate, barrel-stave, and carpet models (Laverty *et al.*, 2011). These models of action can lead to three different outcomes, formation of a transient channel, formation of micelles and dissolution of the membrane, or translocation across the membrane into the cytoplasm without much damage to the membrane. AMPs can therefore be broadly categorised into either membrane or non-membrane acting (Jenssen *et al.*, 2006).

In all membrane permeabilising models, there is an initial attraction between the peptide and the outer envelope of the bacteria. For Gram-negative bacteria, this interaction occurs between the cationic AMPs and the phosphate groups of the LPS. In Gram-positive bacteria, this interaction occurs between AMPs and lipoteichoic acids present on the cell surface (Jenssen *et al.*, 2006).

The hydrophilic groups of an AMP first interact with the negatively charged phospholipid heads of the membrane bilayer, assuming an orientation parallel to the membrane (see first step in all models in Figure 2.5). In the aggregate model (Figure 2.5A) the peptide then inserts perpendicularly into the membrane. There is no specific arrangement of the peptides in the bilayer, resulting in pores that vary greatly in size and lifetime. Partial insertion of peptides into the bilayer leads to a negative curvature and peptide aggregation within the bilayer. As these aggregates collapse peptides have the opportunity to translocate into the cytoplasm (Matsuzaki, 1998, Jenssen *et al.*, 2006, Laverty *et al.*, 2011).

The toroidal pore model (Figure 2.5B) has some similarities to the aggregate model in that the peptide inserts into the membrane perpendicularly. However, in this model there is a specific arrangement of the peptides causing pores of relatively uniform size. The hydrophobic regions of the peptides then cause the lipid monolayers to bend inward to form a pore in such a way that it is lined by a lipid bilayer and peptides on the inside (Hallock *et al.*, 2003, Laverty *et al.*, 2011). Examples of peptides that have been proposed to use this mechanism include Mel, magainins and LL-37 (Jenssen *et al.*, 2006).

The peptides in the barrel-stave model form the staves of a barrel-shaped pore (Figure 2.5C). These peptides also insert perpendicularly in the bilayer by way of van der Waal's

attractions between the hydrophobic side of the peptide and the lipid core, the hydrophilic sides of the peptides face the lumen. The resulting pores in the microorganisms' membrane are all of a similar size (Ehrenstein & Lecar, 1977, Jenssen *et al.*, 2006, Laverty *et al.*, 2011).

The carpet model suggests that the AMPs aggregate on the surface of the membrane, and if the concentration is high enough it will facilitate a detergent-like formation of micelles of the membrane, resulting in membrane disruption (Figure 2.5D) (Bechinger & Lohner, 2006, Jenssen *et al.*, 2006, Laverty *et al.*, 2011).

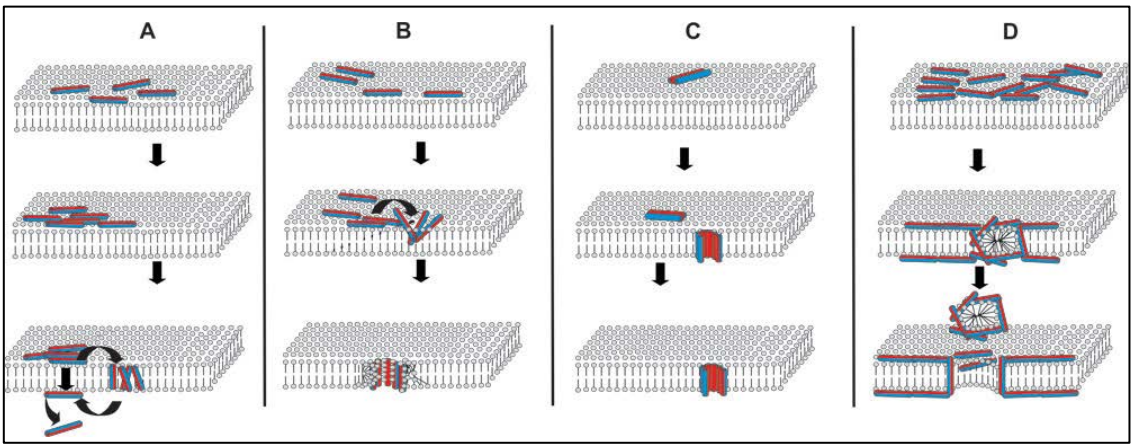

Figure 2.5. Models for AMP plasma membrane penetration (Modified from Jenssen *et al.*, 2006). The bacterial membrane is depicted as a grey lipid bilayer and the peptides, consisting of hydrophilic (red) and hydrophobic (blue) regions, as cylinders. The aggregated model is depicted in (A), the toroidal pore model in (B), the barrel-stave model in (C) and the carpet model in (D).

Newer models of membrane interaction have been introduced. In the revised disordered toroidal pore model, fewer peptides are needed to form a more random pore. AMPs may increase or decrease the thickness of the bacterial bilayer. The peptides may remodel the membrane to form charged lipid clusters surrounding the peptides. Oxidised phospholipids on the surface of the membrane may be targeted to increase peptide adsorption. A peptide may interact with small anions on the intracellular side of the bilayer resulting in a decrease in membrane potential without major damage. On the other hand, in the molecular electroporation model, peptide on the outer membrane can increase the membrane potential enough to render the membrane permeable (Nguyen *et al.*, 2011).

Several AMPs do not cause membrane permeabilisation at their MBC, so an alternative intracellular mechanism of action must be responsible for cell death. Some intracellular modes of bacterial killing include: inhibition of nucleic acid synthesis, protein synthesis, enzymatic activity, cell wall synthesis and DNA binding (Table 2.2) (Jenssen *et al.*, 2006,

Scocchi *et al.*, 2016). It was shown that fluorescently labelled buforin II accumulates intracellularly and gel retardation experiments showed that this peptide binds to bacterial DNA and ribonucleic acid (RNA) (Cudic and Otvos, 2002). Indolicidin has also been shown not to cause membrane damage, and inhibits the synthesis of DNA, RNA and proteins (Laverty *et al.*, 2011). Lactoferricin B also causes inhibition of DNA synthesis of bacteria, and thereby induces filamentation where the bacterium increases in cell length but cannot divide as the septum never develops (Laverty *et al.*, 2011). Human neutrophil peptide (HNP)-I binds primarily to plasma membranes and secondarily to DNA resulting in inhibition of cellular functions (Sharma and Khuller, 2001). Similarly, the peptide PR-39 interferes with bacterial DNA synthesis and protein translation (Cudic and Otvos, 2002, Scocchi *et al.*, 2016). Copsin prevents cell wall synthesis via binding to lipid (Scocchi *et al.*, 2016). Some mammalian AMPs, besides having membrane and intracellular targets in microbes, can also elucidate an immune response, for example, LL-37 induces the selective movement of neutrophils, monocytes and CD4+ T-lymphocyte cells (Laverty *et al.*, 2011).

Table 2.2. Examples of non-membrane permeabilising AMPs (adapted from Scocchi *et al.*, 2016).

Peptides	Mode of action
Buforin II, Tachyplesin I	Bind DNA
Drosocin HNP-1 Indolicidin Lactoferricin B Oncocin Pleurocidin PR-39	Inhibit DNA, RNA and protein synthesis
Apidecin Drosocin Pyrrhocoricin	Inhibit enzymatic activity
Lactoferricin B	Inhibit septum formation
Copsin Nisin Plectasin θ-defensin	Inhibit cell wall synthesis

2.2.6) Eukaryotic cells and antimicrobial peptides

Oral administration is the most common route of drug administration, however, due to digestion, this route remains problematic for peptides (Schall *et al.*, 2012). Topical, pulmonary, transcutaneous or intravenous administration is better suited for peptides. For

intravenous administration, the effects of peptides on the cellular components of blood need to be taken into account. The volume of human blood is composed of 35 – 50% erythrocytes, 1% leukocytes and 49 – 64% plasma (Junqueira and Mescher, 2010). Not only does the concentration of each cell type found in blood differ but also the lifespan. Erythrocytes remain in circulation for 4 months (Bratosin *et al.*, 1995), while the lifespan of leukocytes is variable. Neutrophils have a short lifespan and circulate only 5 days (Pillay *et al.*, 2010). Eosinophils are found in circulation for only 16 to 36 hours, where after these cells migrate to tissues. The entire lifespan of eosinophils can range from 2 to 5 days, or up to 14 days if stimulated by cytokines (Park and Bochner, 2010). The lifespan of mature basophils is estimated to be 60 – 70 hours in circulation, whereas mast cells survive for weeks to months (Siracusa *et al.*, 2011). Lymphocytes have the unique capability to recirculate from tissue to blood, and have a total lifespan of more than 2 months (Young *et al.*, 1995). Monocytes stay in circulation for only a few hours where after they migrate into tissues and differentiate into macrophages. Macrophages have a lifespan ranging from months to years (Parihar *et al.*, 2010).

An ideal AMP for consideration as a therapeutic agent must be shown to have antimicrobial activity at low concentrations and specific selectivity for bacteria cells. Eukaryotic cells contain cholesterol as well as phosphatidylcholine, phosphatidylethanolamine and sphingomyelin, which have no net charge and thus the eukaryotic outer membrane bilayer is neutral (Laverty *et al.*, 2011). This is in contrast to the prokaryotic cell membrane which contains phospholipids such as phosphatidylglycerol, cardiolipin and phosphatidylserine that contribute to the membrane's negative charge (Laverty *et al.*, 2011). The erythrocyte membrane is a typical eukaryotic plasma membrane. It is composed of a phospholipid bilayer with the hydrophobic lipid tails projecting inward and the hydrophilic head groups on the outside. Within the lipid bilayer membrane, proteins can be found that are able to move within the bilayer. Cytoskeletal proteins which form the framework of the cell are also found on the side of the membrane enclosing the cytoplasm. Some of the transmembrane proteins may interact with or be linked to the cytoskeletal proteins. The proteins associated with the erythrocyte membrane are shown in Figure 2.6. Glycophorin C is a transmembrane protein that forms junctional complexes to Band 4.1, which in turn binds to the cytoskeletal elements actin and tropomyosin. Carrier proteins such as Band 3 exchange ions over the cell membrane. Spectrin tetramers are cytoskeletal proteins that form hexagonal scaffolding beneath the cell membrane. Ankyrin binds the spectrin scaffolding to Band 3 proteins. This network of proteins enables erythrocytes to be extremely flexible and to withstand shearing forces resulting from their passage through narrow capillaries (Gartner and Hiatt, 2011).

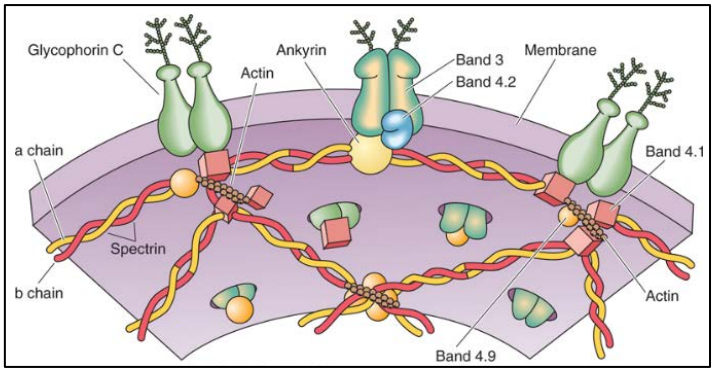

Figure 2.6. Erythrocyte cell membrane and associated proteins (Gartner and Hiatt, 2011). The erythrocyte membrane is composed of a phospholipid bilayer with associated proteins which interact with cytoskeletal proteins.

The cytotoxicity of AMPs is often initially evaluated by measuring the ability of the AMP to induce haemolysis. Mel is a small linear peptide found in the venom of the European honey bee, *Apis mellifera* (Raghuraman and Chattopadhyay, 2005). It is known to be haemolytic, and previous studies have shown that the C-terminal region of the peptide is important for this activity (Blondelle and Houghten, 1991, Raghuraman and Chattopadhyay, 2005). Some amino acids have been shown to be major contributors to the haemolytic activity of Mel, as their omission in synthetic derivatives significantly decreased activity. These amino acids include leucine (Leu) on all positions, Ile on position 17 and 20, and Trp on position 19. To a lesser degree, lysine (Lys) on position 7 and valine (Val) on position 8 also showed a decrease in haemolytic activity when omitted from the peptide sequence (Blondelle and Houghten, 1991).

A limitation of using erythrocytes as a model of mammalian cells is that these differentiated cells lack organelles, RNA and DNA which are essential for cellular replication, growth and differentiation. Types of cells that can be used for this purpose include normal undifferentiated embryonic (e.g. stem cells) or normal differentiated cells (e.g. leukocytes) as well as cancer cell lines (e.g. HeLa cell line).

The advantage of using normal differentiated cells such as leukocytes, is that these cells are a therapeutically relevant cell population. In the laboratory-based development of new AMPs these leukocytes can be used for the evaluation of toxicity. One of the roles of leukocytes is the destruction of pathogenic microorganisms, and AMPs may stimulate leukocytes to enhance this effect. The leukocyte plasma membrane and cytoskeleton plays an important role in this function. The plasma membrane is a phospholipid bilayer with carbohydrates and cholesterol, which contains specialised protein and enzyme factors depending on the type of leukocyte. The cytoskeleton is composed of microtubules, microfilaments and intermediate

filaments. The microtubules are composed of tubulin dimer proteins arranged in a tube with a hollow core, and twisted into a helix. Microtubules radiate from the centrioles in the centre of the cell and these tubules control the recruitment and dissolution of microfilaments in areas of the membrane stimulated to phagocytose. These filaments are composed of actin proteins arranged in a double helix. Microfilaments are located directly below the plasma membrane and provide the contractile element to enable cell movement and phagocytosis. Microfilaments also provide a physical barrier to spontaneous degranulation. During phagocytosis, the oxidative burst supplies the means to kill the pathogens. Evidence exist that the mechanisms which regulate this oxidative process may also be responsible for the regulation of the cytoskeleton. The enzymes involved in the oxidative burst process are also thought to be located in the plasma membrane which implies that both the membrane, and the cytoskeleton is closely involved with leukocyte function and morphology (Oliver, 1978).

A complex system of oxidation and antioxidant activity is regulated by leukocytes as part of the defence against pathogens. Phagocytes produce oxidants during the respiratory burst to kill pathogens. During phagocytosis, nicotinamide adenine dinucleotide phosphate (NADPH) oxidase, which is normally dormant, becomes activated. Activated NADPH oxidase catalyses the formation of superoxide anions (see reaction below). This then leads to the formation of various oxidative molecules, including singlet oxygen, hydrogen peroxide (H_2O_2), hypochlorous acid and chloroamines (Figure 2.7) (Male *et al.*, 2013).

$$NADPH + 2O_2 \xrightarrow{NADPH-oxidase} NADP^+ + 2O_2^- + H^+$$

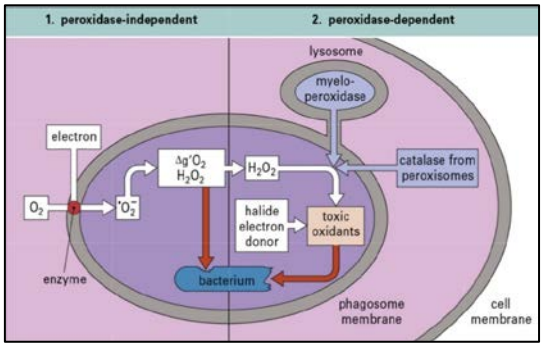

Figure 2.7. Oxygen-dependent microbicidal activity (Male *et al.*, 2013). (1) **Peroxidase-independent pathway.** The enzyme NADPH oxidase in the phagosome membrane reduces oxygen to the superoxide anion ($^{\bullet}O_2^-$). This can give rise to hydroxyl radicals (•OH), singlet oxygen ($\Delta g'O_2$), and H_2O_2, all of which are potentially toxic. (2) **Peroxidase-dependent pathway.** If lysosome fusion occurs, myeloperoxidase (or, under some circumstances, catalase from peroxisomes) acts on peroxides in the presence of halides (preferably iodide). Then additional toxic oxidants, such as hypohalites (HIO, HClO), are generated.

Oxidant and antioxidant effects need to be tightly regulated as an overproduction of ROS would lead to inflammation and cellular damage. Therefore, the amount of ROS produced need to be carefully regulated (Zughaier *et al.*, 2005).

2.2.7) Multifunctional antimicrobial peptides

Several antibacterial AMPs have been found to have additional beneficial effects and these include antiproliferative, antioxidant and anti-inflammatory activities. The AMP, magainin II was isolated from the African clawed frog, *Xenopus laevis*, and has been shown to have antiproliferative activity against bladder cancer cells, with no cytotoxicity toward normal murine or human fibroblasts (Lehmann *et al.*, 2006). Two synthetic peptides, derived from the beetle *Allomyrina dichotoma* defensin, that are active against both Gram-positive and Gram-negative bacteria also show inhibitory effects on inflammatory cellular responses induced by LPS (Motobu *et al.*, 2004).

Infection is often associated with an increase in inflammation and associated increased levels of oxidants such as O_2^- and H_2O_2 (Robinson, 2008). These molecules are produced by immune cells to destroy pathogens, but can cause cellular damage if over-produced or if antioxidants fail to protect these cells (Pavia and Bozza, 2014). Inherent cellular antioxidant activity is due to the presence of antioxidant molecules such as glutathione as well as vitamin C and E. In addition, the antioxidant enzymes catalase, superoxide dismutase and myeloperoxidase protect cells against oxidative damage (Table 2.3). Dietary antioxidants such as polyphenols and peptides provide additional protection against oxidative damage.

Both erythrocytes and leukocytes are relevant cells to use for the study of antioxidant potential. Erythrocyte studies present a relatively simplistic model for antioxidant studies, as there is no cellular signalling or mitochondrial ROS production which complicates interpretation of results (Honzel *et al.*, 2008). In contrast, leukocytes are more complex and have ROS dependent signalling pathways and the mitochondria also produce ROS. Both cell types have some of the same redox enzyme systems (Table 2.3).

Table 2.3. Role of antioxidant enzymes and proteins in erythrocytes and leukocytes (Honzel *et al.*, 2008).

Role of antioxidant enzymes and proteins	Erythrocyte	Leukocyte
Glutathione peroxidase Reduces lipid hydroperoxides to their corresponding alcohols Reduces free H_2O_2 to water Protects integrity of cellular membranes Function depends on selenium Protects nucleated cells from oxidative stress-induced apoptosis	√	√
Glutathione reductase Maintains glutathione in its reduced state	√	√
Catalase Breakdown of H_2O_2 to oxygen and water	√	√
Superoxide dismutase Catalyses dismutation of superoxide to oxygen and H_2O_2	√	√
Myeloperoxidase Produces hypochlorous acid from H_2O_2 and chloride anion during the neutrophil's respiratory burst Oxidises tyrosine to tyrosyl radical using H_2O_2	X	√
Cyclooxygenase COX-1 Contain both cyclooxygenase and peroxidase properties Catalyses the first step in the biosynthesis of prostaglandins, thromboxanes, and prostacyclins	X	Constitutively expressed
Cyclooxygenase COX-2 Contain both cyclooxygenase and peroxidase properties Catalyses the first step in the biosynthesis of prostaglandins, thromboxanes, and prostacyclins	X	Induced with inflammation
Haemoglobin / deoxyhemoglobin Scavenging and transport of O_2, CO_2, NO	√	X

√ Present, X absent

The peptide pheromone plantaricin A, which is synthesized by *Lactobacillus plantarum*, showed protective effects on human keratinocytes which the authors attributed in part to the antioxidant activity of this peptide (Marzani *et al.*, 2012). One plant defensin, SPD1, from sweet potato has been shown to possess antioxidant activity against hydroxyl and peroxyl radicals (Huang *et al.*, 2012). The antioxidant activity of defensin derived peptides has not been widely researched. However, multifunctional peptides have great potential to be further developed as therapeutics as these peptides may eradicate infection and also create a cellular environment that promotes tissue and cellular recovery and healing.

2.3) Background to this study

Research conducted in the Department of Biochemistry, University of Pretoria on the soft tick *Ornithodoros savignyi* identified four fractions from the haemolymph that displayed antibacterial activity against Gram-positive species (Olivier, 2002). The amino-terminal sequence of a peptide in one of the fractions showed homology with scorpion defensins. cDNA cloning using midgut RNA led to the identification of two defensin isoforms, OsDef1 and OsDef2. Synthetic OsDef1 and OsDef2 were tested for antibacterial activity, and OsDef2 was found to be slightly more active (Prinsloo *et al.*, 2013). For this reason, OsDef2 was used as a template for the synthesis of two shorter peptides, namely Os and Os-C (Table 2.4). Disulfide bridges may form between the Cys residues of Os. Peptides without disulphide bridges are easier and cheaper to synthesise (Prinsloo *et al.*, 2013) and for this reason the bioactivity Os-C was also determined.

Table 2.4. Amino acid sequence of tick defensin OsDef2 and C-terminal derived Os and Os-C (Prinsloo *et al.*, 2013).

Name	Amino acid sequence	Mass (Da)	Hydrophobicity	Net charge
OsDef2	GYCPFNQYQCHSHCKGIRGYKGGYCKGAFKQTCKCY	4185.80	0.371	+6
Os	KGIRGYKGGY**C**KGAFKQT**C**K**C**Y	2459.92	0.249	+6
Os-C	KGIRGYKGGYKGAFKQTKY	2150.50	0.045	+6

Both peptides were found to have excellent antibacterial activity, with MBCs ranging between 0.94 – 15 µg/mL (Table 2.5). The Cys-containing peptide, Os was found to be two-fold more active than its Os-C counterpart against the tested bacteria, but equally active against *S. aureus*. Os and Os-C peptides were the most active against *P. aeruginosa* (Prinsloo *et al.*, 2013). Both peptides have the same net charge of +6, but differ in hydrophobicity. The authors suggested that the higher hydrophobicity of Os could be the reason for its increased activity over Os-C (Table 2.4).

Table 2.5. Minimum bactericidal concentration values of synthetic peptides against selected Gram-negative and Gram-positive bacterial strains (Prinsloo *et al.*, 2013).

	Bacterial strain	Os (µg/mL)	Os-C (µg/mL)
Gram-negative	***E. coli***	1.90 (0.77 µM)	3.75 (1.74 µM)
	P. aeruginosa	0.94 (0.38 µM)	1.90 (0.88 µM)
Gram-positive	***S. aureus***	15.00 (6.10 µM)	15.00 (6.98 µM)
	B. subtilis	1.90 (0.77 µM)	3.75 (1.74 µM)

The kinetics of bactericidal activity of Os and Os-C was evaluated using *E. coli* and *B. subtilis*, as representative Gram-negative and Gram-positive strains. The time-course study revealed that Os inactivated 100% of both Gram-positive and -negative bacteria within the first 5 min, whereas Os-C showed 100% bactericidal activity only after 60 min and 120 min against Gram-negative (Figure 2.8A) and Gram-positive bacteria (Figure 2.8B), respectively.

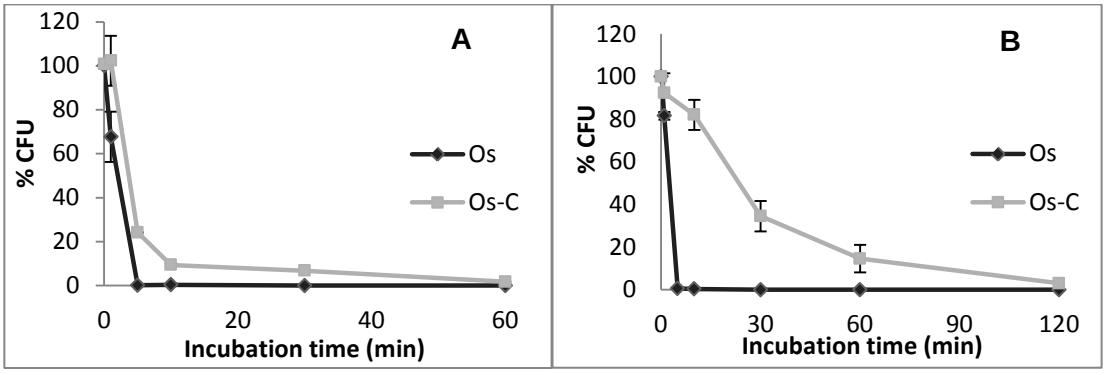

Figure 2.8. Killing kinetics of Os and Os-C against A) *E. coli* and B) *B. subtilis* (Prinsloo *et al.*, 2013). Results are given as % colony forming units (CFU) with respect to the CFU of the untreated bacteria (growth control). 0% CFU indicates complete (100%) bactericidal activity. Error bars represent the standard deviation of two independent experiments performed in triplicate.

Circular dichroism data indicated that in both peptides exhibited random coiled structures in water. However, in SDS, a membrane-mimicking environment, Os had a higher α-helical content. The difference in structure and the amount of time needed to kill bacteria between Os and Os-C may indicate a different mechanism of action for each peptide (Prinsloo *et al.*, 2013). However, this is preliminary data and further detailed studies needed to be undertaken to determine the mode of action of these two peptides to understand how bacterial killing occurs. It is also important to understand the effect that these two peptides may have on eukaryotic cells if these AMPs are to be ultimately developed as antimicrobial agents. In addition, it would also be advantageous to determine if these peptides have additional beneficial effects such as antioxidant activity.

2.4) Aims

The aims of this study were to investigate the effects of Os and Os-C on selected bacterial strains and identify a possible mode of action. Using physiologically relevant cell types, erythrocytes and leukocytes, determine the cytotoxicity of both peptides. Lastly to determine whether Os and Os-C have additional beneficial effects such as cellular antioxidant activity.

2.5) Objectives

1. Determine the effects of Os and Os-C on Gram-positive *B. subtilis* and Gram-negative *E. coli* ultrastructure, cell wall permeability and intracellular targets such as DNA.
2. To study the effects of Os and Os-C on human erythrocyte and leukocyte viability, membrane permeability as well as cellular morphology.
3. To determine if Os and Os-C have antioxidant activity and can effectively protect erythrocytes and leukocytes against oxidative damage.

The experimental strategy to achieve these objectives is presented in Figure 2.9.

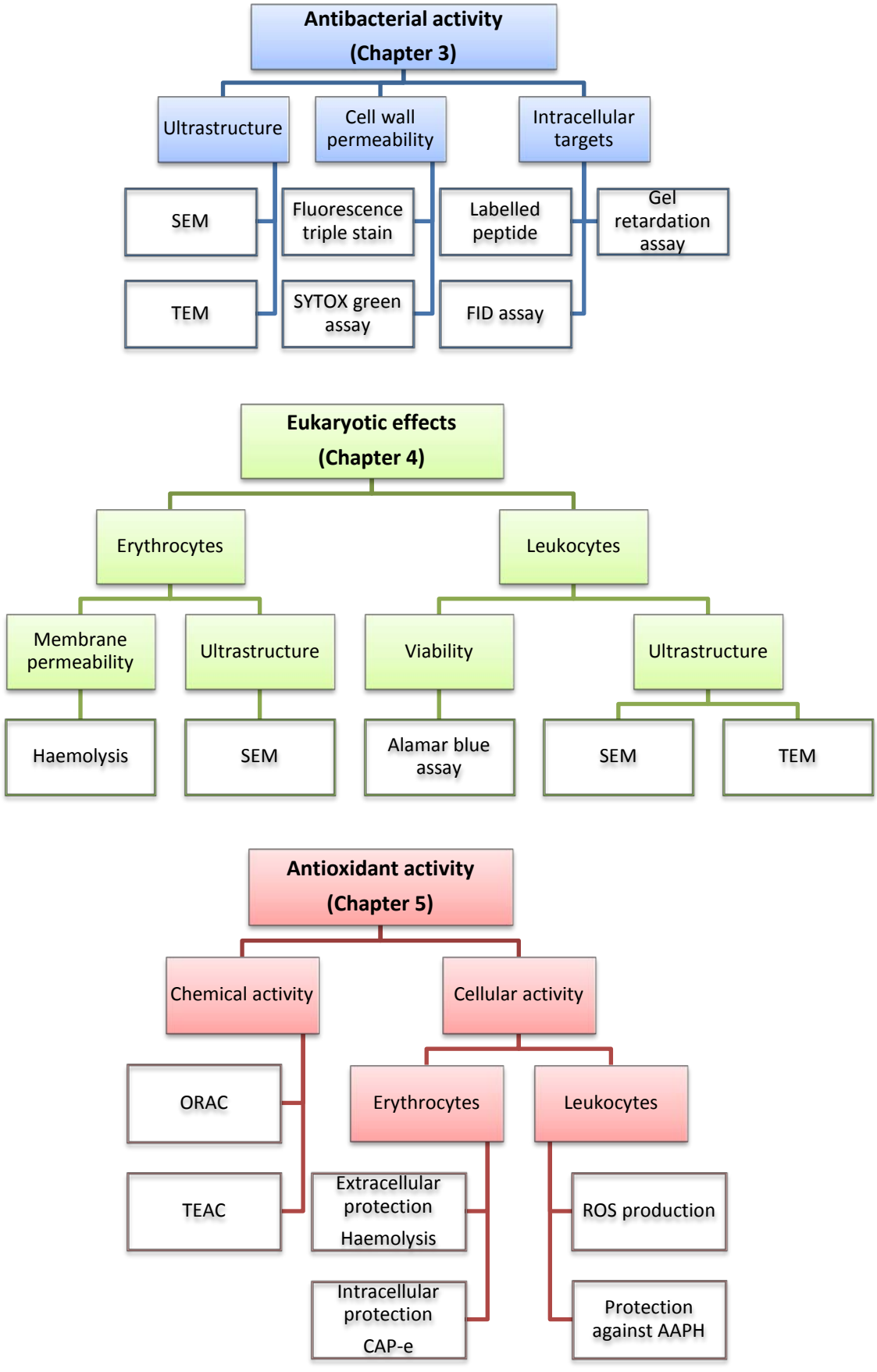

Figure 2.9. Flow diagram of objectives related to the bioactivity of Os and Os-C.

Chapter 3: Mechanism of bacterial killing of Os and Os-C[1]

3.1) Abstract

AMPs have different modes of killing which involve membranes and intracellular targets. Previous *in vitro* studies have shown that Os and Os-C effectively killed bacteria. Os inactivated 100% of both Gram-positive and -negative bacteria within the first 5 min while for Os-C bacteria killing was slower and occurred after 60 min and 120 min for Gram-negative and Gram-positive bacteria, respectively (Prinsloo *et al.*, 2013). The aim of the research described in this chapter was to determine whether Os and Os-C are membrane acting and/or have additional intracellular targets in *E. coli* and *B. subtilis*.

Scanning electron microscopy (SEM) and transmission electron microscopy (TEM) indicated that both peptides adversely affected the cellular structure of both bacteria. Morphology evaluated with SEM revealed bacteria with an indented morphology that indicated a possible loss of membrane integrity similar to that observed with autolysis. TEM revealed cytoplasmic retraction, intracellular granulation and membrane ruffling. Cellular changes induced by Os and Os-C were different from that induced by Mel, an AMP that causes lysis.

Membrane effects were quantified using the SYTOX green assay. At the MBC, permeabilisation did not seem to be the principle mode of killing when compared to Mel. However, fluorescent triple staining showed that the peptides caused permeabilisation of stationary phase bacteria and TEM indicated membrane effects. Studies using fluorescently labelled peptides revealed that the membrane penetrating activity of Os and Os-C was similar to buforin II, a cell-penetrating peptide. Fluorescently labelled Os-C accumulated on *B. subtilis* septa and was unable to penetrate stationary phase *E. coli* cells. Plasmid binding studies showed that Os and Os-C bound *E. coli* plasmid DNA, although fluorescence displacement studies showed a dosage effect for Os only. Differences in the ability to penetrate stationary *E. coli,* localisation of Os-C at *B. subtilis* septa and the preferable binding of Os to DNA indicates that there may be some differences in the mechanism of bacteria killing between Os and Os-C. However, similarities in the morphology following exposure indicates the final consequence of these events is similar.

In conclusion, Os and Os-C effectively kill bacteria and their mode of action is a combination of altered membrane integrity and intracellular effects such as DNA binding.

[1]The results from this chapter was published: Taute, H, Bester, MJ, Neitz, AWH & Gaspar, ARM 2015. Peptides, 71: 179-187.

3.2) Introduction

AMPs are widely studied in an effort to produce novel antibiotics. The mode of killing of an AMP needs to be fully understood if it is to be developed as an antibiotic treatment. AMPs may kill bacteria through a large range of targets. The most prominent target is the bacterial cell membrane. Gram-negative bacteria possess an outer membrane which consists of LPS in a phospholipid bilayer, an inner membrane which consists of a phospholipid bilayer with proteins and a thin peptidoglycan layer in the periplasmic space between the two (Harvey *et al.*, 2013). Gram-positive bacteria, on the other hand, have a thick peptidoglycan layer with teichoic acids which forms a cell wall and a phospholipid cell membrane (Harvey *et al.*, 2013). The selectively permeable outer membrane of Gram-negative bacteria and other protective mechanisms causes these bacteria to be generally more resistant to antibiotics (Hancock and Rozek, 2002). Nevertheless, Gram-negative bacteria have been shown to be susceptible to cationic peptides (Hancock and Rozek, 2002). There are several proposed models of AMP membrane interaction, these are the toroidal pore, aggregate, barrel-stave and carpet models (Laverty *et al.*, 2011). AMPs may either cause the formation of short-lived channels, the disintegration of the membrane or they may translocate into the membrane (Jenssen *et al.*, 2006). Various intracellular targets have also been proposed, such as the inhibition of nucleic acid, protein or cell wall synthesis, or the stimulation of autolytic enzymes (Cudic and Otvos, 2002, Jenssen *et al.*, 2006).

To determine whether the AMPs act on the membrane or intracellular targets, various techniques can be used. The use of microscopy may reveal important insights into the mode of killing of peptides. Using electron microscopy, Hartmann and colleagues (2010) observed that the peptides gramicidin S and peptidyl-glycylleucine-carboxyamide (PGLa) caused damage to the bacterial envelope, disruption of osmoregulation and affected bacterial DNA. Mangoni *et al.* (2004) described a fluorescence triple staining method with which permeability and viability could simultaneously be visualised. Fluorescent labelling of buforin II analogues allowed researchers to observe that substitution or insertion of Pro caused the peptide to become membrane acting, whereas the original peptide translocated to the cytoplasm (Park *et al.*, 2000).

Using these techniques, the effects of Os and Os-C on Gram-positive *B. subtilis* and Gram-negative *E. coli* ultrastructure, cell membrane permeability and intracellular targets such as DNA were determined.

3.3) Materials and methods

3.3.1) Peptides

The peptides Os and Os-C, as well as Os, Os-C and buforin II labelled with 5-carboxyfluorescein (5FAM) on the N-terminus were obtained from GenScript (New Jersey, USA). Antibacterial activity of labelled peptides was confirmed with the colony forming assay. The peptide melittin (Sigma-Aldrich, Johannesburg, South Africa) is a known lytic peptide and was used as a positive control for membrane damage. The purity and molecular mass of the peptides were determined by the vendor by reverse-phase high-performance liquid chromatography (HPLC) and mass spectrometry, respectively. Dithiothreitol (10 nmol) was added to Os prior to lyophilisation to prevent disulphide bond formation between Cys residues. Table 3.1 shows the amino acid sequences and properties of all peptides used.

Table 3.1. Physicochemical properties of peptides used in this study.

Name	Amino acid (AA) sequence	AA length	Mass (Da)	pI	Net charge*
Melittin	GIGAVLKVLTTGLPALISWIKRKRQQ	26	2847.40	12.02	+5
Os	KGIRGYKGGYCKGAFKQTCKCY	22	2459.92	9.98	+6
Os-C	KGIRGYKGGYKGAFKQTKY	19	2150.50	10.70	+6
5FAM-Os	**5FAM**-KGIRGYKGGYCKGAFKQTCKCY	22	2818.23	9.95	+5
5FAM-Os-C	**5FAM**-KGIRGYKGGYKGAFKQTKY	19	2508.79	10.69	+5
5FAM-buforin II	**5FAM**-TRSSRAGLQFPVGRVHRLLRK	21	2793.16	12.71	+5

*Net charge at pH 7

Peptide concentrations were determined by measuring the absorbance (Abs) of Tyr or Trp residues at 280 nm and using the equation below:

$$c = \frac{MW \times df \times Abs}{no.of\ Tyr/Trp \times Extinction\ coefficient}$$

where c is the peptide concentration in mg/mL; MW is the molecular weight of the peptide, and df is the dilution factor. The extinction coefficients of Tyr and Trp are 1200 and 5560 AU/mmole/mL, respectively (Lamichhane *et al.*, 2011). The concentration of the fluorescently labelled peptides was determined with the same equation, by measuring the absorbance of

5FAM at the excitation wavelength (492 nm) and using its extinction coefficient (78 000 AU/mmole/mL) (Buranasompob, 2005).

Stock solutions of the peptides were prepared in sterile $dddH_2O$ with the following concentrations; 1.2 mg/mL of Os (488.33 µM) and Os-C (557.92 µM), 3.4 mg/mL of Mel (1190 µM), 430 µg/mL of 5FAM-Os (154 µM), 380 µg/mL of 5FAM-Os-C (152 µM) and 382 µg/mL of 5FAM-buforin II (137 µM). The stock solutions were kept in aliquots of 20µl in polypropylene tubes at -20°C until needed. Dilutions from this stock solution were made as needed in sterile $dddH_2O$. As a negative control in all experiments, the peptide was replaced with an equal volume of sterile $dddH_2O$.

3.3.2) Bacterial strains

The bacterial strains *E. coli* (ATCC 700928) and *B. subtilis* (ATCC 13933) were used for all experiments. Both bacterial strains were kept at -80ºC until needed. To establish bacterial colonies, the strain needed was streaked onto a Luria-Bertani (LB) agar plate. The plate was incubated at 37ºC for 16-18 hours. On the day before experimentation, a bacterial culture was prepared by inoculating 20 mL of LB broth with a colony from the agar plate. The bacterial culture was grown at 37ºC for 16-18 hours in a shaking incubator. The culture was then diluted 100 times and sub-cultured in LB broth until an OD_{600} of 0.5 per cm (exponential growth phase) was reached.

3.3.3) Poly-L-lysine coated coverslips

To ensure attachment of bacterial cells to a surface suitable for microscopy, glass coverslips were coated with poly-L-lysine. Poly-L-lysine is a positively charged polymer which coats the glass surface and offers enhanced attachment to negatively charged cells through electrostatic interaction (Sitterley, 2008). As the poly-L-lysine is positively charged, there would be minimal interaction with the positively charged peptides under investigation. Round coverslips with a diameter of 10 mm were obtained from Lasec (Johannesburg, South Africa). The coverslips were cleaned with an alkaline wash solution containing 10% NaOH (w/v) and 60% ethanol (*v/v*) by shaking for at least 2 hours. The coverslips were then rinsed seven times with double distilled water (ddH_2O) and sterilised with 99.9% ethanol for at least 30 minutes. Coverslips were then transferred to a sterile environment to dry. Dried coverslips were submerged in poly-L-lysine (70000 – 150000 kDa, Sigma-Aldrich, Johannesburg, South Africa) for 2 hours. After the poly-L-lysine solution was removed, coverslips were

rinsed seven times with sterile dddH_2O and dried for at least three days before use. Coated coverslips were stored under sterile conditions at room temperature.

3.3.4) Ultrastructure of selected bacterial strains

To investigate the effects of Os and Os-C on the ultrastructural morphology of *E. coli* and *B. subtilis*, SEM and TEM was used.

Scanning electron microscopy

The sample preparation methods of Mangoni *et al.* (2004) were adapted for this study. *E. coli* and *B. subtilis* bacterial strains in the exponential growth phase were diluted to a cell concentration of $1x10^6$ CFU/mL in 10 mM sodium phosphate buffer, pH 7.4 (NaP; 2 mM $NaH_2PO_4 \cdot H_2O$ and 8 mM $HNa_2PO_4 \cdot 2H_2O$). The two synthetic peptides were added to separate vials containing the bacterial suspensions to obtain final concentrations of the respective MBCs. The MBCs were previously determined as 0.77 µM for Os and 1.74 µM for Os-C for both *E. coli* and *B. subtilis* at a cell density of $1x10^6$ CFU/mL (Prinsloo *et al.*, 2013). Bacteria were also exposed separately to Mel, which was used as a positive control for damage, at a concentration of 25 µM. Issam *et al*. (2015) measured the MBC of Mel to be 21 µM for *E. coli* and 10.5 µM for *B. subtilis* using $1x10^8$ CFU/mL. Lyu *et al.* (2016) found the MBC of Mel to be between 2 – 4 µM for *E. coli* and 2 µM for *B. subtilis* at a cell density of $1x10^5$ CFU/mL. The bacteria were exposed to the various peptides for 30 min at 37°C in a shaking incubator. After exposure the bacterial suspension was transferred to poly-L-lysine coated coverslips and allowed to attach for 90 minutes at 30°C. To remove any bacterial cells not firmly attached, the coverslips were rinsed twice with NaP buffer. Cells were then immediately fixed with a solution of 2.5% gluteraldehyde and 2.5 %formaldehyde in 0.075 M sodium phosphate buffer (NaH_2PO_4, $NaHPO_4 \cdot 2H_2O$, pH 7.4). After one hour of fixing, the samples were rinsed three times with 0.075 M phosphate buffer for 10 minutes before being placed in a secondary fixative of 1% osmium tetraoxide solution for 30 minutes. The samples were again rinsed in 0.075 M phosphate buffer three times for 10 minutes. The bacteria on the coverslips were then dehydrated with a series of ethanol dilutions; 30%, 50%, 70%, 90% and three changes of 100%. The coverslips were dried with the use of hexamethyldisilazane (HMDS), mounted with carbon tape on aluminium stubs, coated with carbon, and viewed with an Ultra plus field emission gun (FEG) SEM (Zeiss, Oberkochen, Germany).

Transmission electron microscopy

There are several methods available to prepare bacterial samples for TEM. These include chemical fixation, high pressure freezing and negative staining. A standard sample preparation technique was used for chemical fixation. *E coli* and *B. subtilis* cells in the exponential phase were adjusted to a cell density of $64x10^6$ CFU/mL. The cell suspension was centrifuged to make a dense pellet. The pelleted cells were fixed with 2.5% gluteraldehyde and formaldehyde in 0.075 M phosphate buffer. After one hour of fixing, the samples were rinsed three times with 0.075 M phosphate buffer for 10 minutes before being placed in a secondary fixative of 1% osmium tetraoxide solution for 30 minutes. The samples were again rinsed in 0.075 M phosphate buffer three times for 10 minutes. The bacteria were then dehydrated with a series of ethanol dilutions; 30%, 50%, 70%, 90% and three changes of 100%. The cells were then infiltrated with 50% Embed 812 resin (SPI supplies, Pennsylvania, USA) in ethanol for 1 hour, then with 100% resin for 4 hours. The resin was replaced with fresh resin, and polymerised in moulds for 72 hours. Subsequently, 100 nm sections were made with the Leica Ultramicrotome (Leica Microsystems GmbH, Wetzlar, Germany) using a 45° diamond knife (Diatome, Pennsylvania, USA). These sections were picked up on copper grids and contrasted with 4% aqueous uranyl acetate and Reynolds' lead citrate and rinsed with water. The contrasted sections were viewed and images taken on the JEM-2100F TEM (JEOL, Tokyo, Japan).

The negative staining methods were adapted from Prigent-Combaret *et al.* (2000). *E. coli* and *B. subtilis* cells in the exponential phase were diluted to a cell density of $1x10^6$ CFU/mL. A volume of 90 µL of cell suspension was incubated with 10 µL peptide for 10 minutes at 37°C. The final concentrations were at the MBCs of Os (0.77 µM) and Os-C (1.74 µM). Mel (25 µM) was used as a positive control for damage, and water was used as a negative control. Copper grids were coated with a layer of Formvar 1595 E polymer (Merck Millipore, Johannesburg, South Africa) as a support for the cells and then coated with carbon to make it conductive. The cell suspension was dropped onto the grid and allowed to air dry. A drop of uranyl acetate was used as the negative stain, this was allowed to dry at room temperature. The cells were imaged with the JEM-2100F TEM (JEOL, Tokyo, Japan).

The method for high pressure freezing and freeze substitution (FS) were based on the methods described by Venter *et al.* (2013). *E coli* and *B. subtilis* cells in the exponential phase were adjusted to a cell density of $64x10^6$ CFU/mL. A volume of 990 µL of these cells were exposed to 10 µL of a final concentration of 2 µM Mel, Os or Os-C or water for 10 minutes at 37°C. After exposure of selected bacteria to the peptides, the suspension was

centrifuged to make a dense pellet. The pellet (1 µL) was used to fill the cavity (1.2 mm in diameter and 200 µm deep) of a gold plated flat specimen carrier (Leica Microsystems GmbH, Wetzlar, Germany). The samples were immediately frozen under high pressure in the Leica EM Pact (Leica Microsystems GmbH, Wetzlar, Germany). To remove all water from the samples, FS was carried out with the Leica EM AFS2 (Leica Microsystems GmbH, Wetzlar, Germany) in 2% osmium tetroxide, 0.1% uranyl acetate and 97.9% acetone. The samples were kept at -90°C for 42 hours, heated to -60°C over a 15 hour period, left at -60°C for 8 hours, heated to -30°C over a 15 hour period, left at -30°C for a further 8 hours after which the samples were allowed to warm up to room temperature. Samples were infiltrated with, and embedded in Embed 812 (SPI Supplies, PA, USA). Ultra-thin sections of 100 nm were prepared with the Leica Ultramicrotome (Leica Microsystems GmbH, Wetzlar, Germany) using a 45° diamond knife (Diatome, Pennsylvania, USA). These sections were picked up on copper grids and contrasted with 4% aqueous uranyl acetate and Reynolds' lead citrate and rinsed with water. The contrasted sections were viewed and images taken on the JEM-2100F TEM (JEOL, Tokyo, Japan).

3.3.5) Membrane permeability assays

SYTOX green assay

In order to quantify the extent of bacterial cell wall permeabilisation after exposure to the peptides, the SYTOX green (Life Technologies, Johannesburg, South Africa) assay was used. The methods were adapted from Roth *et al.* (1997). SYTOX green gives an indication of permeabilisation, as it is unable to penetrate intact membranes. Upon entering a cell, SYTOX green binds to DNA and its fluorescence increases markedly (Roth *et al.*, 1997). Bacterial strains were grown to the exponential growth phase and diluted to a cell density of $1x10^6$ CFU/mL. The cells were incubated with SYTOX green at a final concentration of 0.1 µM in 10 mM NaP buffer, pH 7.4 for 15 minutes at 37°C in a shaking incubator. A volume of 90 µL of the bacteria and SYTOX green mixture was then exposed to 10 µL of a concentration range of Mel, Os and Os-C (final concentrations between 0.1 – 10 µM) for 1 hour at 37°C in a shaking incubator in a black, flat bottom, polystyrene Costar 96-well plate (Corning, New York, USA). The control was exposed to the same volume of sterile $dddH_2O$ only. The plate was then transferred to the SpectraMax Paradigm microplate reader (Molecular Devices, California, USA) and the fluorescence of each well measured using an excitation of 488 nm and emission of 530 nm.

Fluorescent triple staining

In this study, a triple staining method was used, based on the method described in Mangoni *et al.* (2004), using 5-cyano-2,3-ditolyl tetrazolium chloride (CTC), 4',6-diamidino-2-phenylindole (DAPI) and fluorescein 5(6)-isothiocyanate (FITC). This triple stain enables the simultaneous viewing of total (stained by DAPI) and viable cells (stained by CTC), as well as cells with modified membrane permeability (stained by FITC). Stationary phase *E. coli* and *B. subtilis* cultures were adjusted to a cell density of $64x10^6$ CFU/mL in 10 mM NaP buffer, pH 7.4. A volume of 90 µL of the cell suspension was exposed to 10 µL peptide for 10 minutes at 37°C in a shaking incubator. The final concentrations were 0.77 µM for Os and 1.74 µM for Os-C and concentrations 10x lower (0.07 µM and 0.17 µM). The cells were also exposed to the positive control, Mel, at a concentration of 2.5 µM for 10 minutes at 37°C in a shaking incubator. The bacterial suspensions were subsequently incubated with 900 µL of 5 mM CTC in 10 mM NaP buffer pH 7.4 for 2 hours at 37°C in a shaking incubator. To allow adhesion of cells to the surface of poly-L-lysine coated coverslips, the CTC-bacteria mixture was added to the wells of a 24-well Cellstar polystyrene plate (Greiner Bio-One GmbH, Kremsmünster, Austria) containing the coverslips and incubated at 30°C for 90 min. The coverslips were rinsed with NaP buffer, then a volume of 1 mL of 10 µg/mL DAPI in phosphate buffered saline (PBS[a], 0.137 M NaCl, 2.7 mM KCl, 10 mM Na_2HPO_4, 2 mM KH_2PO_4, pH 7.4) was added and incubated at 30°C for 30 min. The coverslips were rinsed with NaP buffer and 1 mL FITC solution (6 µg/mL in 10 mM NaP buffer) added and incubated at 30°C for 45 min. Thereafter the coverslips were rinsed with NaP buffer again, mounted on slides with antifade mounting medium (Sigma-Aldrich, Johannesburg, South Africa) and viewed with the Zeiss LSM 510 Meta Confocal Microscope (Carl Zeiss NTS GmbH, Oberkochen, Germany). The excitation and emission wavelengths used for CTC were 450 nm and 630 nm, for FITC 490 nm and 520 nm and for DAPI 359 nm and 461 nm, respectively. Images of all three dyes were taken separately and overlaid with the Carl Zeiss AIM LSM imaging software into a single image containing the three colour signals.

3.3.6) Gel retardation assay

The DNA of prokaryotic cells is localised in the cytoplasm, has no nuclear membrane or associated histone proteins but exists as a supercoiled structure. Most bacteria also contain separate small pieces of DNA called plasmids (Actor, 2012). If AMPs cross the cell envelope, plasmid/genomic DNA, RNA and/or negatively charged proteins are therefore likely targets. The gel retardation assay was used to determine if peptides bind to plasmid DNA. Ionic interactions between the cationic peptide and plasmid DNA reduce the charge on

the plasmid and subsequently the migration in the agarose gel is retarded. To investigate the effect of peptides on DNA, 2.5 µL 10 µg/mL pBR322 vector from *E. coli* (Sigma-Aldrich, Johannesburg, South Africa) was exposed to 2.5 µL of different concentrations of Os, Os-C and Mel for 1 hour at 37°C. 2,2'-Azobis(2-amidinopropane) dihydrochloride (AAPH) was used as a positive control for DNA damage, and ddH_2O was used as a negative control. A volume of 5 µL of loading solution (40% sucrose and 0.13% bromophenol blue) was added. The samples were analysed on a 1% agarose gel in TAE buffer (0.8 mM Tris, 0.4 mM glacial acetic acid, 10 mM ethylenediaminetetraacetic acid, pH 8.0). The gel was post stained with a 3X staining solution of GelRed (Biotium, California, USA) as per the manufacturer's instructions for 1 hour, and imaged with the UVIdoc HD5 gel documentation system (Uvitech, Cambridge, UK). The intensity of three points on each band was measured using the image analysis freeware ImageJ 1.45s (National Institutes of Health, USA), this was done twice. Multiple comparisons were tested by one-way ANOVA followed by the Tukey post hoc test to test for significant difference to the control (GraphPad Prism v6.01, California, USA).

3.3.7) Fluorescent intercalator displacement assay

To confirm results from the SYTOX green membrane permeabilisation assay and the gel retardation assay, the fluorescent intercalator displacement (FID) assay was used. Tse and Boger (2004) described the principle of the assay with ethidium bromide and thiazole orange. A fluorescent dye which intercalates with DNA results in an increased amount of fluorescence upon binding. A test compound which is DNA binding, will displace the intercalator and result in a decrease in fluorescence (Tse and Boger, 2004). The method for the current study was adapted from two previous studies which used ethidium bromide as intercalator (Geall and Blagbrough, 2000, Tse and Boger, 2004). SYTOX green has been shown to bind DNA by intercalation (Thakur and colleagues, 2015), and was chosen for the FID assay in the present study. A volume of 2.5 µL of 10 mg/mL pBR322 vector from *E. coli* (Sigma-Aldrich, Johannesburg, South Africa) in 0.1 M PBS[b] (81 mM $Na_2HPO_4.2H_2O$, 19 mM $NaH_2PO_4.H_2O$, 0.15 M NaCl, pH 7.4) was incubated with 95 µL of 1 µM SYTOX green in 10 mM NaP buffer in a 96-well polystyrene, flat bottom plate for 15 min at 37°C to allow for equilibration. A volume of 2.5 µL of Mel, Os and Os-C at concentrations of 1 – 50 µM was added and incubated for a further 60 min. The fluorescence intensity was then measured with the FLUOstar OPTIMA plate reader from BMG Labtechnologies (Offenburg, Germany) using an excitation wavelength of 492 nm and an emission wavelength of 520 nm. The fluorescence was expressed as the percentage of the maximum fluorescence of SYTOX

green and was corrected for background fluorescence (free SYTOX green in solution) using the formula below. Each peptide concentration was repeated in triplicate.

$$\%\ Fluorescence = \frac{(sample\ fluorescence) - (background\ fluorescence)}{(maximum\ fluorescence) - (background\ fluorescence)} \times 100$$

3.3.8) Localisation of peptides

To determine whether Os and Os-C were able to enter intact *E. coli* and *B. subtilis*, cells incubated with fluorescently labelled peptide were observed with confocal fluorescence microscopy. Exponential and stationary phase *E. coli* and *B. subtilis* were adjusted to a cell density of 64x10^6 CFU/mL in NaP buffer. A volume of 90 µL of the cell suspension was exposed to 10 µL of 5FAM-Os, 5FAM-Os-C and 5FAM-buforin II (final concentrations of 7.6 µM) for 2 hours at 37°C in a shaking incubator. Buforin II is a non-membrane acting AMP that is known to cross the cell membrane and was used as a positive control (Park *et al.*, 1998). The bacterial cells were immobilised onto poly-L-lysine coated coverslips which were placed in a 24-well Cellstar polystyrene plate (Greiner Bio-One GmbH, Kremsmünster, Austria). The coverslips were rinsed with NaP buffer, and the cells counterstained with 10 µg/mL DAPI in PBS[a]. The coverslips were rinsed with PBS[a] and mounted on glass slides with polyvinyl alcohol mounting medium with DABCO® (Sigma-Aldrich, Johannesburg, South Africa) and viewed with the Zeiss LSM 510 Meta Confocal Microscope (Carl Zeiss NTS GmbH, Oberkochen, Germany). For visualisation, an excitation wavelength of 490 nm and emission wavelength of 520 nm was used for the 5FAM labelled peptides, and 359nm and 461 nm for DAPI. Images of the two dyes were taken separately and overlaid with the Carl Zeiss AIM LSM imaging software into a single image containing the two colour signals.

3.3.9) Data analysis

Each quantitative assay consisted of three repeats of each concentration, and the experiment was repeated three times. Multiple comparisons were tested by one-way ANOVA followed by the Tukey post hoc test for significant difference between the different peptides. Linear regression fit and comparison of the slopes for statistical significance was done on a scatterplot for the FID assay (Graphpad Prism v6.01, California, USA). Significance was set at $p < 0.05$.

3.4) Results

3.4.1) Peptides alter the ultrastructural morphology of bacterial cells

The effects of Os and Os-C were investigated on *E. coli* and *B. subtilis* membranes with SEM at their respective MBCs. Control bacteria displayed a rough surface with no apparent cellular debris and typical cell shape (Figure 3.1A and E). Mel is a known lytic AMP that causes damage to a wide range of bacterial cell membranes, and was chosen as a positive control (Pandey *et al.*, 2010). Mel caused distinct blebbing of bacterial membranes with no apparent change in cell shape (Figure 3.1B and F). Bacterial cells exposed to Os (Figure 3.1C and G) and Os-C (Figure 3.1D and H) showed a collapse of the cell structure indicated by indentations of the cell membrane.

Three sample preparation methods were used to investigate the effect of Mel, Os and Os-C on *B. subtilis* and *E. coli* with TEM. This was chemical fixation, high pressure freezing and negative staining. Negative staining is an easy and rapid method for single cell suspension samples which may give an indication of membrane effects (Figure 3.2A). This methodology allows the bacteria to be exposed to their respective MBCs, however, it does not allow for high resolution examination of the cells. Chemical fixative or high pressure freezing (HPF) on the other hand, would give more detailed information on any ultrastructural changes. Chemical fixing is a conventional method which makes use of aldehyde-protein cross-links to stabilise cellular structures (Junqueira and Mescher, 2010). However, the process leaves cells with altered membranes, as can be seen in Figure 3.2B. HPF with FS is a newer technique, which results in a much smoother membrane appearance (Figure 3.2C). Therefore, negative staining was used to demonstrate membrane effects at the MBCs and HPF with FS was also used to observe any additional morphological changes.

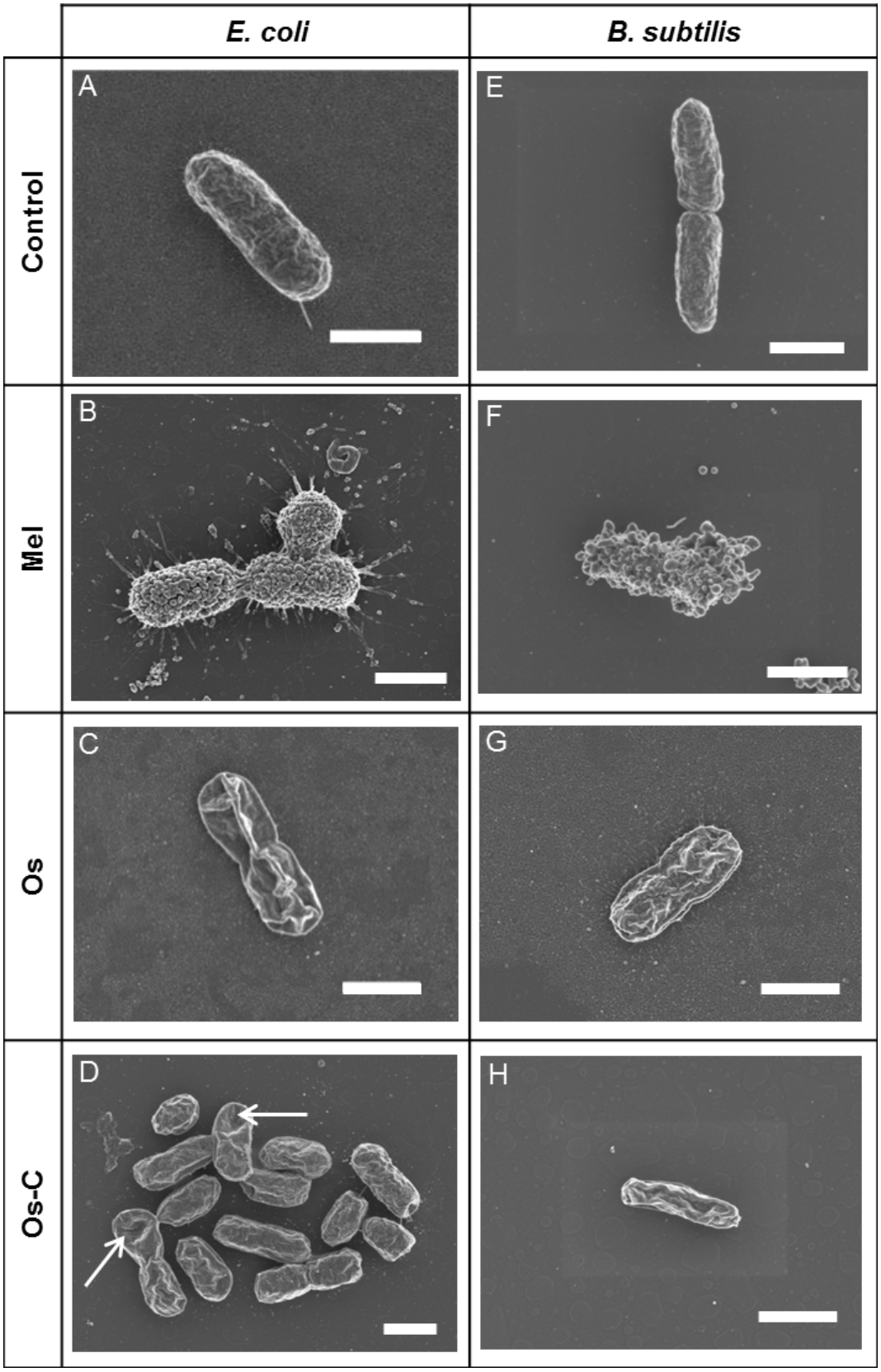

Figure 3.1. Membrane effects of Mel, Os and Os-C on *E. coli* (A – D) and *B. subtilis* (E – H) with scanning electron microscopy after 30 min exposure. A, E) Control, B, F) bacteria treated with 25 µM Mel showing membrane blebbing, C, G) bacteria treated with 0.77 µM Os, D, H) bacteria treated with 1.74 µM Os-C. The arrows in Figure D indicate indentation of the cell membrane. Scale bars = 1 µm.

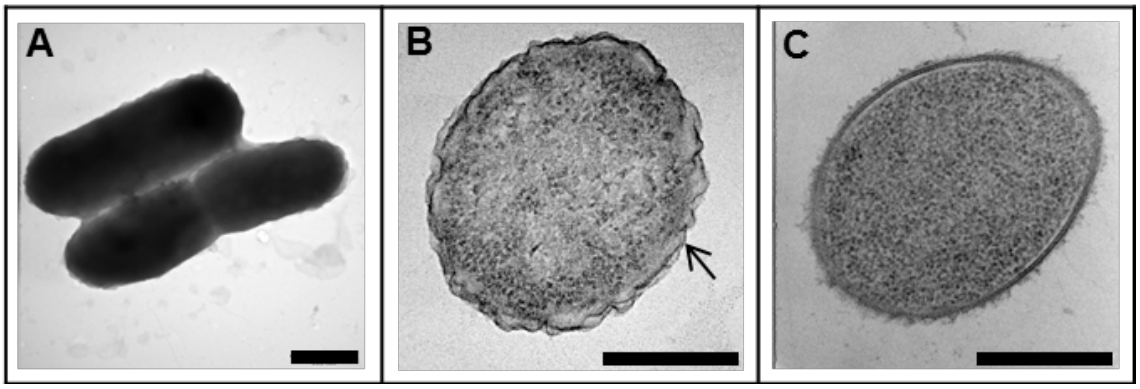

Figure 3.2. Comparison of different sample preparation techniques of *E. coli* control cells for TEM. A) Negative staining, B) chemical fixing, and C) HPF with FS. Arrow indicates altered wavy appearance of the bacterial membrane. Scale bars = 500 nm.

Negative staining revealed control cells with a uniformly electron dense appearance (Figure 3.3A & E). Mel exposed *E. coli* cells presented with membrane blebbing (Figure 3.3B), whereas *B. subtilis* cells showed electron translucent areas within the cell (Figure 3.3F). Os and Os-C caused cytoplasmic retraction in both *E. coli* and *B. subtilis* cells, this was not as clear in *E. coli* exposed to Os (Figure 3.3C, D, G & F).

Using the HPF technique with FS resulted in control cells which showed a regular cell shape with intact cell membranes and a homogeneous cytoplasm (Figure 3.4A & E, 5A & E). The cell content of some of the control cells were slightly pulled away from the cell membrane, due to sample preparation. Mel caused clear intracellular changes and membrane ruffling in both *E. coli* and *B. subtilis* cells (Figure 3.4B & F, 3.5B & F). The cytoplasm of cells exposed to Mel contained electron dense fibres interspersed with electron translucent areas. *E. coli* cells exposed to Os and Os-C generally showed retraction of the intracellular content accompanied by indentation of the cell envelope (Figure 3.4C, D & H). Both Os and Os-C exposed *E. coli* presented with a granulated or more extremely clumped intracellular content (Figure 3.4D & G). A large number of *E. coli* cells also had membrane ruffling (Figure 3.4C, D & G).

B. subtilis cells exposed to Os showed cytoplasmic retraction and the intracellular content appeared granulated (Figure 3.5C & G). Cells exposed to Os-C also presented with granulated or clumped cytoplasm, but only a small number of cells showed cytoplasmic retraction (Figure 3.5D & H).

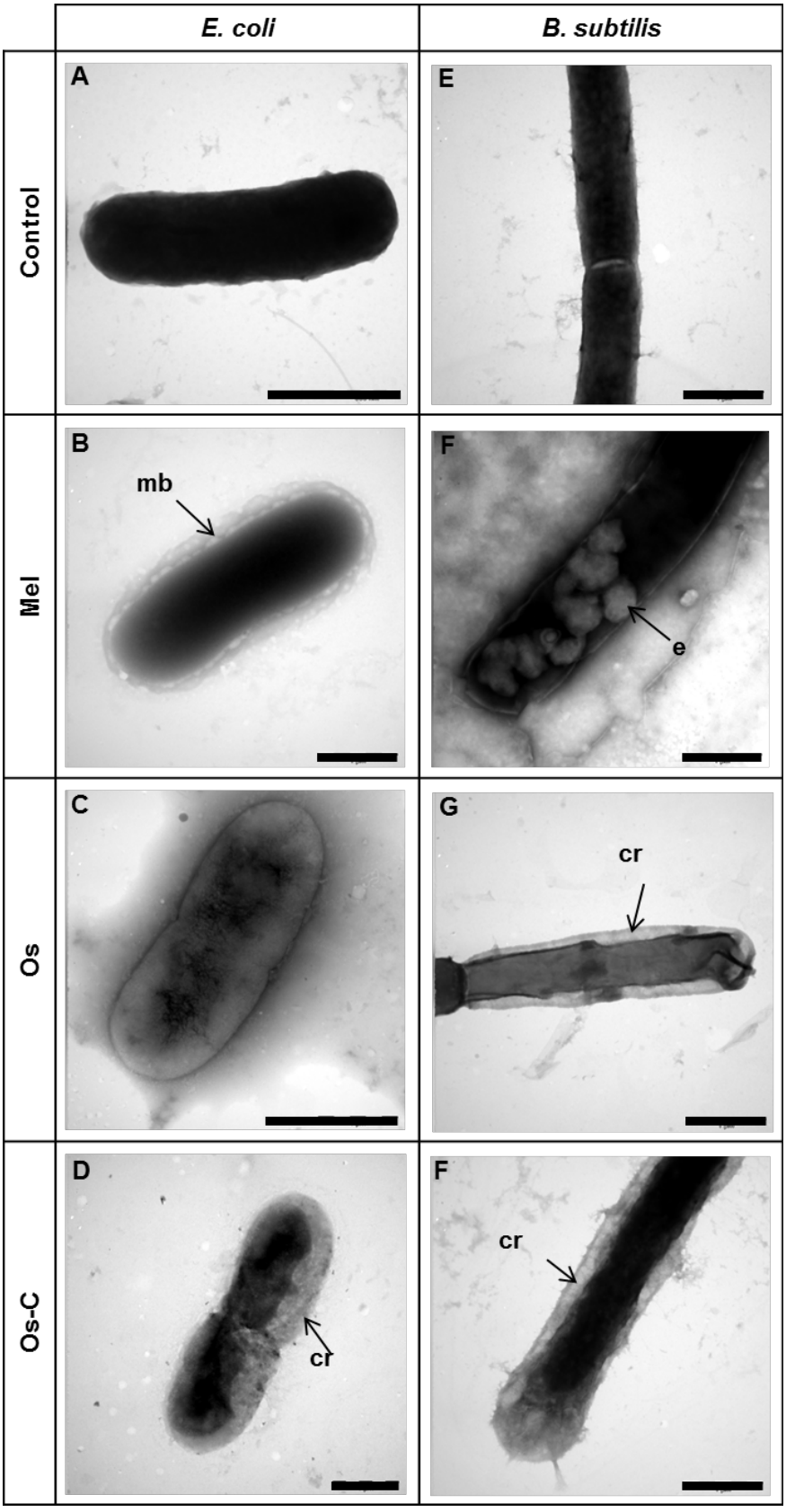

Figure 3.3. TEM of negatively stained *E. coli* (A – D) and *B. subtilis* (E – F) exposed to MBCs of Mel, Os and Os-C for 10 min. A, E) Control, B, F) 25 µM Mel, C, G) 0.77 µM Os, D, H) 1.74 µM Os-C. cr) cytoplasmic retraction, e) electron translucent area, mb) membrane blebbing. Scale bars = 1 µm.

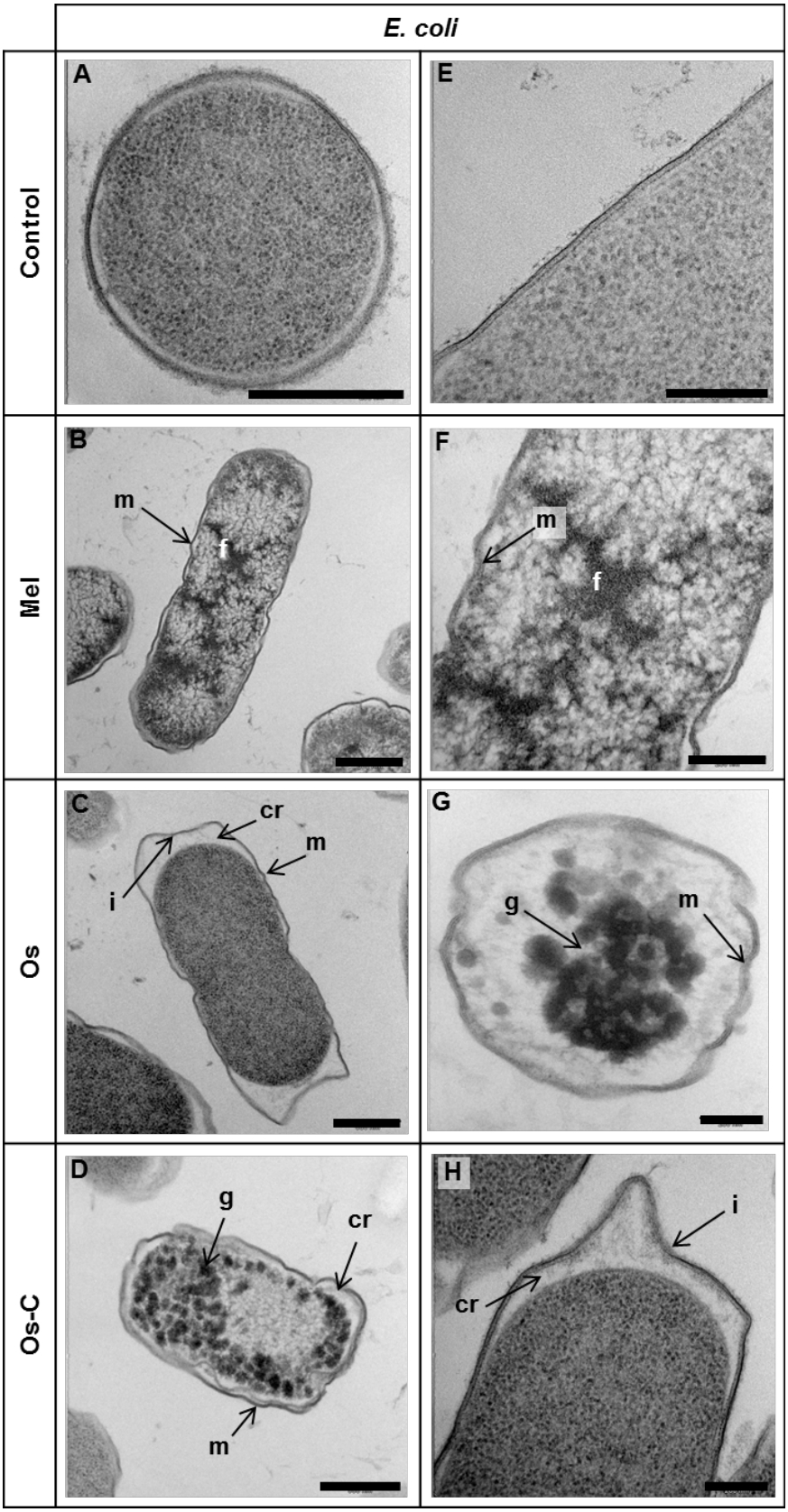

Figure 3.4. Ultrastructure of high pressure frozen *E. coli* exposed to 2 µM Mel, Os and Os-C for 10 min. A, E) Control, B, F) Mel, C, G) Os, D, H) Os-C. cr) cytoplasmic retraction, f) electron dense fibres, g) intracellular granulation, i) indentation of cell envelope, m) membrane ruffling. Scale bars A – D) 500 nm, E – H) 200 nm.

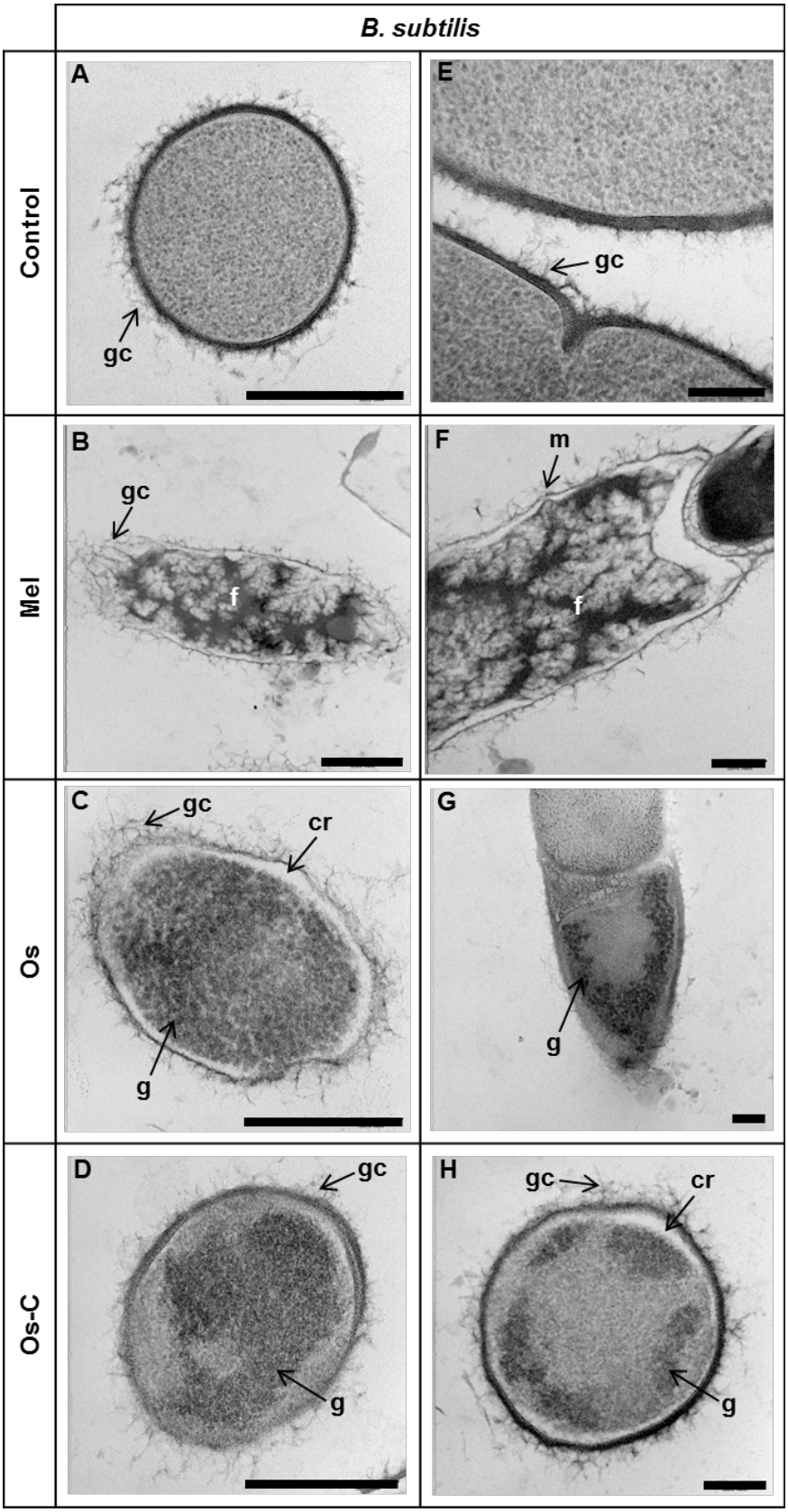

Figure 3.5. Ultrastructure of HPF *B. subtilis* exposed to 2 µM Mel, Os and Os-C for 10 min. A, E) Control, B, F) Mel, C, G) Os, D, H) Os-C. cr) cytoplasmic retraction, f) electron dense fibres, g) intracellular granulation, gc) glycocalyx, m) membrane ruffling. Scale bars A – D) 500 nm, E – H) 200 nm.

3.4.2) Membrane permeabilisation by peptides

SYTOX green is an unsymmetrical cyanine dye unable to enter intact cell membranes and its fluorescence increases significantly when bound to nucleic acids (Roth *et al.*, 1997). If the integrity of the cell membrane is compromised following exposure to the peptides, SYTOX green can enter the bacteria and bind to nucleic acids resulting in an increase in fluorescence emission. Compared to the control (no peptide) an increase in SYTOX green influx was observed for Mel exposure at a concentration of 1 µM and lower in both *E. coli* and *B. subtilis* cells (Figure 3.6). Os caused an increase in membrane permeability of *E. coli* cells only at 0.2 µM (concentration 3.9 fold lower than MBC of 0.77 µM) and of *B. subtilis* cells at 0.2 µM and 0.5 µM (concentration 1.5 fold lower than MBC). Os-C caused significant permeabilisation of both bacterial membranes at sub-inhibitory concentrations of 0.1 µM and 0.2 µM, 17.4 and 8.7 fold lower than the MBC (1.74 µM), respectively. The permeabilisation observed at 0.2 µM for both Os and Os-C was significantly lower than Mel in both bacteria. In *B. subtilis* cells, Os caused more permeabilisation than Os-C at a concentration of 0.5 µM. Neither Os nor Os-C caused significant permeabilisation ($p > 0.05$) at the concentrations spanning the MBCs in *E. coli* or *B. subtilis* cells (Figure 3.6). For all peptides at higher concentrations, the SYTOX green uptake decreased significantly below that of the control. This decrease was much more pronounced in the 5 and 10 µM concentrations of Os than the equivalent Os-C concentrations. Os also caused a decrease in fluorescence significantly lower than that of Mel at 10 µM in both *E. coli* and *B. subtilis*.

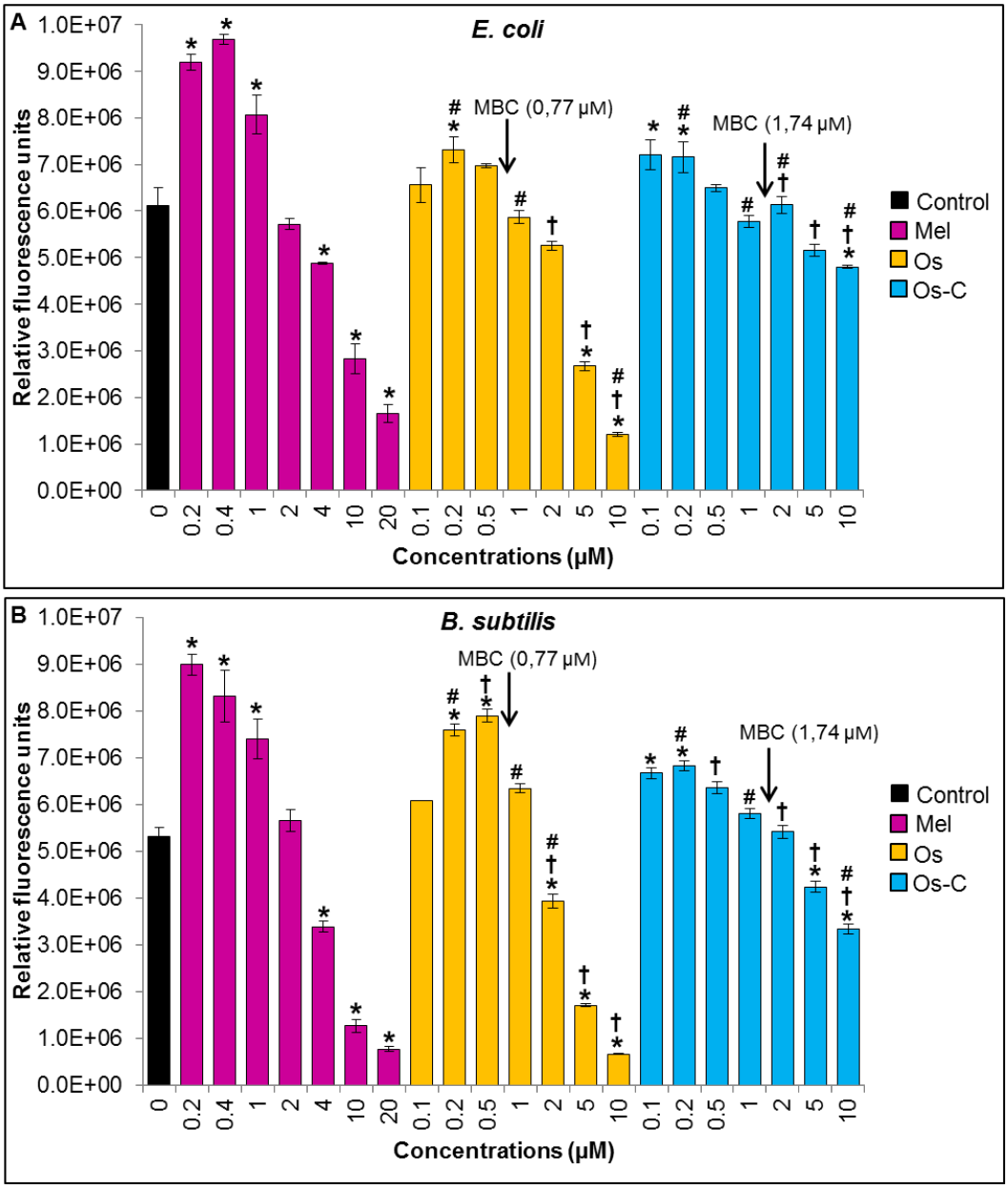

Figure 3.6. Membrane permeabilisation of A) *E. coli* and B) *B. subtilis* exposed to Mel, Os and Os-C for 1 hour. Permeabilisation was measured as an increase in SYTOX green fluorescence (relative fluorescence units) after addition of the peptides. Error bars represent the SE of three independent experiments, n = 9. Asterisks indicate significant difference to the control ($p < 0.01$), crosses indicate significant difference between corresponding concentrations of Os and Os-C, hash indicates significant difference to the same concentration of Mel ($p < 0.05$). Arrows indicate the minimum bactericidal concentrations (MBC) of Os and Os-C.

In order to visualise membrane permeabilisation and the effect of Os and Os-C on bacterial viability in the stationary phase of growth, a combination of fluorescent dyes was used. The triple stain enables the simultaneous viewing of total, viable, as well as cells with altered membrane permeability. CTC stains viable cells (red), DAPI (blue) stains all DNA and FITC (green) only stains cells with permeabilised membranes (Mangoni *et al.*, 2004). Control cells of both *E. coli* and *B. subtilis* showed no permeabilisation, and most of the cells fluoresced red, which indicated viability (Figure 3.10A and 3.8A). Cells exposed to 2.5 µM Mel had permeabilised membranes, with cells that were not viable (Figure 3.7B and 3.8B). Cells exposed to sub-lethal concentrations (10 times lower than MBC) of Os (Figure 3.7C and 3.8C) and Os-C (Figure 3.7E and 3.8E) had permeabilised membranes and viable cells, while at the MBCs only a few viable cells were present (Figure 3.7D & F and 3.8D & F). The peptides also seemed to cause a higher degree of cellular clumping than observed in the control cultures.

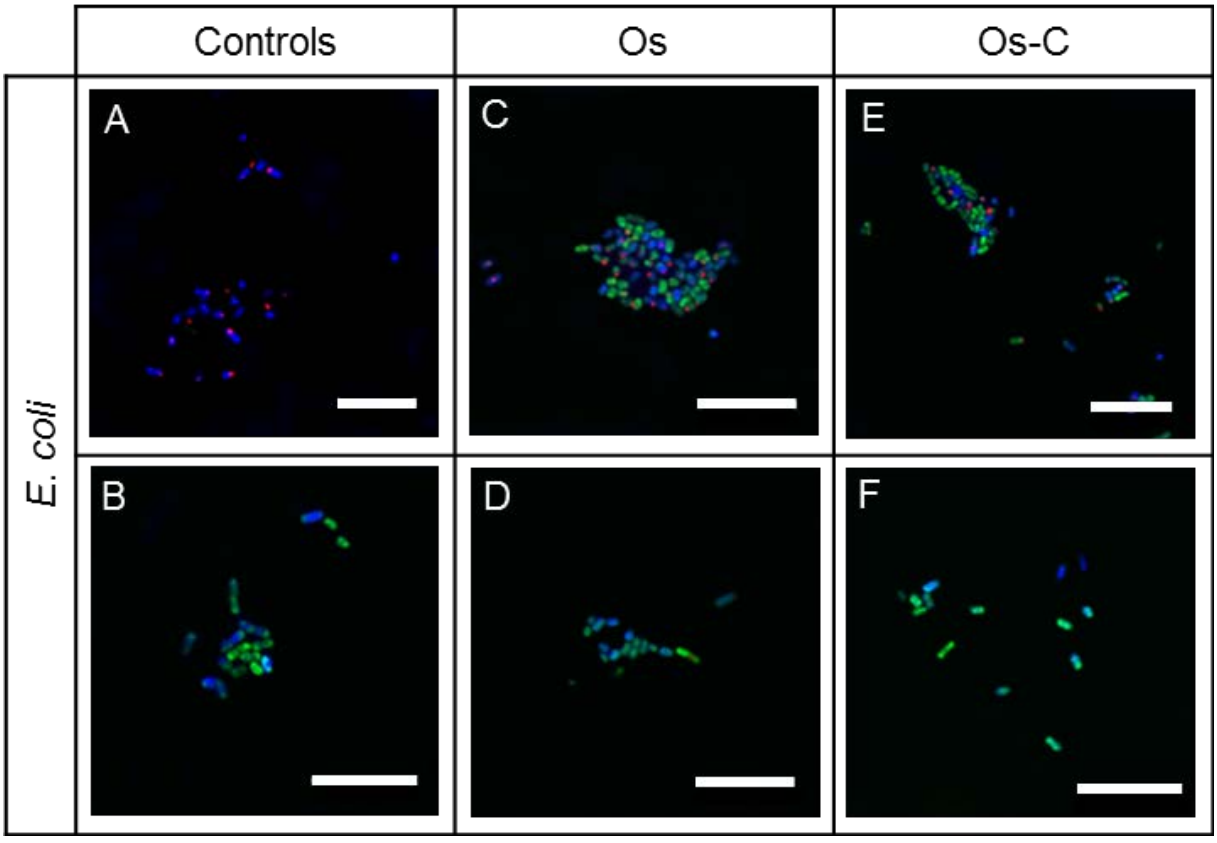

Figure 3.7. *E. coli* in the stationary phase of growth exposed to Mel, Os and Os-C for 10 min. Cells were stained with DAPI (blue) which stains all DNA, CTC (red) which indicates viability, and FITC (green) which indicates permeabilised membranes. A) Control, B) 2.5 µM Mel, C) 0.077 µM Os, D) 0.77 µM Os, E) 0.174 µM Os-C, F) 1.74 µM Os-C. Scale bars = 10 µM.

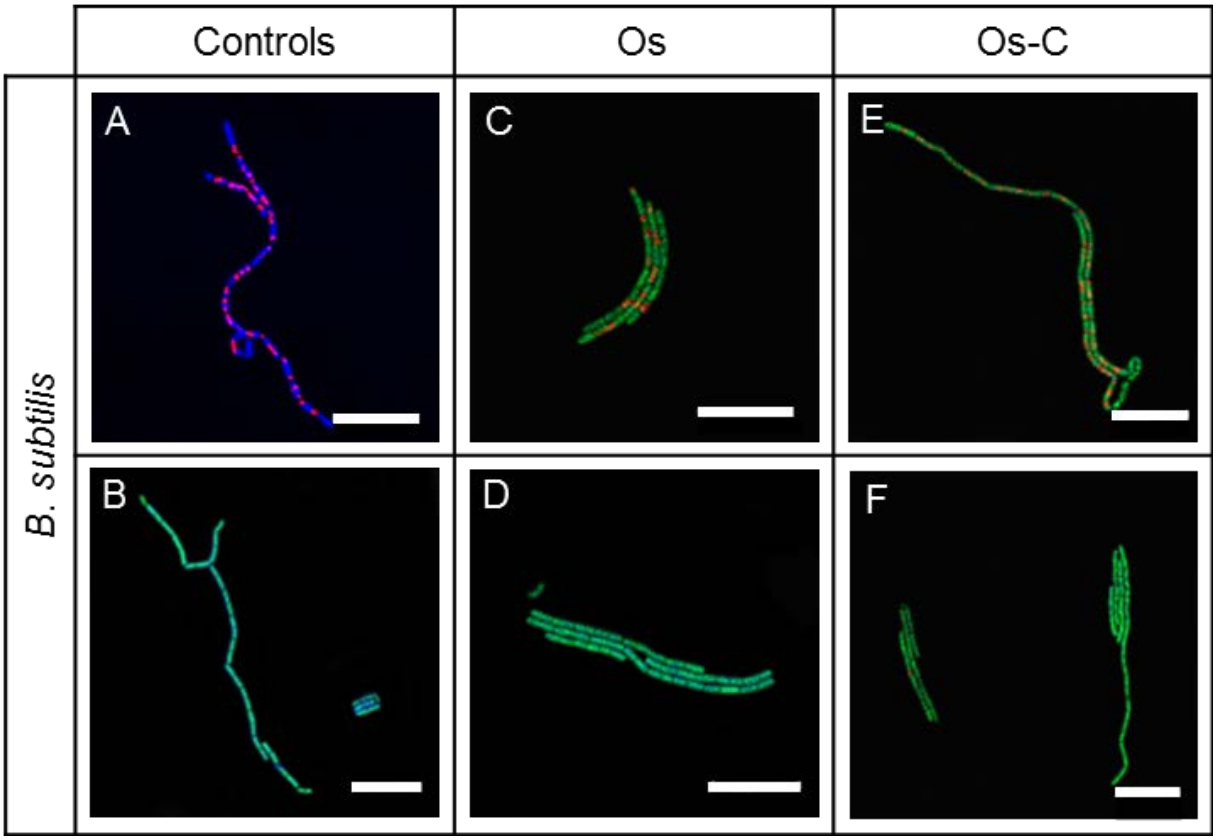

Figure 3.8. *B. subtilis* in the stationary phase of growth exposed to Mel, Os and Os-C for 10 min. Cells were stained with DAPI (blue) which stains all DNA, CTC (red) which indicates viability, and FITC (green) which indicates permeabilised membranes. A) Control, B) 2.5 µM Mel, C) 0.077 µM Os, D) 0.77 µM Os, E) 0.174 µM Os-C, F) 1.74 µM Os-C. Scale bars = 10 µM.

3.4.3) Peptides bind plasmid DNA

The gel retardation assay was used to determine whether peptides bind to plasmid DNA (pBR322 vector from *E. coli*). Ionic interactions between the cationic peptide and plasmid DNA reduce the charge on the plasmid and subsequently the migration is retarded. Peptide binding can also cause quenching of plasmid dye fluorescence or may cause the transformation of supercoiled plasmid DNA to the open circular and linear forms as an indication of DNA damage (Ueda *et al.*, 1985, Ehrenfeld *et al.*, 1987, Lewis *et al.*, 1988). The plasmid DNA is in a supercoiled form before exposure. A single-strand break results in a relaxed circular form of DNA, and a double strand break results in a linear form of DNA (Wei *et al.*, 2006). These three forms of DNA migrate at different rates in a gel, and would be seen as bands at different locations. Most supercoiled DNA samples contain some degree of circular DNA depending on the batch (Wei *et al.*, 2006). This can be seen in the negative control in Lane 1 of Figure 3.9 which featured both Band A and a light Band B. Plasmid in Lane 2 and 3 were exposed to 2.5 mM and 5 mM AAPH, respectively. This resulted in an

increase in the amount of circular or linear DNA observed as Band B with a much higher intensity than the control as measured with ImageJ ($p < 0.05$) and Band A disappeared (Wei *et al.*, 2006). The average intensity value for each Band is presented in Table 3.2.

Several studies report the interaction between plasmid DNA and peptide as weight ratios, whereas charge ratios as used in this study would provide a correct stoichiometric indication of the interaction that occurs. In order to compare the present findings to other studies, the weight ratios were also reported. The migration position of the plasmid DNA was unaltered, and remained supercoiled following exposure to Mel at a charge per pmol ratio of 1:0.2 (pDNA:peptide) (Lane 4) as compared with the control in Lane 1 (Figure 3.9). Exposure to Mel at a charge ratio of 1:0.8 resulted in the formation of an additional band, Band C, close to the well (Lane 5) which indicated bound DNA, and a significantly lower intensity of Band A as compared with the control ($p < 0.01$). In Lane 6 (Mel 1:1.6) and Lane 7 (Mel 1:8.3), Bands A and B were absent and only Band C was present. Os had an effect on plasmid DNA at all concentrations, forming a light Band C with Bands A and B at charge ratios of 1:0.1 (Lane 8) and 1:0.5 (Lane 9). There was a marked decrease in intensity of Band A in Lane 10 ($p < 0.01$), and disappearance of all bands in Lane 11 (1:5). Os-C had no effect on plasmid structure at charge ratios of 1:0.1 and 1:0.5 (Lane 12 and 13). However, at charge ratios of 1:1 and 1:5 there was a decrease or loss of Band A and formation of Band C (Lane 14 and 15).

	pDNA	Melittin				Os				Os-C			
Weight ratio	**1:**	0.3	1.4	2.8	14.2	0.1	0.6	1.2	6.1	0.1	0.5	1	5.4
Charge ratio	**1:**	0.2	0.8	1.6	8.3	0.1	0.5	1	5	0.1	0.5	1	5

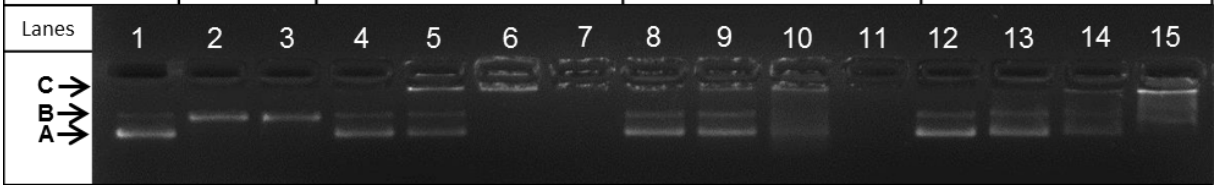

Figure 3.9. pBR322 vector from *E. coli* exposed to AAPH, Mel, Os and Os-C on an agarose gel stained with GelRed. 1) ddH_2O, 2) 2.5 mM AAPH, 3) 5mM AAPH, 4) 1 µM Mel, 5) 5 µM Mel, 6) 10 µM Mel, 7) 50 µM Mel, 8) 0.5 µM Os, 9) 2.5 µM Os, 10) 5 µM Os, 11) 25 µM Os, 12) 0.5 µM Os-C, 13) 2.5 µM Os-C, 14) 5 µM Os-C, 15) 25 µM Os-C. A) Supercoiled pDNA, B) circular / linear pDNA, C) bound pDNA. The weight ratio and charge per pmol ratio of pDNA:peptide is indicated above the corresponding Lanes 4 – 15.

Table 3.2. Intensity values of bands on the agarose gel in Figure 3.9 as measured with ImageJ.

	Control	AAPH (mM)		Mel (µM)				Os (µM)				Os-C (µM)			
		2.5	5	1	5	10	50	0.5	2.5	5	25	0.5	2.5	5	25
Lanes:	**1**	**2**	**3**	**4**	**5**	**6**	**7**	**8**	**9**	**10**	**11**	**12**	**13**	**14**	**15**
Band C	-	-	-	-	124.4	112.3	80.3	76.7	86.9	91.8	-	-	-	66.5	141.5
Band B	63.2	101.7*	93.5*	63.2	62.2	-	-	71.8	74	63.1	-	67	70.2	57.9	73.9
Band A	120.4	-	-	90.3	74.5*	-	-	102.6	100.2	67.3*	-	104.6	92	63.1*	-

Values are the average of 6 measured points for each band. Asterisks indicate significant difference to the control, - indicates absence of a band.

The FID assay was used to better quantify the ability of the peptides to bind to pDNA and displace bound SYTOX green. A decrease in fluorescence is an indication of the amount of displaced SYTOX green, and thus the DNA binding capacity of the peptide. The concentrations of Os and Os-C used were chosen to correspond with the pDNA:peptide ratios used in the gel retardation assay. At 5 µM, Mel, at a charge ratio of 1:1 did not displace SYTOX green while at 25 µM (charge ratio of 1:8.3, Figure 3.10A), the percentage fluorescence was reduced by 75%. Os displaced 50% of the intercalator at 5 µM, a pDNA:peptide charge ratio of 1:1, and at 25 µM (ratio of 1:5), 76.4% of the intercalator was displaced. Both Mel and Os showed a dosage dependant increase in displacement (Figure 3.10B). The dose-effect was confirmed by a linear fit with an R^2-value of 0.97 (slope -2.785) for Mel. Os showed a logarithmic decrease in fluorescence ($R^2 = 0.9777$), showing that lower concentrations of Os were able to displace a higher ratio of SYTOX per molecule than higher concentrations of peptide. Os-C caused the lowest amount of displacement, ranging between 23.5% and 36.4% for all concentrations tested. No dosage effect was observed for Os-C. From the line equations it could be calculated that 19.34 and 6.68 µM, Mel and Os respectively displaced 50% SYTOX green.

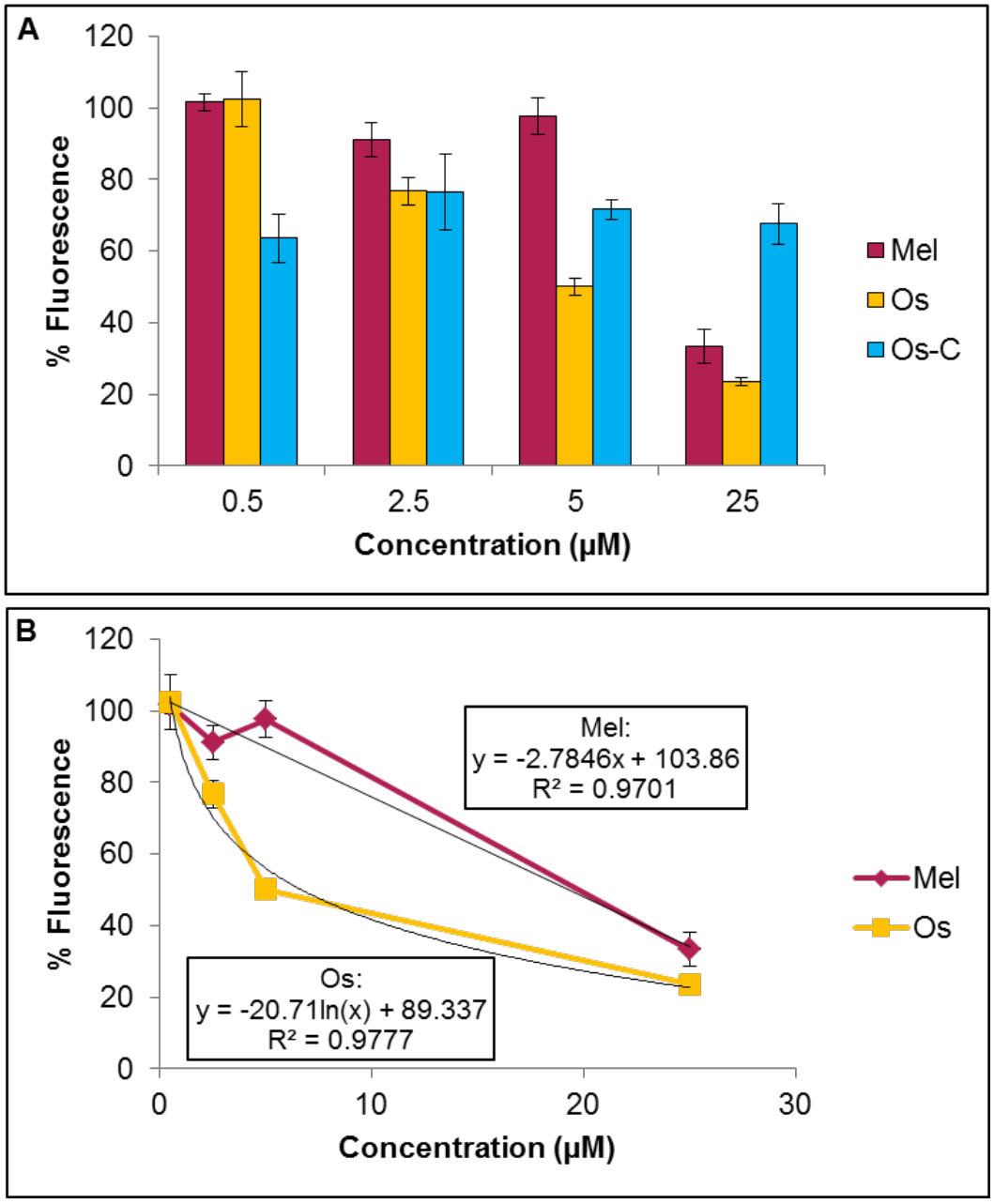

Figure 3.10. FID assay on pBR322 vector from *E. coli* exposed to 0.5 – 25 µM Mel, Os and Os-C for 1 hour. A) Bar chart, B) line fit curve showing dosage effect for Mel and Os. Data was expressed as a percentage of the untreated sample ± standard deviation of three repeats, n = 3.

3.4.4) Localisation of peptides

To determine whether the peptides are able to cross membranes, both exponential and stationary phase bacteria cells were exposed to fluorescently labelled Os, Os-C and buforin II. The peptides were labelled at the N-terminal with the fluorescent molecule 5FAM which fluoresces green. The cells were counterstained with DAPI which fluoresces blue. Cells exposed to buforin II showed green fluorescence consistent with a cell-penetrating peptide (Figure 3.11A & D, 3.12A & D) (Park *et al.*, 1998, Park *et al.*, 2000). Cells exposed to labelled Os and Os-C also fluoresced green (Figure 3.11B, C, E and 3.12B, C, E & F), except for stationary phase *E. coli* cells exposed to Os-C (Figure 3.11F). In the presence of Os-C some of the septa of *B. subtilis* cells were stained, while in other cells the entire cell stained green (Figure 3.12C & F and 3.13).

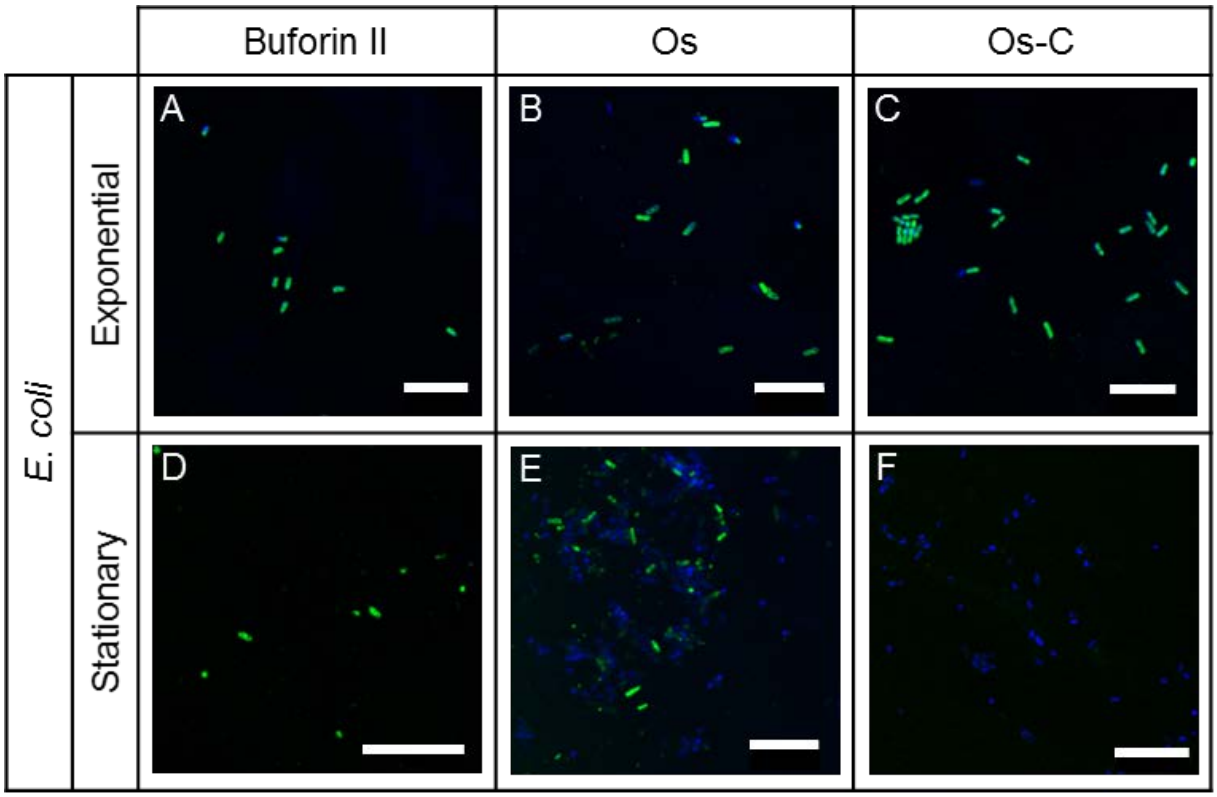

Figure 3.11. Localisation of 5FAM labelled peptides in *E. coli* in exponential (A – C) and stationary phase (D – F) after 2 hours. Exposed to 7.6 µM A, D) 5FAM-buforin II, B, E) 5FAM-Os and C, F) 5FAM-Os-C (green) and counter stained with DAPI (blue). Scale bars = 10 µm.

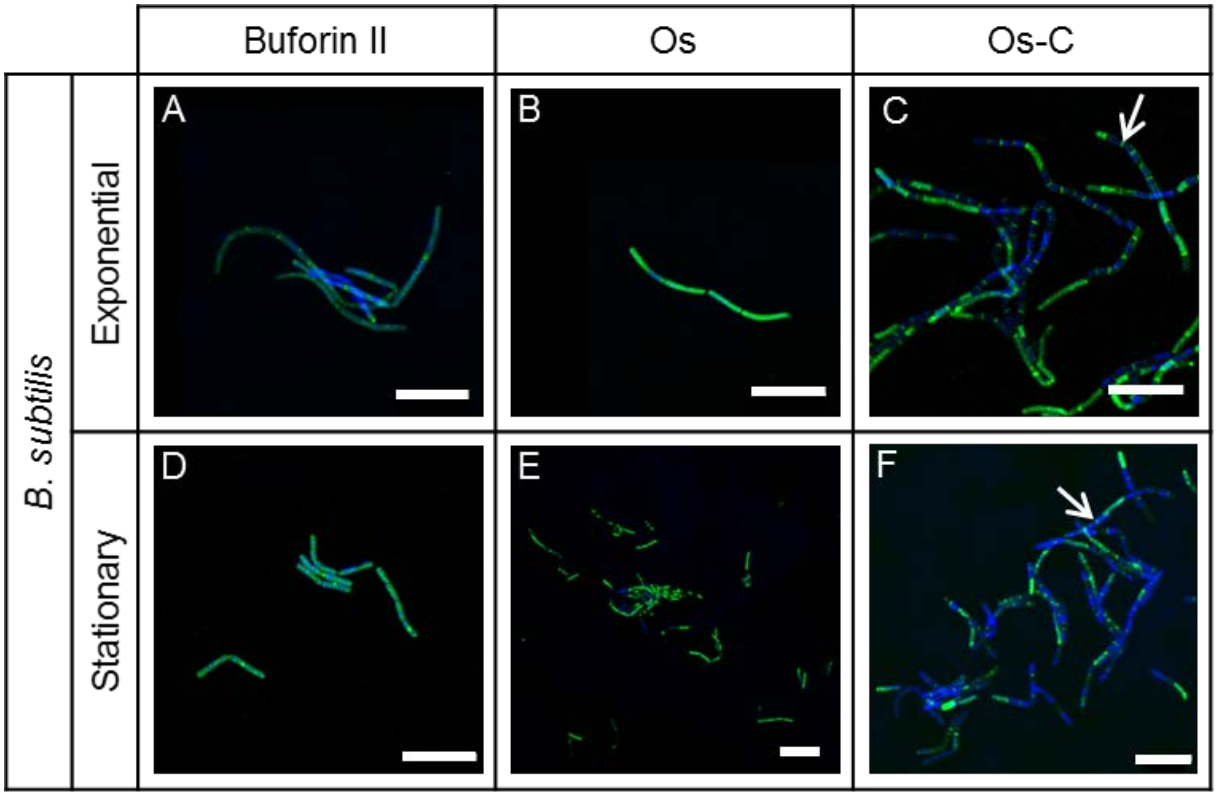

Figure 3.12. Localisation of 5FAM labelled peptides in *B. subtilis* in exponential (A – C) and stationary phase (D – F) after 2 hours. Exposed to 7.6 µM A, D) 5FAM-buforin II, B, E) 5FAM-Os, and C, F) 5FAM-Os-C (green) and counter stained with DAPI (blue). Arrows indicate stained septa in B. subtilis. Scale bars = 10 µm.

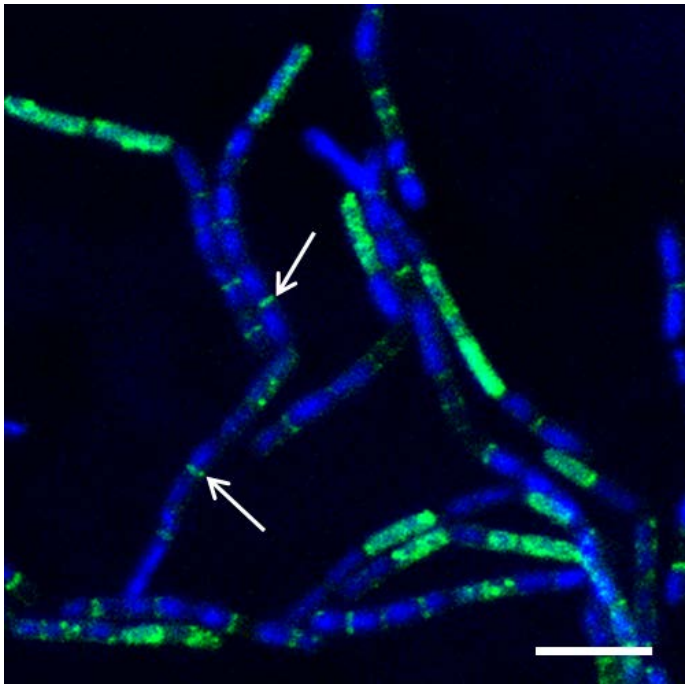

Figure 3.13. Labelling of septa of *B. subtilis* cells in the stationary phase by 5FAM-Os-C after 2 hours exposure. Exposed to 7.6 µM 5FAM-Os-C (green) and counter stained with DAPI (blue). Arrows indicate stained septa. Scale bar = 5 µm.

3.5) Discussion

The peptides under investigation were previously found to be active against both Gram-positive and Gram-negative bacteria, whereas the original peptide OsDef2 was only active against Gram-positive bacteria (Prinsloo *et al.*, 2013). The authors also found that Os-C had a slower killing rate than Os suggesting a different mode of action (Prinsloo *et al.*, 2013). The focus of the present study was to investigate the mode of action of peptides Os and Os-C on Gram-positive *B. subtilis* and Gram-negative *E. coli* bacteria. More specifically, to determine whether Os and Os-C are membrane acting, and/or have additional intracellular targets such as the ability to bind DNA.

SEM results indicated that the cellular content of *E. coli* and *B. subtilis* cells was lost and this results in the collapse of cellular structure indicated by indented membranes and cells which appeared flattened and empty. In contrast to cells exposed to Mel, no membrane blebbing was observed on bacterial cells exposed to either Os or Os-C. This is evidence that the mechanisms of action for these peptides are different from Mel. The nucleoid was not visible in the HPF controls as observed with TEM. However, the formation of electron dense fibres in the Mel exposed bacterial cells is reminiscent of the nucleoid structure observed in chemically fixed bacteria. Therefore, it is likely that the cells exposed to Mel were under enough stress to cause DNA damage. Mel also caused membrane blebbing of *E. coli* cells as observed with negatively stained TEM samples, at the same concentrations as used for SEM. HPF samples exposed to Mel, and some Os and Os-C exposed samples caused membrane ruffling. Meincken *et al.* (2005) previously found an increase in the membrane roughness of *E. coli* cells exposed to Mel. The authors attributed this membrane roughness to an increase in the surface area of the membrane, after Mel incorporation into the outer membrane of the bacterial cell (Meincken *et al.*, 2005). The ruffled appearance observed in the present study may similarly be caused by peptide integration into the membrane. In recent years there has been an increase in research on programmed cell death in bacteria. Dewachter *et al*. (2015) describe programmed cell death in *E. coli* cells with a mutation in the ObgE gene with similar features to eukaryotic apoptosis. Expression of the mutant protein resulted in loss of membrane potential, DNA condensation and fragmentation, translocation of phosphatidylserine to the outer membrane and membrane blebbing (Dewachter *et al*. 2015). Membrane blebbing observed after exposure to Mel in the current study may be caused by triggering of programmed cell death in *E. coli* and *B. subtilis*. However, this needs

to be confirmed with biochemical assays similar to those used to investigate eukaryotic apoptosis.

The morphology of cells exposed to Os and Os-C was different to that of cells exposed to Mel, suggesting a different mode of action. TEM revealed that Os and Os-C caused membrane indentation and the cytoplasm was pulled away from the cell envelope. This correlates with the SEM results which showed indentations and collapse of the cell structure after exposure to Os and Os-C. The cytoplasmic retraction observed in *E. coli* is similar to cells undergoing plasmolysis in a hyperosmotic environment (Cota-Robles, 1963, Bayer, 1967). Pilizota and Shaevitz (2013) found that solutes unable to freely penetrate the outer membrane did not cause plasmolysis, but rather caused a complete shrinkage of the cell. Only solutes that were outer membrane permeable caused plasmolysis as a result of the difference in osmotic pressure between the cytoplasm and periplasmic space (Pilizota and Shaevitz, 2013). It is therefore possible that Os and Os-C acts only on the outer, but not the inner membrane of Gram-negative bacteria, resulting in an influx of extracellular fluids into the periplasmic space. SEM also revealed *B. subtilis* cells with reduced size after exposure to Os and Os-C. This is indicative of cell shrinkage rather than cell swelling.

The SYTOX green assay is a commonly used method which measures permeabilisation of the inner membranes of bacteria (Aragão *et al.*, 2008). Mel caused permeabilisation of both *E. coli* and *B. subtilis* cells at 1 µM concentration and lower. Os and Os-C caused permeabilisation at concentrations below 0.5 µM. However, this was significantly less permeabilisation than Mel at equivalent concentrations. Os and Os-C caused no significant increase in permeabilisation at concentrations spanning the MBCs of each peptide. It was previously observed that cells which were permeabilised by an AMP but were not lysed showed a low level of SYTOX green fluorescence as compared with cells which were lysed (Roth *et al.*, 1997). It is therefore possible that Os and Os-C permeabilised the cells without causing lysis. This is supported by the triple staining results which indicate membrane permeabilisation to FITC. At higher concentrations above 1 µM of Mel, Os and Os-C, the SYTOX green signal decreased to well below that of the control. DNA fragmentation and/or degradation caused by the bactericidal effects of the peptides may lead to a decrease in SYTOX green binding which in turn leads to a decrease in fluorescence. Alternatively, the peptides may translocate into cells, bind to DNA and compete with SYTOX green for binding sites, which will also lead to a decrease in, or quenching of fluorescence. This was observed with the FID assay, which showed displacement of bound SYTOX green after exposure to the peptides. For Mel and Os a dosage dependent decrease in SYTOX green fluorescence

was measured. The binding ability of Os was 3 fold greater than Mel. Although Os-C did bind plasmid DNA, the observed effect was not dosage dependent.

During infection, bacteria often encounter less than desirable conditions and periods of limited growth are common (Kolter *et al.*, 1993, Mascio *et al.*, 2007). Treatment of infections with antibiotics is often not effective against non-multiplying populations of bacteria and may lead to clinical relapse of the infection (Coates *et al.*, 2002). It is therefore important to determine the activity of a possible antibiotic against non-multiplying or slow multiplying bacteria. For this reason, the effect of Os and Os-C on stationary phase bacteria was also investigated.

Ten-minute exposure to Mel caused membrane permeabilisation and associated loss of viability of *E. coli* and *B. subtilis* cells in the stationary phase, as seen with fluorescent triple staining. High concentrations of Os and Os-C caused membrane permeabilisation with only a few viable cells remaining while low concentrations of Os and Os-C, the peptides caused sufficient membrane permeabilisation to allow the penetration of the non-permeable fluorescent dye fluorescein, while the cells remain viable. In contrast to this, 5FAM-labelled Os-C was unable to enter stationary phase *E. coli* cells. It is possible that the concentration used was too low to allow penetration of the peptide, as the MBCs for the labelled peptide were unknown. However, this is another indication that Os-C has lower activity than Os. The triple staining results indicated that the peptides may act on intracellular targets prior to the killing of bacteria. Using the triple staining method, the peptide temporin-L was previously also found to cause membrane permeabilisation without cell death. The authors concluded that the mechanism of bacterial killing of temporin-L differs at low and high concentrations, and at low concentrations might have intracellular targets (Mangoni *et al.*, 2004). Furthermore, cellular clumping was observed in bacterial cultures exposed to Os and Os-C. Some AMPs were found to cause bacterial clumping or agglutination, which was necessary for bacterial killing (Torrent *et al.*, 2012). Similarly, Os and Os-C may be forming aggregates on the bacterial cell surface, which leads to agglutination of bacteria. It is possible that the peptides may aggregate on the bacterial cell surface, where interaction between the positive peptides and the negatively charged surface components causes partial neutralisation of charge. Consequently this would cause a disruption of the outer membrane, or cell wall, which would allow entry of the peptides into the cell (Zhao, 2003, Hancock and Sahl, 2006). The addition of a large fluorescent label to a small peptide may change the amphipathic balance of the peptide and therefore the membrane interaction and possibly the mode of action. The labelled peptides were confirmed to retain activity (results not shown). However, these results need to be confirmed by a different method.

The DNA retardation assay revealed that Mel, Os and Os-C caused the inhibition of pDNA migration at charge ratios (pDNA:peptide) close to or above 1:1. The positively charged peptides most likely formed ionic bonds with the negatively charged DNA. The migration of the DNA:peptide complex will be less than the DNA alone. This resulted in the formation of an additional band below the well. In some of the cases, the plasmid DNA stayed partially within the well, or did not migrate indicating complete neutralisation of charges on the DNA, e.g. 25 µM Mel and Os. SYTOX green results showed a more pronounced decrease in fluorescence for Os than for Os-C at 5 µM and 10 µM. This, the absence of pDNA at 10 µM and the higher degree of intercalator displacement suggested that Os binds more effectively to DNA than Os-C. Buforin II is a non-membrane acting AMP, which has been shown to have a high affinity for DNA and RNA (Park *et al.*, 2000). Buforin II was previously found to bind pDNA at a weight ratio of above 1:0.25 (pDNA:peptide) (Park *et al.*, 1998). Another AMP, indolicidin, has been shown to cause membrane permeabilisation without cell lysis, and to have possible intracellular targets through which it kills bacteria (Hsu *et al.*, 2005). Indolicidin retarded the movement of DNA at pDNA:peptide weight ratios of above 1:0.2 (Hsu *et al.*, 2005). Os starts to cause pDNA retardation at weight ratios above 1:0.2 and Os-C above 1:1, as seen by the formation of Band C. When comparing the weight ratios, it appears that Os-C binds less tightly to pDNA than buforin II and indolicidin, while Os binds at the same weight ratio. The binding phenomena observed with both the gel retardation and FID assays is most probably the reason for the decrease in SYTOX green fluorescence in the membrane permeabilisation assay observed for *E. coli* and *B subtilis* at high concentrations of Mel and Os while only a minor decrease in fluorescence was observed for Os-C. The difference in binding observed between Os and Os-C is not purely a charge effect, as the net charge of the two peptides are the same. The ability of Os to bind pDNA is not due to the presence of Cys residues as Mel, buforin II and indolicidin lack Cys residues.

To be able to alter the functioning of an intracellular target, peptides need to cross the cell membrane. Fluorescently labelled peptides which are purely membrane acting will show fluorescence only on the membrane. This result was observed in a study done by Park *et al.* in 2000, where a fluorescently labelled analogue of buforin II was observed on the cell surface, without entering the cell unlike the original fluorescently labelled buforin II. In the present study, fluorescence was observed throughout entire cells, indicating the ability of these peptides to cross membranes of both *E. coli* and *B. subtilis.* Labelled Os and Os-C was observed in both stationary and exponential phase cells, except for stationary phase *E. coli* exposed to Os-C. This is an indication that Os-C is unable to affect *E. coli* cells which are dormant. Some septa of *B. subtilis* cells showed green fluorescence, with the adjacent

cells not labelled, while other cells were completely filled. However, no morphological changes to the septa were observed with TEM. The peptides PR-26 (Shi *et al.*, 1996a), PR-39 (Shi *et al.*, 1996b), indolicidin (Subbalakshmi and Sitaram, 1998) and microcin (Salomon and Farías, 1992) were previously found to cause filamentation which may be caused by the inhibition or alteration of membrane proteins required for septum formation (Brogden, 2005). Sochaki and colleagues (2011) observed that fluorescently labelled LL-37 more readily entered *E. coli* cells at the septal regions of dividing cells. However, the research group did not find any evidence for LL-37 preference to septating *B. subtilis* cells (Barns and Weisshaar, 2013). Rapidly dividing *B. subtilis* cultures often lead to the formation of strings of cells as a result of slow septum degradation (Graumann, 2012). As a result of this, the septa of *B. subtilis* cells are visible for a longer time-period than that of *E. coli*. It is possible that Os-C accumulates on *E. coli* septa as well, although it is not observed with the current methodology. The septum peptide accumulation might indicate that Os-C either gains entry into the periplasmic space via the septal region, or that Os-C may have an effect on the function of the cytoplasmic membrane proteins of the septa of *B.subtilis*. Further studies are necessary to elucidate this septal effect.

3.6) Conclusion

Both Os and Os-C caused a collapse of the cell structure and granulation of the intracellular contents of *E. coli* and *B. subtilis* cells. Fluorescently labelled peptides were able to cross membranes. TEM reveals that both peptides may insert into cell membranes causing permeabilisation. Differences between Os and Os-C was that Os more effectively bound pDNA, fluorescently labelled Os-C accumulated on the septa of *B. subtilis* and was unable to penetrate stationary phase *E. coli* cells. These observed differences may account for the differences in killing times especially of *B subtilis* although ultrastructural findings are that the consequence of exposure is similar especially when compared to Mel.

Chapter 4: Effect of Os and Os-C on human blood cells

4.1) Abstract

Os and Os-C effectively kills bacteria, however, to develop these AMPs as therapeutic agents it is necessary to determine if Os and Os-C is only specific for bacteria and has no effect on human cells. Whether the therapeutic application involves intravenous, topical or aerosol administration, blood cells such as erythrocytes and leukocytes, will be exposed to the administered AMPs. In addition, leukocytes play an important role in the immunological response to foreign molecules such as peptides.

In this chapter the effects of Os and Os-C on the viability and ultrastructure of human peripheral erythrocytes, mononuclear (MN) and polymorphonuclear (PMN) leukocytes were investigated. Neither peptide (0-100 µM for 30 minutes) caused haemolysis or altered the ultrastructure of erythrocytes compared to Mel, a potent AMP that has limited therapeutic application due to its haemolytic activity at concentrations as low as 10 µM. At 100 µM the morphology of the erythrocytes exposed to Os and Os-C was normal while 10 µM Mel induced echinocyte formation.

Leukocyte viability was evaluated after exposure for 24 hours to Mel, Os and Os-C. In MN cells 0.5 µM Mel and 100 µM Os caused a statistically significant decrease in cell viability while Os-C had no effect. In PMN cells loss of cell viability was observed at 2 µM Mel and neither Os and Os-C were cytotoxic.

Ultrastructural analysis with SEM revealed that 50 µM and 100 µM Os caused MN cellular lysis similar to that caused by 1 µM Mel. No effect was observed with Os-C. In PMN cells, 1 µM Mel caused lysis, 50 and 100 µM Os had no effect and Os-C caused activation. TEM revealed that Mel and Os induced morphological features associated with oncosis/apoptosis in MN cells. In PMN cells, Mel induced apoptosis and Os induced oncosis/apoptosis.

In conclusion, Os and Os-C had no effect on human erythrocytes. Leukocyte cytotoxicity was only observed at concentrations at 130 times higher than the MBC of Os, 0.77 µM for *E. coli* and *B. subtilis*. Os-C caused leukocyte activation.

4.2) Introduction

AMPs are promising alternatives for the treatment of topical and systemic infections. In such a treatment strategy, AMPs must be shown to be highly specific for bacteria i.e. must not compromise the viability and function of cells and tissues of the human body. Some AMPs have previously been shown to have cytotoxic effects and are thus unsuitable for use as antibiotic treatments. An antimicrobial which targets bacterial membranes in a detergent-like manner will likely also have a cytotoxic effect on mammalian cell membranes (Laverty and Gilmore, 2014). An example of such a peptide is Mel (Pratt *et al.*, 2005). In patients, these cytotoxic effects may present as a range of effects from irritation at the wound site, to more severe vascular injuries, seizures or cardiac arrhythmias (Mandell *et al.*, 2001, Laverty and Gilmore, 2014). Some AMPs have been shown to target microbes specifically, while showing no or little toxicity to mammalian cells (Matsuzaki, 2009) and several of these AMPs are being evaluated in clinical trials (Chapter 2, Table 2.1). This specificity has been attributed to the difference between bacterial and mammalian membrane composition, as described in Chapter 2, Section 2.2.6.

Following either topical, intravenous or aerosol administration, blood cells, namely the erythrocytes and leukocytes, would be exposed to an AMP. Three possible effects could occur; cytotoxicity to all cell types, cytotoxicity to a specific cell population or no cytotoxicity. Erythrocytes are the predominant cell found in blood. Mature erythrocytes contain no DNA or organelles and have a typical eukaryotic cellular bilayer. The slightest damage to the membrane results in haemoglobin (Hb) leakage which can be quantified (Tabart *et al.*, 2009, Ximenes *et al.*, 2010). In many studies on AMPs, the first level of testing is done on erythrocytes and therefore data generated in the present study can be compared with many other investigations (Nakajima *et al.*, 2003, Yan *et al.*, 2012). In contrast, the leukocytes are nucleated, contain organelles and based on their immunological function respond rapidly to the presence of foreign proteins and/or antigens and in addition are capable of rapid ROS production upon exposure to oxidative damage or inflammatory signals. Leukocytes perform various specific functions within the immune system such as phagocytosis of foreign bodies, secretion of antibodies, cytokines and histamine (Widmaier, 2006). Leukocytes include neutrophils, basophils, eosinophils, monocytes and lymphocytes, the latter being the most abundant cell type of the immune system. PMN cells, also known as granulocytes, include eosinophils, basophils and neutrophils and are characterised by multi-lobed nuclei and a granular cytoplasm (Junqueira and Mescher, 2010). MN cells are also called agranulocytes and include lymphocytes and monocytes (Junqueira and Mescher, 2010). Table 4.1 provides information on the abundance, lifespan in circulation and the function of specific leukocytes.

Table 4.1. Summary of abundance, lifespan and functional characteristics of leukocytes.

Cell type		% of leukocytes[a]	Lifespan in circulation	Function[b]
Mononuclear (MN)	Lymphocyte	20 - 25%	Total 2 months, able to recirculate[c]	Antigen recognition, natural killer cells, immune response
	Monocyte	3 – 8%	Few hours[d]	Differentiate into macrophages, phagocytosis
Polymorphonuclear (PMN)	Neutrophil	60 – 70%	5 days[e]	Phagocytosis, acute inflammation
	Eosinophil	2 – 4%	16 – 36 hours[f]	Phagocytosis, granule release, allergic reaction, activation of neutrophils
	Basophil	< 1%	60 – 70 hours[g]	Phagocytosis, granule release, allergic reaction, acute inflammation

[a]Gartner and Hiatt, 2011, [b]Male *et al.*, 2013, [c]Young *et al.*, 1995, [d]Parihar *et al.*, 2010, [e]Pillay *et al*., 2010, [f]Park and Bochner, 2010, [g]Sirachusa *et al*., 2011

Lymphocytes form part of the adaptive immune system which via antigen receptors recognise antigens. Natural killer cells, derived from immature lymphocytes, kill virus-infected cells and certain tumour cells. Lymphocytes have various sub-populations of cells including cytotoxic T cells, helper T cells and B cells, all of which play a role in the regulation and activation of the immune response. Monocytes, eosinophils, basophils and neutrophils are all phagocytic cells. Monocytes differentiate into macrophages in tissues where the particular tissue type determines their morphology and specific functions. However, the primary role of macrophages is to remove particulate matter such as microbes, aged cells or tumour cells. Neutrophils play an important role in acute inflammation to protect the body against microbes through phagocytosis and are attracted to sites of inflammation by chemotactic stimuli. Eosinophils and basophils, besides functioning as phagocytes, are both also able to release granules. Eosinophils contain granular proteins which are toxic to large pathogens which cannot be phagocytosed, induce histamine release from mast cells, activate neutrophils and platelets, and cause allergic reactions. Basophils differentiate into mast cells when leaving the circulation. Both basophils and mast cells are capable of rapid degranulation upon allergic stimulation. Degranulation leads to the release of histamine and heparin, which causes the adverse symptoms of allergy, but which also plays a role in parasite destruction and enhances acute inflammation (Male *et al.*, 2013). The study of the effects of peptides on peripheral blood leukocytes could give important insights into their influence on the immune system. The effects of AMPs on leukocytes can be direct toxicity or cellular stimulation or activation related to the functions described above.

In this chapter, the effects of the peptides Os and Os-C were investigated on erythrocytes and leukocytes. The haemolysis and Alamar blue (AB) assays were used to evaluate toxicity to erythrocytes and PMN and MN leukocytes respectively. Changes to the ultrastructure of these cells following exposure to Os and Os-C was determined with SEM and TEM.

4.3) Materials and methods

4.3.1) Blood collection

Ethical clearance was obtained from the Research Ethics Committee of the Faculty of Health Sciences of the University of Pretoria to collect blood from healthy, consenting donors (Protocol nr 452/2014). A volume of between 5 mL and 10 mL venous blood was collected using a sterile needle inserted into a 5 mL vacuum extraction blood tube containing 3.2% sodium citrate for erythrocyte studies and potassium ethylenediaminetetraacetic acid (EDTA) for leukocyte studies (Lasec, Johannesburg, South Africa). The tubes were labelled only with the researcher's name and date of collection.

4.3.2) Haemolysis assay

Haemolysis is frequently used to determine peptide cytotoxicity. Damage to erythrocyte membranes leads to the release of Hb which can be quantified spectrophotometrically. The method of Nakajima and colleagues (2003) was followed. Erythrocytes were collected by centrifugation at 200 x gravity (*g*) for 30 min and washed with isotonic phosphate buffered saline (isoPBS: 0.137 M NaCl, 3 mM KCl, 1.9 mM NaH_2PO_4, 8.1 mM Na_2HPO_4, pH 7.4). A 5% (*v/v*) dilution of erythrocyte cells was prepared in isoPBS and kept at 4°C. Before experimentation, the erythrocyte suspension was warmed to room temperature and rinsed with isoPBS. A volume of 90 µL of the 5% erythrocyte suspension was exposed to 10 µL of a range of peptide concentrations of Os and Os-C (0.25 - 100 µM) for 30 minutes at 37°C. The erythrocytes were then collected by centrifugation, the absorbance of the supernatant was determined at 570 nm and data was calculated as:

$$\%\ \boldsymbol{haemolysis} = \frac{A_{peptide} - A_{0\%}}{A_{100\%} - A_{0\%}} \times 100$$

where $A_{peptide}$ is the absorbance of erythrocytes exposed to the peptide, $A_{0\%}$ is the absorbance of erythrocytes exposed to isoPBS (0% haemolysis) and $A_{100\%}$ is the absorbance of erythrocytes exposed to 2% SDS (100% haemolysis).

4.3.3) Scanning electron microscopy of erythrocytes

SEM was used to investigate the ultrastructural effects of the peptides on erythrocytes. Erythrocytes were collected and exposed in the same manner as in Section 4.3.2. After exposure to the peptides, a standard sample preparation method for SEM was used. The erythrocytes were fixed with a mixture of 2.5% gluteraldehyde and 2.5% formaldehyde in 0.075 M phosphate buffer (NaH_2PO_4, $NaHPO_4 \cdot 2H_2O$, pH 7.4). After one hour, the samples were rinsed three times with 0.075 M phosphate buffer for 10 minutes before being placed in a secondary fixative of 1% osmium tetraoxide solution for 30 minutes. The samples were again rinsed in 0.075 M phosphate buffer three times for 10 minutes. The erythrocytes were then dehydrated with a series of ethanol dilutions; 30%, 50%, 70%, 90% and three changes of 100%. The erythrocytes were suspended in HMDS for 30 minutes, centrifuged and resuspended in fresh HMDS. A volume of 200 µL of erythrocyte suspension was dropped on a glass coverslip, air dried, coated with carbon and examined with an Ultra plus FEG SEM (Zeiss, Oberkochen, Germany).

4.3.4) Leukocyte isolation

A volume of 6 mL whole blood was carefully layered over 3 mL Histopaque 1077 and 3 mL Histopaque 1119 (Sigma-Aldrich, Johannesburg, South Africa), and centrifuged for 30 min at 500 x*g*. The upper layer containing MN cells and lower layer of PMN cells was collected into separate tubes and washed twice with Roswell Park Memorial Institute 1640 (RPMI) medium (Highveld Biological, Johannesburg, South Africa) containing 2% foetal bovine serum (FBS) (Highveld Biological, Johannesburg, South Africa), centrifuged each time for 10 min at 250 x*g*. Following this, the pelleted leukocytes were treated with 4 mL of ddH_2O for 30 sec to haemolyse any remaining erythrocytes. To restore the physiological isotonic conditions, 4 mL of 1.8 % (w/v) saline was immediately added. The leukocyte cell suspension was again centrifuged and resuspended in RPMI/FBS. The cell concentration of both the MN and PMN cell suspensions were determined by counting with a haemocytometer. Trypan blue (0.2%) was used to exclude any non-viable cells from the count. The cell concentration was adjusted to $1x10^6$ cells/mL, and a volume of 90 µL plated in a sterile tissue cultured 96-well plate.

4.3.5) Leukocyte viability assay

AB is a non-fluorescent dye which turns pink and fluorescent upon reduction in live cells by cytosolic and mitochondrial enzymes (Hamid *et al.*, 2004). The colour change may be measured spectrophotometrically or fluorescently (Collins and Franzblau, 1997), it allows the use of cells in suspension and is ideal for the evaluation of leukocyte activity.

To determine the toxic effect of the peptides, the AB assay was modified from the methods of Catrina *et al.* (2009). The cells were exposed to a concentration range of Mel, Os and Os-C between 0.5 µM and 100 µM for 24 hours at 37°C and 5% CO_2. Sterile $dddH_2O$ was added to the control wells. A 20 mM stock solution of AB was prepared in isoPBS. The stock solution was diluted to a working solution of 1.2 mM in isoPBS, and sterile filtered with a 0.2 µM cellulose acetate syringe filter (Lasec, Johannesburg, South Africa). AB was added to the leukocyte suspension to obtain a final concentration of 400 µM. The cell suspension was incubated for another 24 hours at 37°C and 5% CO_2. Fluorescence was measured at an excitation wavelength of 492 nm and emission wavelength of 590 nm on the FLUOstar Omega (BMG Labtech, Germany). Cytotoxicity was calculated by determining the percentage difference between the treated and control cells using the following formula (Invitrogen, USA):

$$\%\ of\ control = \frac{Fl_{treated}}{Fl_{control}} \times 100$$

where $Fl_{treated}$ is the fluorescence measurement of a treated well and $Fl_{control}$ is the fluorescence measurement of the control well.

4.3.6) Ultrastructure of leukocytes

To investigate the ultrastructural effects of the peptides on leukocytes both SEM and TEM was used. MN and PMN leukocytes were isolated as described in Section 4.2.5. The cell density was adjusted to $1x10^6$ cells/mL.

Scanning electron microscopy

Poly-L-lysine coated coverslips were placed in sterile 24-well tissue culture plates. The coverslips were prepared as in Chapter 3, Section 3.3.3. A volume of 90 µL of the cell suspension was pipetted onto the coverslip, and 10 µL of selected concentrations of the

peptide was added. The final concentrations of peptides were 1 µM Mel, 50 µM and 100 µM Os and Os-C, respectively. The cells were then incubated for 20 hours at 37°C and 5% CO_2. The coverslips were rinsed once with isoPBS and fixed with 2.5% gluteraldehyde and 2.5% formaldehyde in 0.05 M PBS[b] (40.5 mM $Na_2HPO_4.2H_2O$, 9.5 mM $NaH_2PO_4.H_2O$, 75 mM NaCl, pH 7.4) for one hour. The samples were rinsed three times with 0.05 M PBS[b] for 10 min each. Post fixation was done with 1% osmium tetraoxide for one hour, after which the coverslips were rinsed three times with 0.05 M PBS[b] again. The attached cells were dehydrated with an increasing series of ethanol (30%, 50%, 70%, 90%, and three times 100%) for 10 minutes each. The cells were then dried overnight with HMDS. The coverslips were mounted on an aluminium stub with carbon tape, coated with carbon and viewed with an Ultra plus FEG SEM (Zeiss, Oberkochen, Germany).

Transmission electron microscopy

A volume of 90 µL of the $1x10^6$ cells/mL suspension was plated into a 96-well tissue culture plate. The cells were incubated for 4 hours before peptide was added. A volume of 10 µL of peptide was added to obtain the final concentrations: 0.5 µM and 1 µM Mel, 50 µM and 100 µM Os and Os-C. Incubation followed for 18 hours at 37°C and 5% CO_2. The cells were then fixed by adding 200 µL of prewarmed fixative containing 2.5% gluteraldehyde and 2.5% formaldehyde in 0.05 M PBS[b] for 30 min. The medium-fixative mixture was removed and replaced with pure fixative for 1 hour. The fixed cells were then rinsed three times with 0.05 M PBS[b] for 10 min each. Postfixation was carried out with 1% osmium tetraoxide for 30 min, and rinsed again with 0.05 M PBS[b] three times for 10 min. Dehydration was done with an increasing series of ethanol; 30%, 50%, 70%, 90%, and three times 100% for 10 min each. The cells were then infiltrated in the plate with 50% Embed 812 resin (SPI supplies, Pennsylvania, USA) in ethanol for 1 hour, then with 100% resin for 4 hours. The resin was replaced with fresh resin, and polymerised within the wells for 72 hours. To remove the bottom of the embedded plate, it was melted with a dissection teasing needle warmed with a Bunsen burner. This was then cut into small blocks, which was mounted onto a premade resin block with commercial epoxy resin glue. The plastic from the bottom of the plate was carefully trimmed away with a single edge razor blade (SPI supplies, Pennsylvania, USA) and glass knife. Monitor sections were made with a glass knife and viewed with a light microscope to ensure the presence of cells in the resin block. Subsequent 100 nm sections were made with the Leica Ultramicrotome (Leica Microsystems GmbH, Wetzlar, Germany) using a 45° diamond knife (Diatome, Pennsylvania, USA). These sections were picked up on copper grids and contrasted with 4% aqueous uranyl acetate and Reynolds' lead citrate and

rinsed with water. The contrasted sections were viewed and images taken on the JEM-2100F TEM (JEOL, Tokyo, Japan).

4.3.7) Data analysis

Each quantitative assay consisted of three repeats of each concentration, and the experiment was repeated three times. The data is presented as means ± SE. Multiple comparisons were tested by one-way ANOVA followed by the Tukey post hoc test for significant difference between the different peptides (Graphpad Prism v6.01, California, USA). Significance was set at $p < 0.05$.

4.4) Results

4.4.1) Erythrocyte membrane integrity is unaffected

The peptides were evaluated for their ability to cause lysis of human erythrocytes. All peptides were tested at a concentration range of 2.5 - 100 µM. Even at 100 µM, a concentration 130x the MBC for Os and 58x the MBC for Os-C, no significant erythrocyte lysis was observed for either peptide (Figure 4.1A). A maximum of 0.9% haemolysis was observed for Os at 50 µM and 0.3% for Os-C at 100 µM (Figure 4.1B). In contrast, Mel which served as the positive control for damage, caused a dosage related increase in haemolysis (Figure 4.1A). At concentrations of 25 µM and higher, Mel caused more than 100% haemolysis, indicating that it is a better haemolytic agent than 2% SDS.

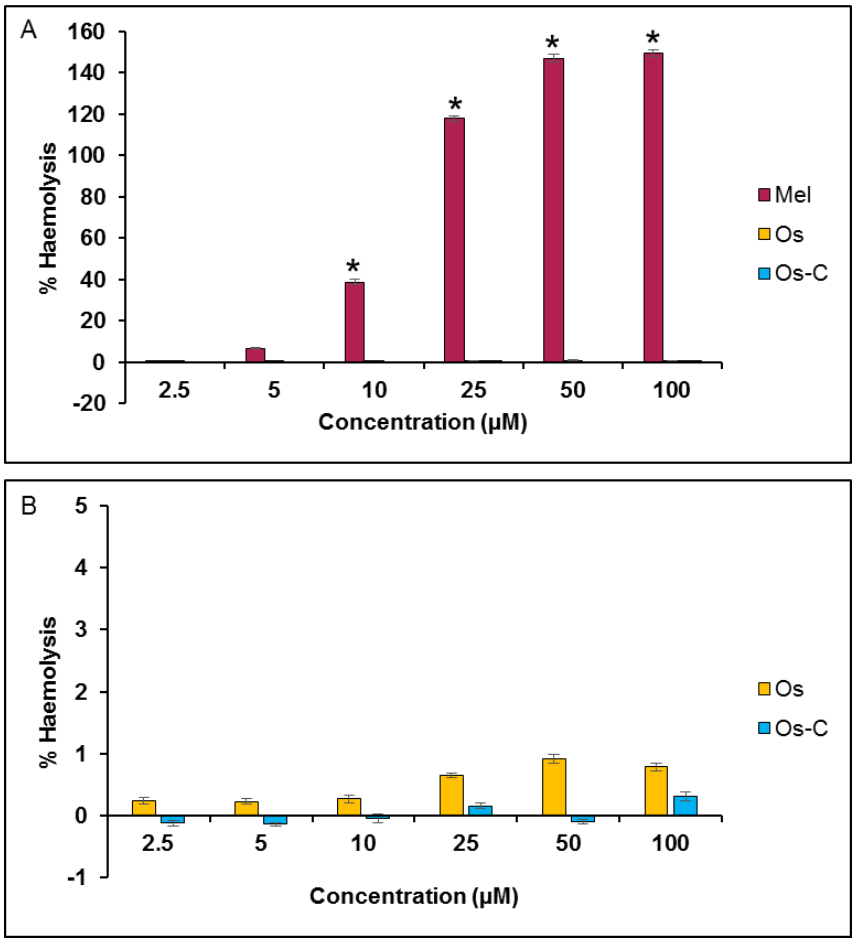

Figure 4.1. Haemolysis of erythrocytes after exposure to 0.25 – 100 µM Mel, Os and Os-C for 30 min. A) Represents 0 – 100%, B) represents a selection of the data (0 – 5%) to show the effect of Os and Os-C. Data expressed as mean ± SE. Asterisks indicate a significant difference between Mel and Os and Mel and Os-C at the same concentration ($p < 0.05$, $n = 9$).

4.4.2) Ultrastructural effects of peptides on erythrocytes

The effect of Mel, Os and Os-C on the erythrocyte ultrastructure was evaluated with SEM. The control sample (no peptide) showed a mixture of cell shapes, cells with a typical round biconcave shape, and cells with a more convoluted appearance and a few crenated cells (Figure 4.2A and E). Cells with a crenated appearance are also known as echinocytes. The presence of a few of these cells in the control group could be due to sample preparation or the presence of mature erythrocytes which had not yet been removed from circulation. Mel caused most of the cells to change to echinocytes (Figure 4.2B and F) at concentrations as low as 10 µM which correlates with 38.6% haemolysis (Figure 4.1A). At higher Mel concentrations, the cell numbers decreased too much for imaging to be possible. Os and Os-C had no observable effect on the membranes of human erythrocytes (Figure 4.2C, D, G and H). The same mixture of cell shapes was observed as in the control sample even at the highest peptide concentration of 100 µM.

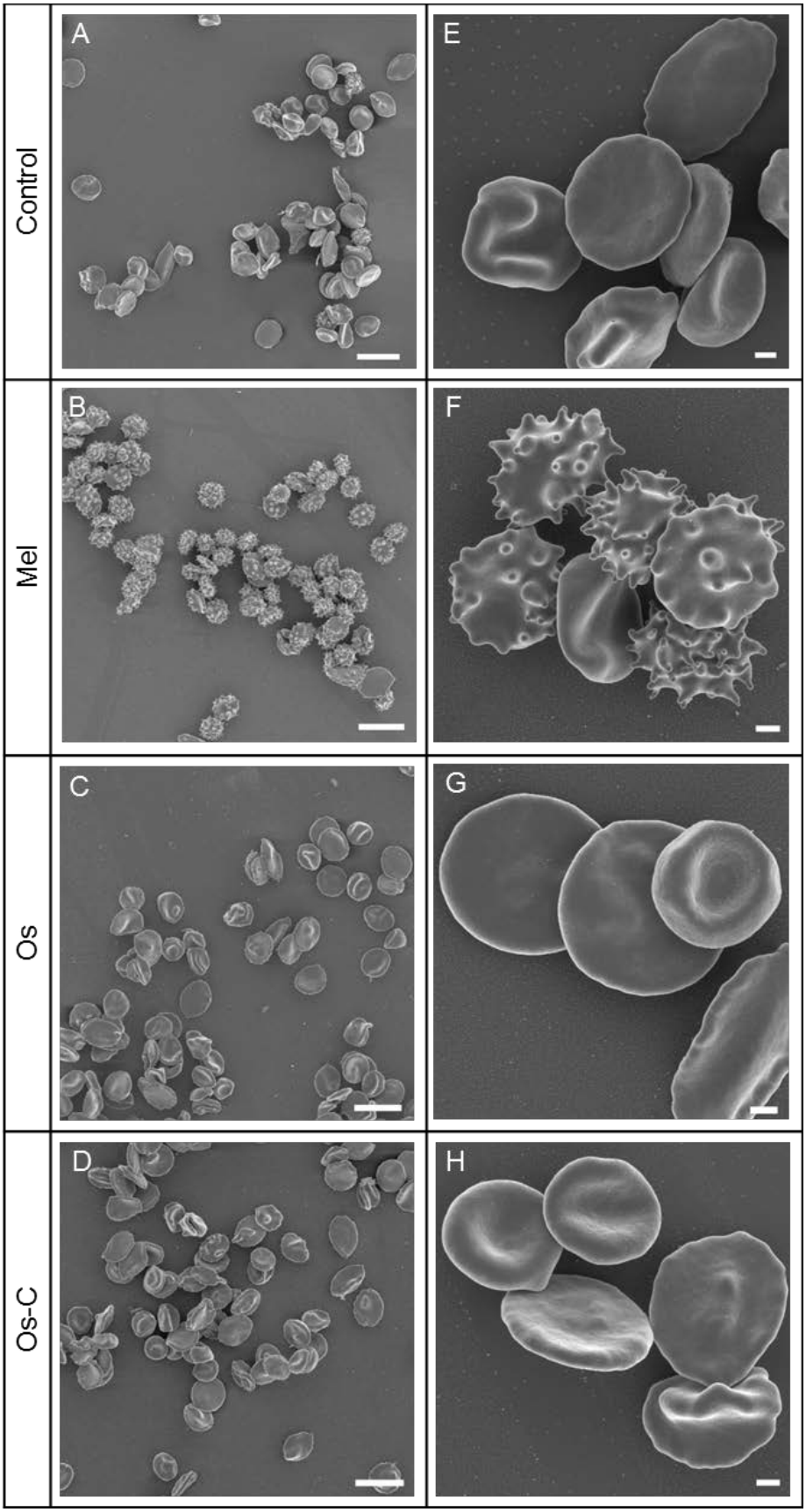

Figure 4.2. Ultrastructural effects of Mel, Os and Os-C on human erythrocytes evaluated with SEM after 30 min. A, E) Control, B, F) 10 µM Mel, C, G) 100 µM Os, D, H) 100 µM Os-C. Scale bars A - D) 10 µm, E - H) 1 µm.

4.4.3) Leukocyte viability

The influence of Mel, Os and Os-C on the viability of MN and PMN leukocytes was determined with the AB assay. The MN group of cells contains mostly lymphocytes and a few monocytes, while the PMN group of cells contains mostly neutrophils, eosinophils and to some lesser extent basophils (English and Andersen, 1974, Junqueira and Mescher, 2010). The AB assay measures the enzymatic reduction potential of the cell, as the non-fluorescent molecule is reduced within an active cell to fluoresce. Mel caused a decrease in reducing capability of both MN and PMN leukocytes. MN cells were more sensitive, showing almost complete toxicity at 2 µM (2.28% viability relative to the control) and significant difference to the control at all concentrations (Figure 4.3A). Mel caused significant reduction in PMN cell viability only at concentrations of 2 µM and higher (Figure 4.3B). The viability of MN cells was reduced following exposure to 100 µM of Os, a concentration 130 times higher than its MBC (0.77 µM) for *E. coli* and *B. subtilis*. Os-C showed no significant difference to the control at any of the concentrations tested. Os and Os-C had no significant effect on PMN cells.

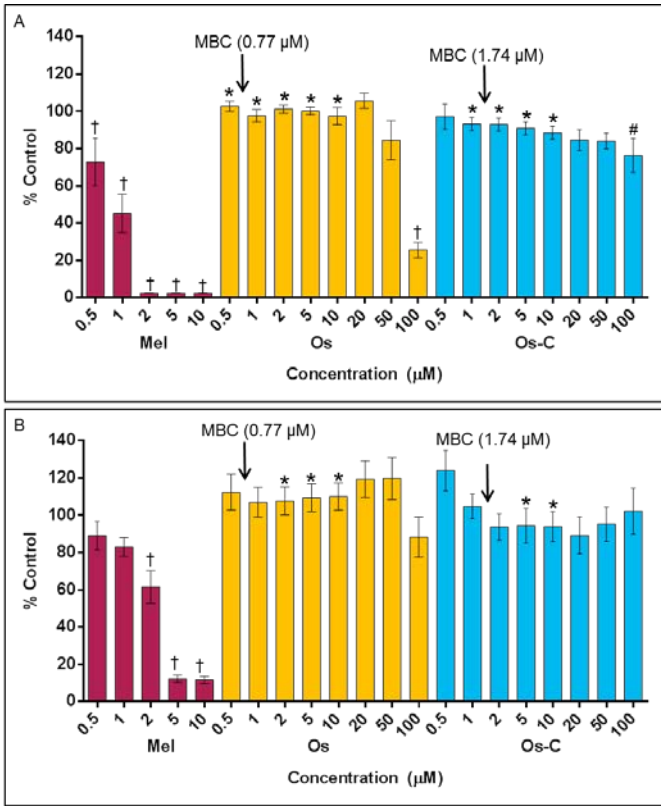

Figure 4.3. Leukocyte viability after exposure to Mel (0 – 10 µM), Os and Os-C (0 – 100 µM) for 24 hours, measured with the AB assay. A) MN cells and B) PMN cells. Crosses indicate significant difference to the control where no peptide was added (100%), arrows indicate the minimum bactericidal concentrations (MBC), asterisks indicate significant difference to Mel of the same concentration, and hash indicates significant difference to Os of the same concentration ($p < 0.05$, $n = 9$).

4.4.4) Ultrastructural changes to leukocytes

The effects of Mel, Os and Os-C on MN and PMN cellular morphology and structure were evaluated with SEM and TEM, respectively. SEM provides insights into the membrane effects of the peptides, while TEM allows further detailed analysis of membrane as well as organelle structure.

With SEM two typical morphology types were observed for MN cells not exposed to peptide (Figure 4.4A and B). These are cells with a more flattened appearance, often with pseudopodia (Figure 4.4A) and smaller round cells with microvilli covering the surface of the cell (Figure 4.4B). The latter morphology is consistent with normal lymphocytes (Zucker-Franklin *et al.*, 1981). Mel caused severe membrane damage or possibly complete loss of the membrane at a concentration of 1 µM (Figure 4.4C and D). Os caused membrane damage at both 50 µM and 100 µM (Figures 4.5A and B). However, at 50 µM, fewer cells were affected. Cells exposed to Os-C showed no membrane damage (Figure 4.5D and E). MN cells exposed to 100 µM Os-C appeared to be in a more activated state, some had more protrusions or pseudopodia extending from the cell body (Figures 4.5E).

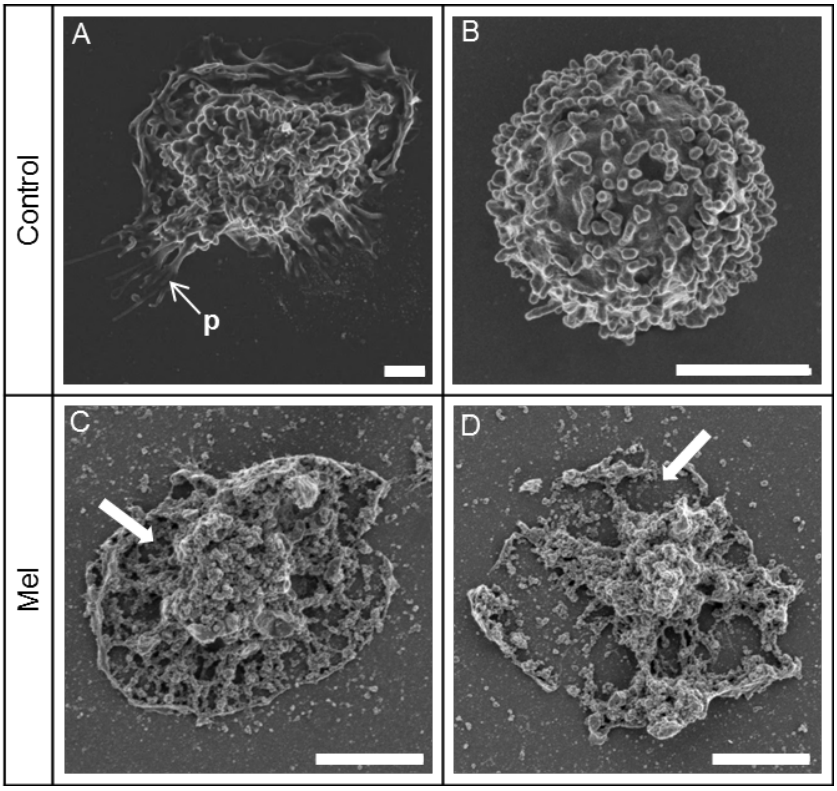

Figure 4.4. Membrane effects of MN cells not exposed and exposed to Mel for 20 hours and imaged with SEM. A,B) Control, C, D) 1 µM Mel. Arrows indicate membrane damage, p) pseudopodia. Scale bars = 2 µm.

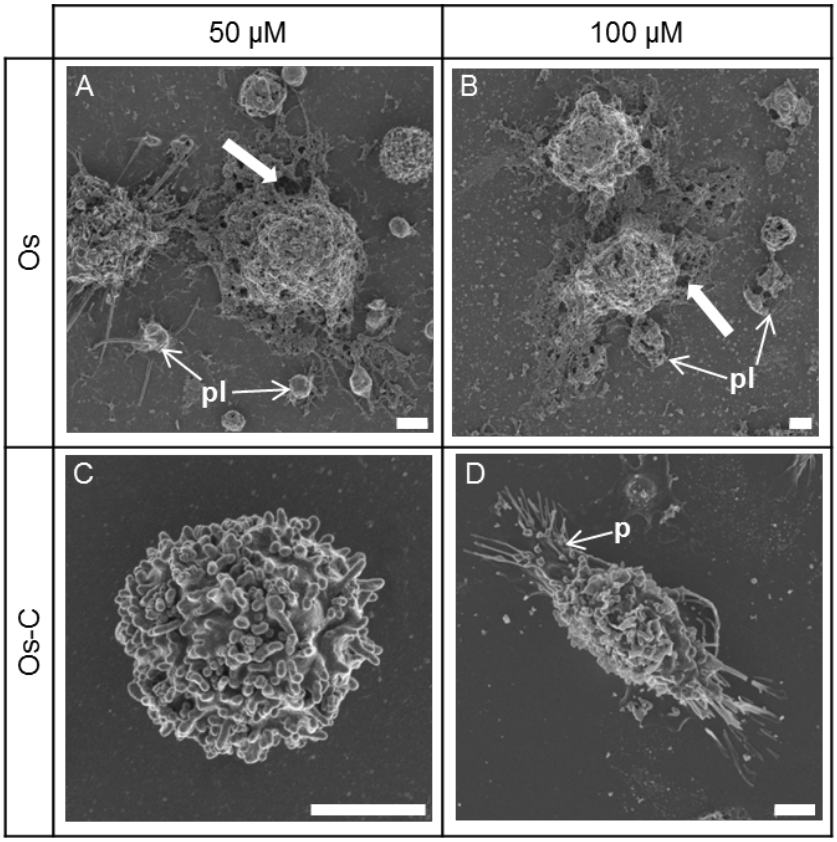

Figure 4.5. Membrane effects of MN cells exposed to Os and Os-C for 20 hours and imaged with SEM. A) 50 µM Os, B) 100 µM Os, C) 50 µM Os-C, D) 100 µM Os-C. Arrows indicate membrane damage, p) pseudopodium, pl) platelets not washed away during leukocyte separation. Scale bars = 2 µm.

PMN control cells also showed two types of morphology, a smaller round cell with a mostly smooth membrane (Figure 4.6A) and a more flattened larger cell type with pseudopodia (Figure 4.6B). PMN cells exposed to 1 µM Mel were damaged in a similar way to MN cells, with large holes in the cell structure (Figure 4.6C and D). The 50 µM concentration of Os seemed to have no effect on PMN cells, as can be seen with the two representative cell types shown in Figures 4.7A and B. However, a large amount of cell damage was observed with 100 µM Os (Figure 4.7C). After exposure to 50 µM Os-C, the cellular morphology was similar to the control. However, there was an increase in the amount of long thin filopodia from the cell membrane for both cell types (Figures 4.7D and E). PMN cells exposed to 100 µM Os-C underwent a change in cell shape, with the formation of pseudopodia similar to cells responding to a chemotactic molecule (Figure 4.7F). These cells generally had more membrane ruffles as compared with the control, and some cells had filopodia extending from the pseudopodia.

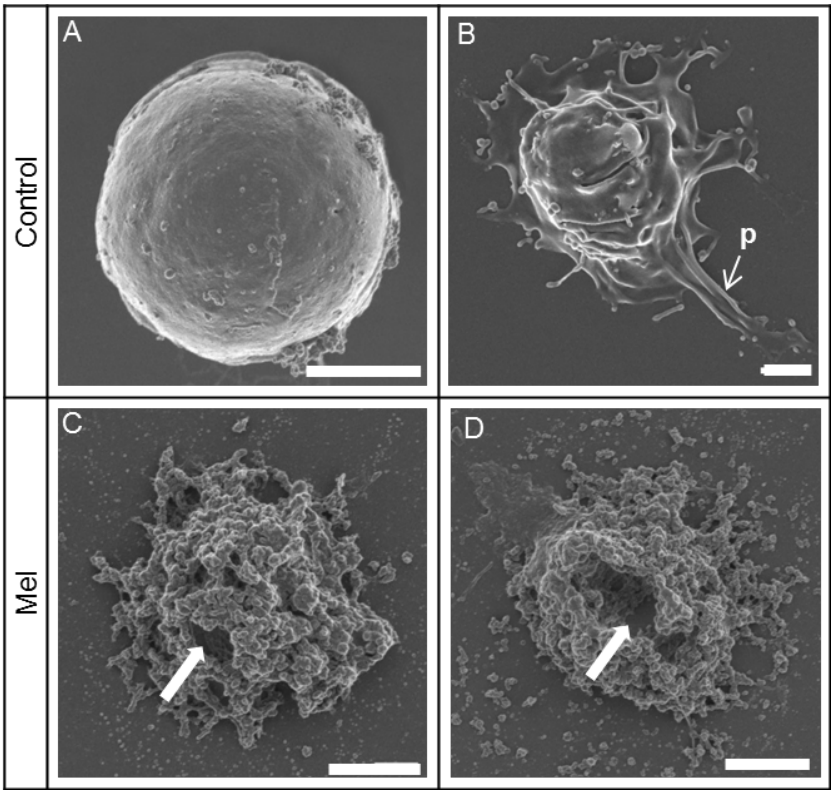

Figure 4.6. SEM of PMN leukocytes, not exposed and exposed to Mel for 20 hours. A, B) Control, C, D) 1 µM Mel. Arrows indicate membrane damage, p) pseudopodia. Scale bars = 2 µm.

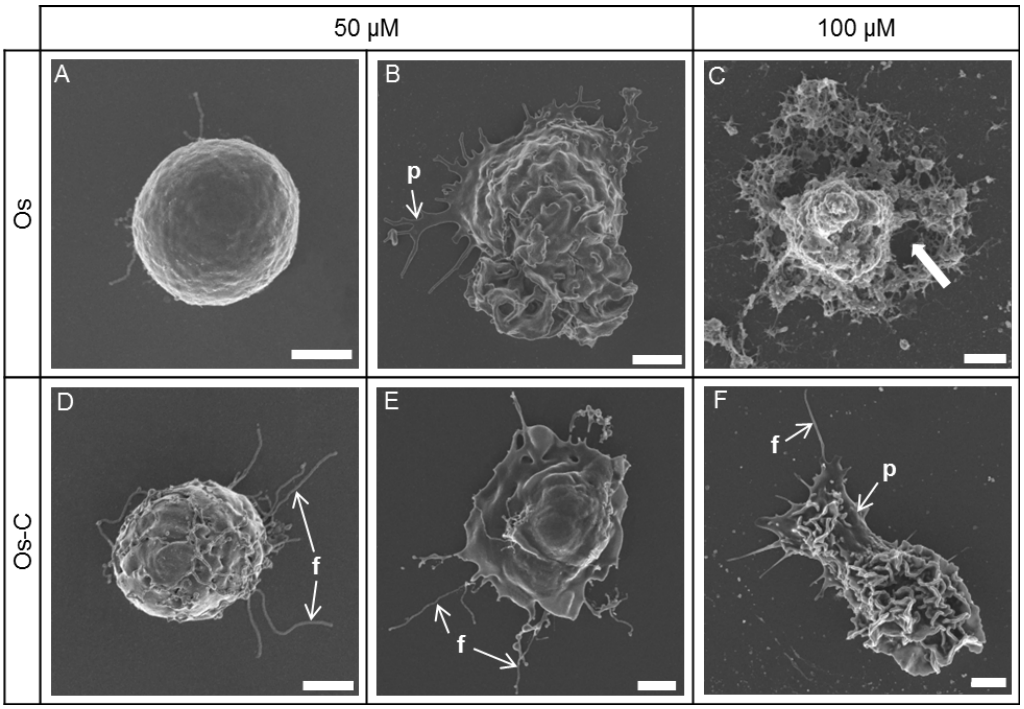

Figure 4.7. SEM of PMN leukocytes exposed to Os and Os-C for 20 hours. A, B) 50 µM Os, C) 100 µM Os, D, E) 50 µM Os-C, F) 100 µM Os-C. Arrows indicate membrane damage, f) filopodia, p) pseudopodia. Scale bars = 2 µm.

TEM revealed control MN cells (exposed only to water) which had a rounded shape with microvilli (Figure 4.8A). These cells generally contained a large nucleus with peripheral heterochromatin, interrupted by euchromatin only at the nuclear pores. The shape of nuclei ranged from having a large indentation to being almost perfectly round. Most control cells possessed only a small amount of cytoplasm. Centrioli could be observed in some cells (Figure 4.8B). The control cells contained small amounts of rough endoplasmic reticulum (RER), and mitochondria and Golgi were easily observed. This is consistent with the ultrastructure of lymphocytes in interphase (Zucker-Franklin *et al.*, 1981).

All concentrations of Mel caused a decrease in MN cell viability was observed. No cells could be observed in the sample which was exposed to 1 µM Mel and therefore cells incubated with 0.5 µM Mel were used. Most of the cells exposed to 0.5 µM Mel, contained large electron dense bodies, which are most likely lipid bodies (Figures 4.8D – F). In contrast to membranous organelles that possess a double phospholipid membrane, lipid bodies have only a single phospholipid membrane and this difference is used for the identification of lipid bodies (Melo *et al.*, 2011). Some cells also had electron lucent vacuoles of different sizes which were either empty or contained some material while some cells also had pseudopodia (Figure 4.8D).

In the presence of 50 µM Os many MN cells were similar in appearance to the control (Figure 4.9A), although a few damaged MN cells were also observed (Figures 4.9B and C). These cells generally appeared to have lost intracellular content, with some vesicles containing heterogeneous material, while microvilli were absent (Figure 4.9B). The nucleus appeared abnormal, with the disappearance of euchromatin, and only severely condensed heterochromatin on the periphery (Figure 4.9B). In some cells mitochondria could still be observed, however, they had mostly lost their cristae, and appeared to have undergone membrane damage (Figure 4.9C). After exposure to 100 µM Os, few cells with relatively normal morphology remained, and most of those showed a separation of the inner and outer nuclear membranes (Figure 4.9D). Most cells had an appearance similar to that described for the damaged cells exposed to 50 µM Os (Figure 4.9E). Some cells had large gaps in the plasma membrane, and little nuclear material remained (Figure 4.9F).

MN cells exposed to Os-C did not show the same extent of damage as observed with Mel or Os. However, these cells did appear to be different from the control. Some cells had large vacuoles, either empty or containing some material (Figures 4.10A, F - H). Some cells were enlarged with long filopodia (Figure 4.10A), others were elongated with a large pseudopod (Figure 4.10C and G). The elongated cells generally had larger amounts of RER than seen

in control cells (Figure 4.10D). A few cells contained electron lucent lipid bodies with a dark perimeter (Figure 4.1E). No major ultrastructural differences were observed between 50 µM and 100 µM concentrations of Os-C.

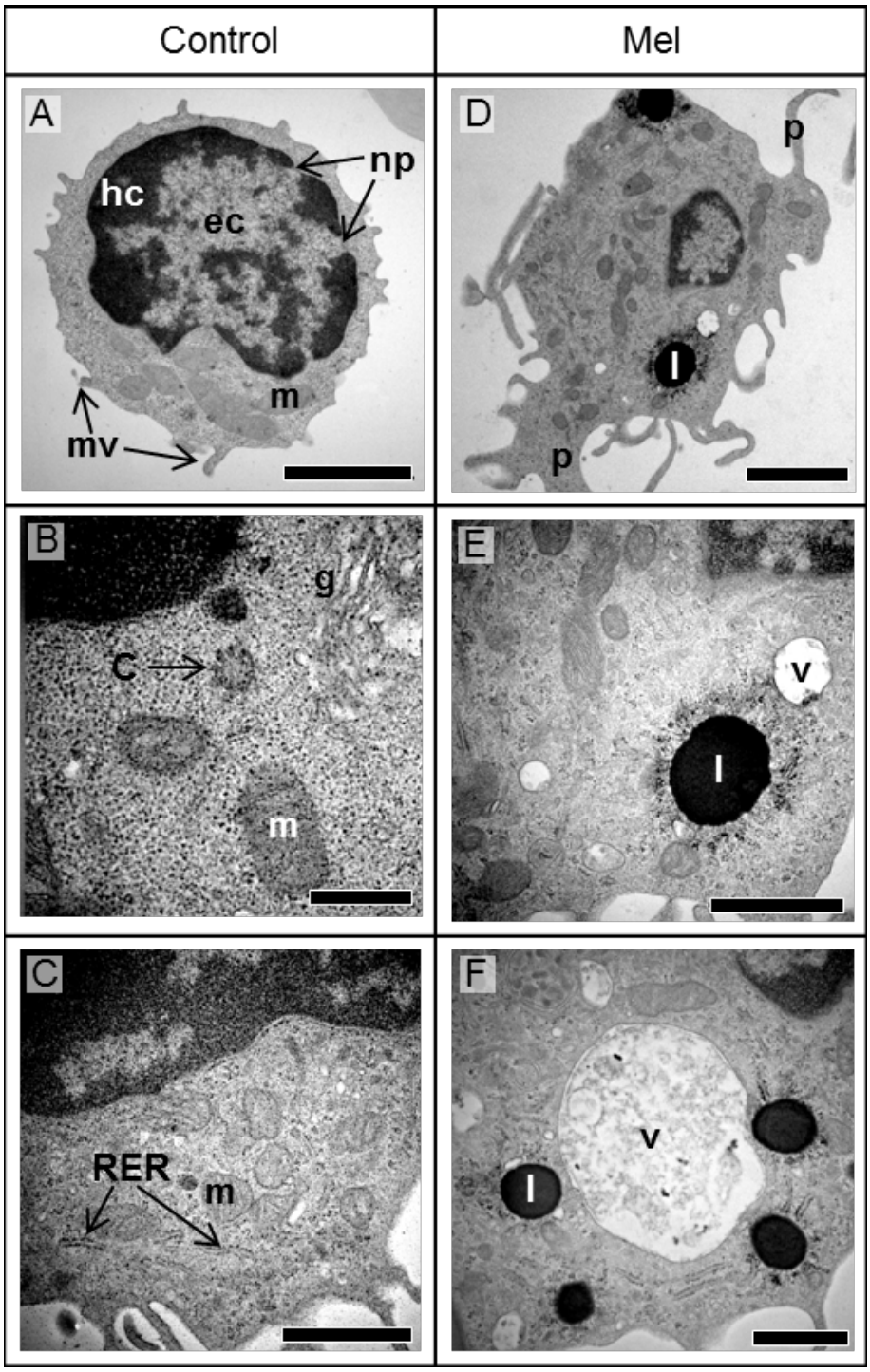

Figure 4.8. TEM images of MN cells not exposed and exposed to Mel for 18 hours. A - C) Control, D - F) 0.5 µM Mel. E) higher magnification of D. c) centriole, ec) euchromatin, hc) heterochromatin, g) Golgi, l) lipid body, m) mitochondria, mv) microvilli, np) nuclear pore, p) pseudopodia, RER) rough endoplasmic reticulum, v) vacuole. Scale bars A & D) 2 µm, B) 500 nm, C, E & F) 1 µm.

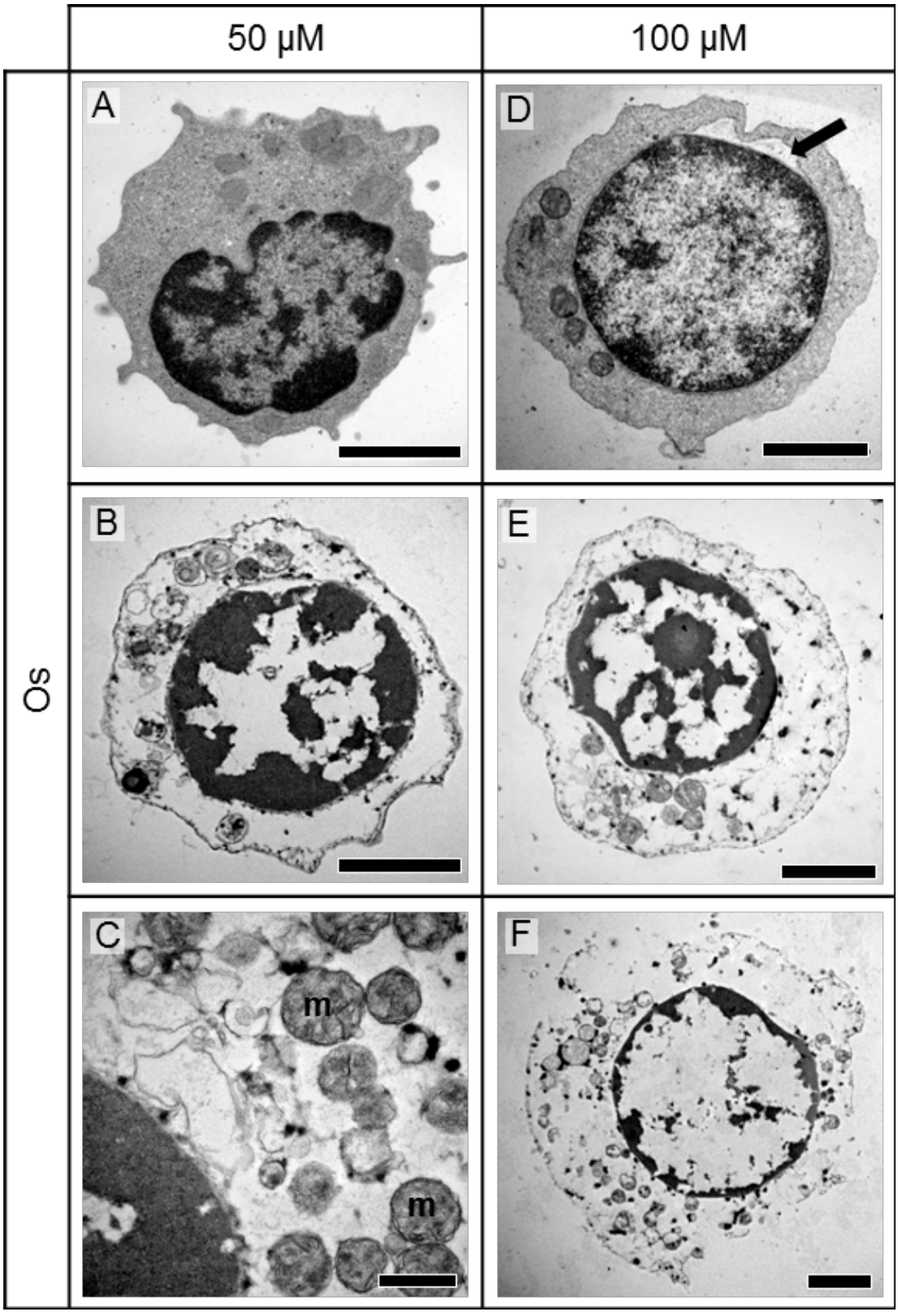

Figure 4.9. TEM images of MN cells exposed to Os for 18 hours. A - C) 50 µM, D - F) 100 µM. Arrow indicates separation of inner and outer nuclear membrane, m) mitochondria. Scale bars = 2 µm, except C) 500 nm.

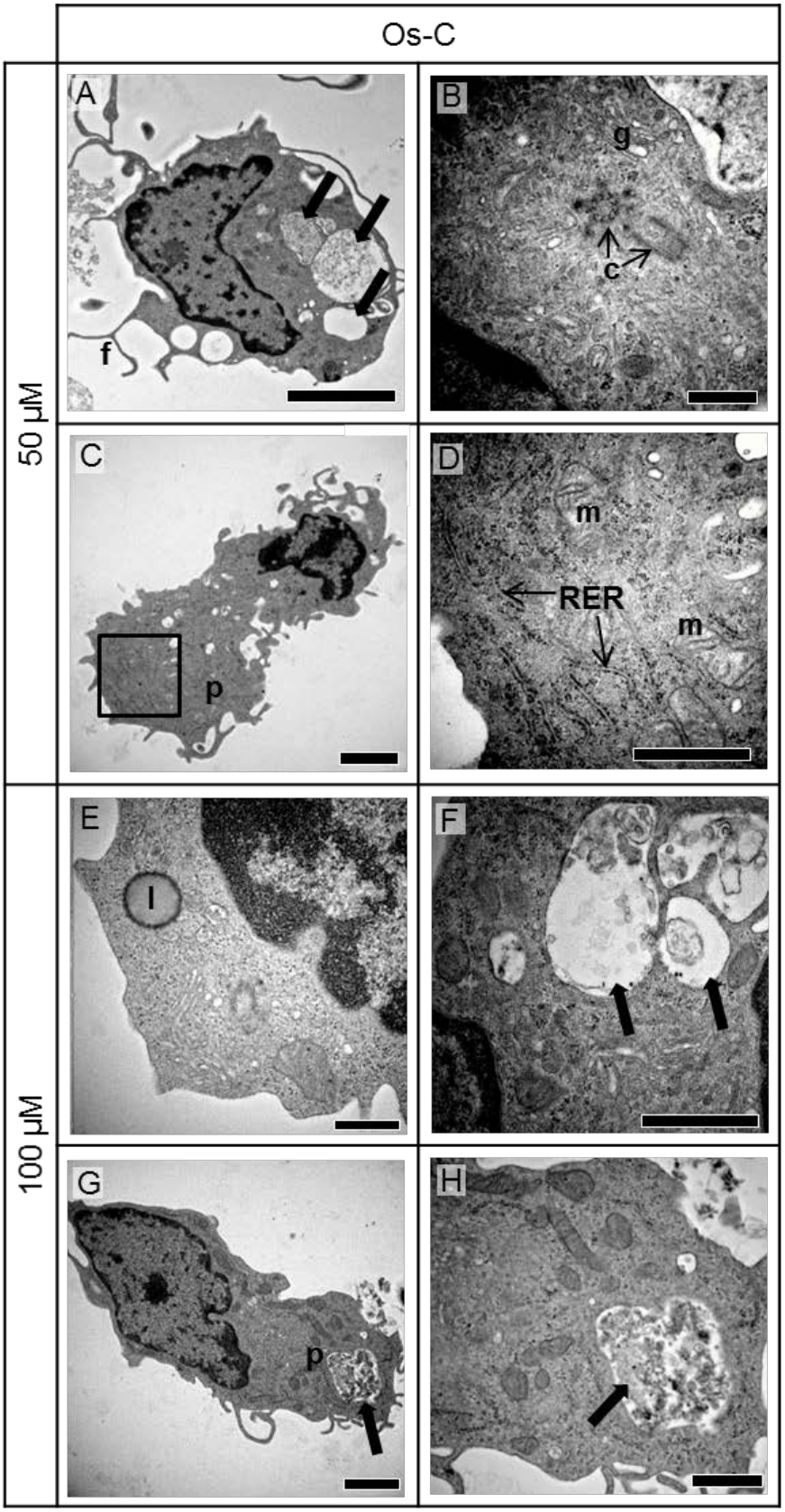

Figure 4.10. TEM images of MN cells exposed to Os-C for 18 hours. A - D) 50 µM, E - H) 100 µM. B, D, H) Higher magnification of A, C, G, respectively. Square in C indicates area magnified in D. Arrows indicate vacuoles, c) centrioli, f) filopodia, g) Golgi, l) lipid body m) mitochondria, p) pseudopodia, RER) rough endoplasmic reticulum. Scale bars A) 5 µm, B, E) 500 nm, C, G) 2 µm, D, F, H) 1 µm.

The nuclei of typical PMN cells are generally multi-lobed, with heterochromatin on the periphery and euchromatin in the centre (Zucker-Franklin *et al.*, 1981). The control group of PMN cells in the current study, which were exposed only to water, presented with abnormal morphology. These cells all had round nuclei with completely condensed chromatin (Figure 4.11A - C). The granules also appeared to be in various states of degradation. Mel caused the formation of inclusions within the cytoplasm and lipid bodies at 0.5 µM (Figure 4.11D). Lipid bodies display various degrees of osmophilia in response to inflammatory stimuli (Melo *et al.*, 2011). It also affected the nucleus by the appearance of more electron lucent areas, and some cells had fragmented nuclei (Figures 4.11D). Few cells remained after exposure to 1 µM Mel, and those that did appeared to have undergone apoptosis showing vacuolisation and membrane blebbing (Figure 4.11F).

The 50 µM concentration of Os caused marginalisation of the condensed chromatin, and large inclusions within the cells (Figures 4.12A and B). Some cells were damaged as in Figure 4.12C. Few cells remained after exposure to 100 µM Os, most of these were extremely damaged presenting with disintegrated membranes, no intact organelles and in some cases the disappearance of the nucleus (Figure 4.12D – F).

Most PMN cells exposed to 50 µM Os-C did not display major differences in ultrastructure compared to the control (Figure 4.13A and B). However, some of these cells showed an increase in the amount of vacuolisation (Figure 4.13C). The 100 µM concentration of Os-C caused the formation of large vacuoles (Figures 4.13D and E), and in some cases caused marginalisation of the condensed chromatin (Figures 4.13D and F).

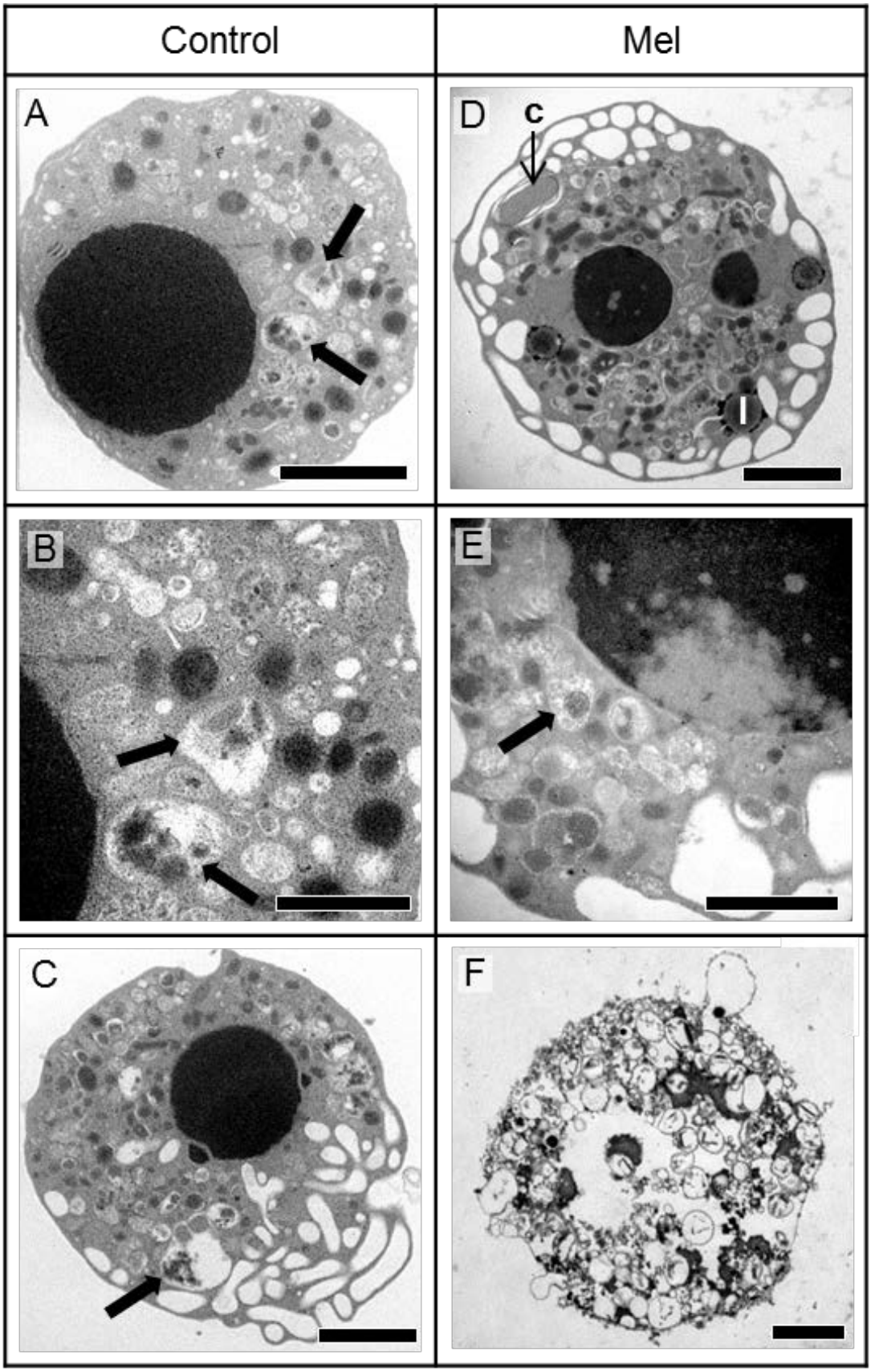

Figure 4.11. TEM of PMN leukocytes not exposed and exposed to Mel for 18 hours. A - C) Control, D - E) 0.5 µM Mel, F) 1 µM Mel. Arrows indicate degrading granules, c) cytoplasmic inclusions, l) lipid body. Scale bars A, C, D & F) 2 µm, B & E) 1 µm.

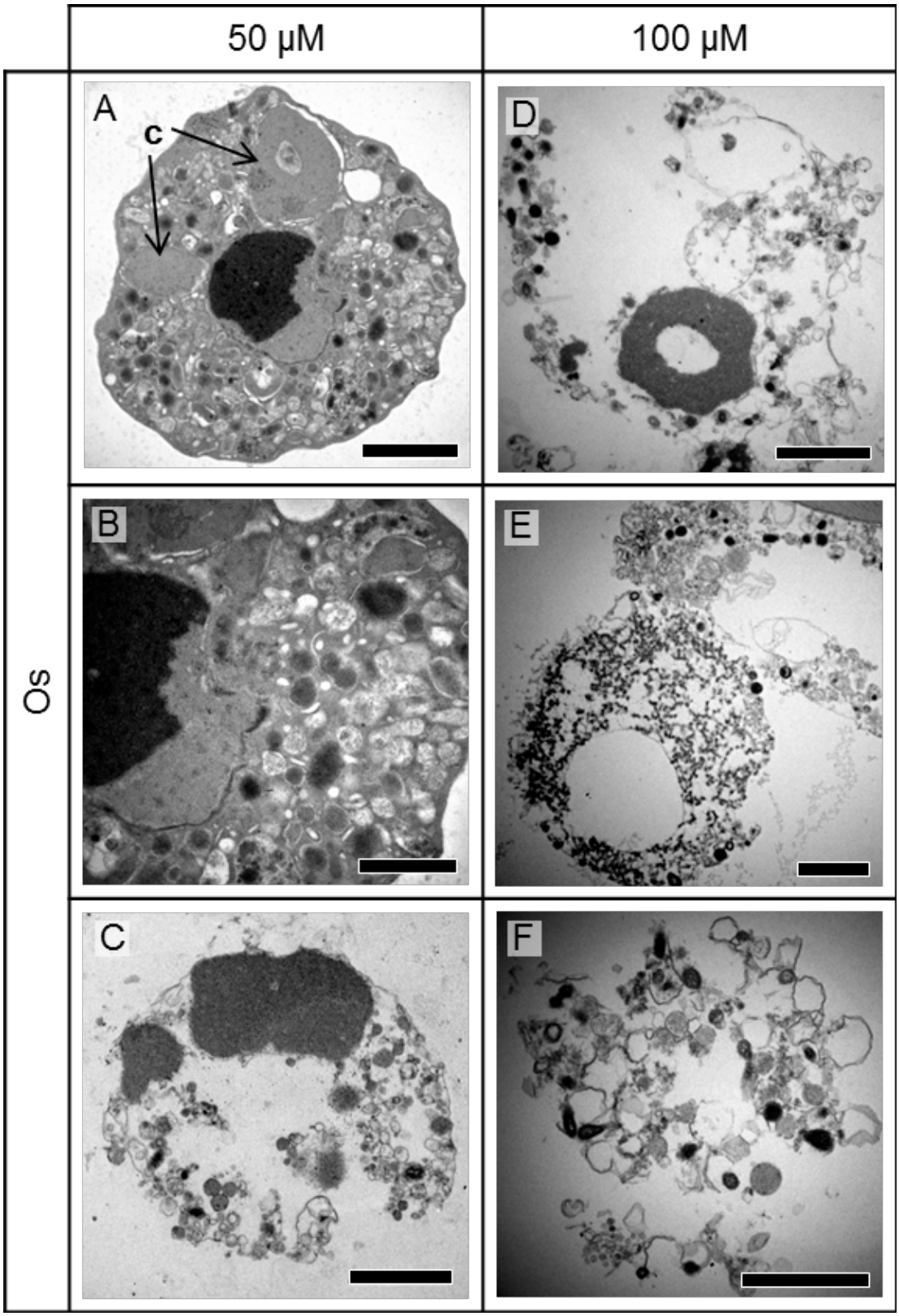

Figure 4.12. TEM of PMN leukocytes exposed to Os for 18 hours. A - C) 50 µM, D - F) 100 µM. c) Cytoplasmic inclusions. Scale bars B) 1 µm, the rest 2 µm.

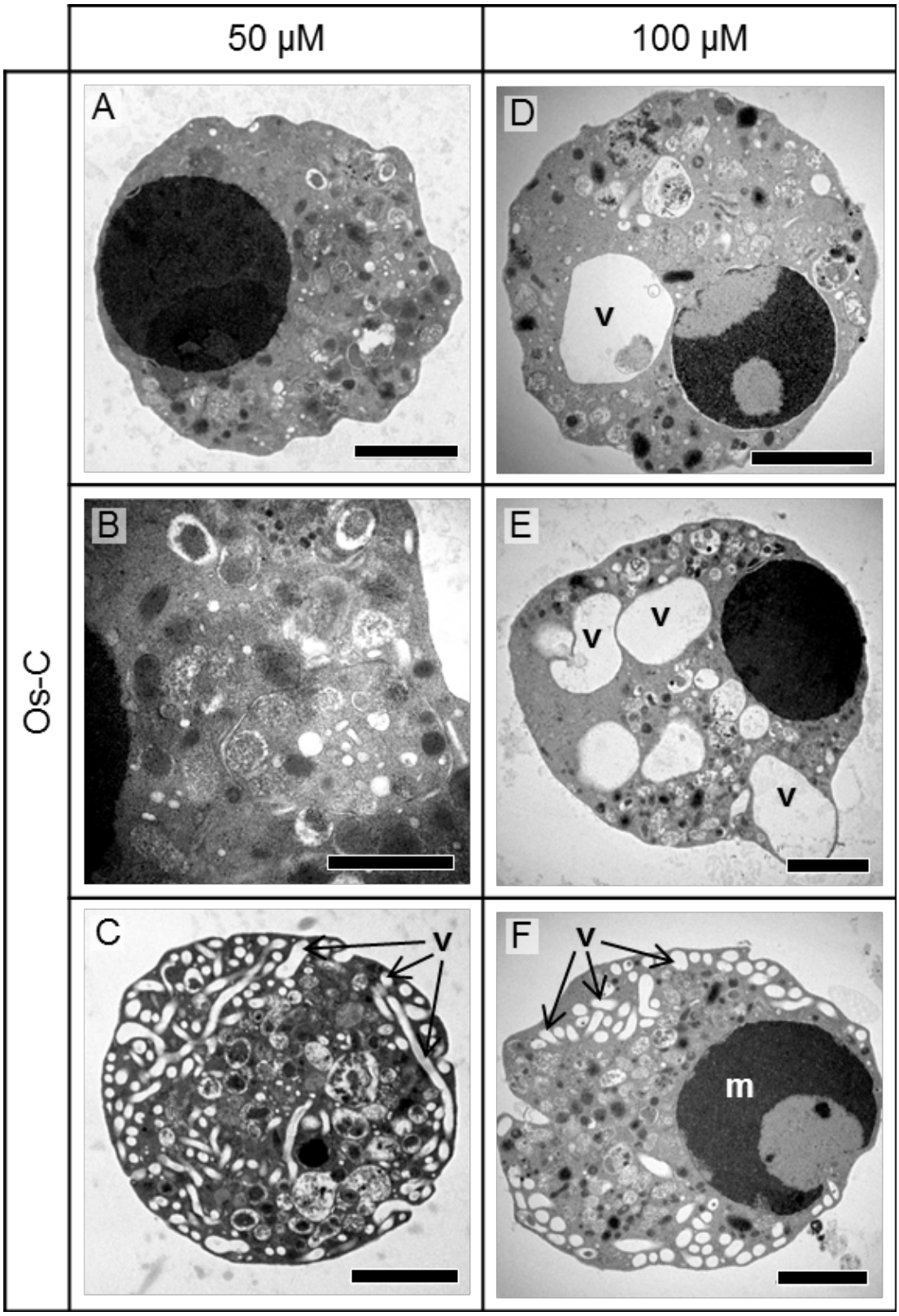

Figure 4.13. TEM of PMN leukocytes exposed to Os-C for 18 hours. A - C) 50 µM, D - F) 100 µM. B) higher magnification of A. m) marginalisation of chromatin, v) vacuoles. Scale bars B) 1 µm, the rest 2 µm.

4.5) Discussion

To evaluate the suitability of Os and Os-C as therapeutic peptides, the effects of the peptides on human blood cells were investigated. Haemolysis results indicated that neither Os nor Os-C caused significant damage at any of the concentrations tested. At 10 µM, Mel caused 38.6% haemolysis and the formation of echinocytes. Nakao and colleagues (2011) previously reported that Mel caused echinocyte formation. It has been suggested that Mel inserts into the outer monolayer of the erythrocyte membrane, which causes crenation of the cell (Katsu *et al.*, 1989, Nakao *et al.*, 2011). Gramicidin S and mastoparan from *Polistes jadwagae* similarly cause crenation of erythrocytes (Nakao *et al.*, 2011). Echinocyte formation is also associated with eryptosis which is the programmed cell death of erythrocytes and is characterised by cell shrinkage, phosphatidylserine exposure and membrane blebbing (Malik *et al.*, 2015, Ran *et al.,* 2015). Associated biochemical changes result in increased intracellular Ca^{2+}, ROS, and ceramide levels, rapid depletion of ATP and activation of caspases (Malik *et al.*, 2015). The induction of apoptosis in nucleated and organelle containing cells is similar, and this is the basis of research where Mel is evaluated as an anticancer agent (Kong *et al.*, 2016). The concentrations used in these studies range between 0.35 – 70 µM, this is of concern as they may be cytotoxic to noncancerous cells such as erythrocytes limiting their application as systemic anticancer agents (Yang *et al*., 2007, Zhang *et al.*, 2007, Kong *et al.*, 2016).

Os and Os-C did not have the same effects on erythrocytes, indicating that these peptides do not interact with the cell membrane as was observed for Mel. Although haemolysis testing is widely used to determine AMP toxicity, it cannot evaluate dysfunction in erythrocytes with unbroken membranes (Ran *et al.,* 2015). Membrane disturbances which are not associated with haemolysis are related to a number of disorders such as anaemia, thrombogenic activation, exposure of phosphatidylserine which contributes to chronic renal failure, Wilson's disease and other malignancies (Ran *et al.,* 2015). Therefore, it is essential to further investigate whether Os and Os-C may disrupt other erythrocyte biochemical pathways that do not result in haemolysis.

Malik *et al.* (2015) used fluorescent probes to measure phosphatidylserine externalisation, intracellular ROS, Ca^{2+} and ceramide levels, and cell volume in erythrocytes after exposure to gramicidin. The authors found that gramicidin caused phospholipid scrambling of the erythrocyte membrane, increase in intracellular Ca^{2+} and up-regulation of ceramide. There was also a concurrent increase in cell volume (Malik *et al.*, 2015). Similar methods can be used to ascertain whether Os and Os-C disrupts other biochemical pathways in erythrocytes.

The effects of Os, Os-C and Mel were evaluated on human peripheral MN and PMN leukocytes. The exposure time of 18-24 hours was longer than the 30 min used for erythrocytes. This was done as the cell viability (AB) assay required longer incubation times for the accurate and reproducible quantification of cell viability. In addition, a longer incubation time used for leukocytes allows uptake, protein or DNA targeting, pathway activation and metabolism of Os and Os-C.

Several cellular pathways can contribute to cell death and these include apoptosis, oncosis, necrosis and autophagy. Apoptosis is characterised by cellular shrinking, condensation and margination of chromatin, ruffling of the plasma membrane and the formation of apoptotic bodies (Table 4.2). This type of cell death typically does not lead to inflammation. Oncosis is associated with cellular and organelle swelling, and necrosis refers to features which appear after the cell has died such as cellular and nuclear lysis and subsequent inflammation (Table 4.2) (Van Cruchten and Van Den Broeck, 2002). In a cell culture environment, extended exposure to an apoptosis inducing factor would be expected to eventually lead to apoptotic necrosis, as there are no macrophages to phagocytose the apoptotic bodies. The membranes of apoptotic bodies would eventually become destabilised leading to increased membrane permeability and necrotic lysis. Cells which have undergone oncosis would lead to oncotic necrosis. Autophagy is a process of degradation of intracellular components in order to reuse the constituents (Mcleod and He, 2010, Iba *et al.*, 2013). It is characterised by autophagosomes, large vacuoles which contain cytosol and organelle components, and a lack of chromatin condensation (Table 4.2). The vacuoles fuse with lysosomes, which degrade the content without damaging the cell. If autophagy is overstimulated, a cell will undergo apoptosis (Iba *et al.*, 2013). Autophagy has been shown to be mechanisms of both homeostasis and cell death in lymphocytes and neutrophils (Mcleod and He, 2010, Iba *et al.*, 2013). Cells which have undergone autophagic cell death are phagocytosed by adjacent cells, and as such do not lead to inflammation (Iba *et al.*, 2013).

MN cells are lymphocytes and monocytes which do not contain specific granules (Gartner and Hiatt, 2011). Lymphocytes typically have a rounded symmetrical appearance with numerous microvilli on the cell surface (Holt *et al.*, 1972). The surface of lymphocytes becomes more irregular when activated (Holt *et al.*, 1972). Inactive lymphocytes display round or oval nuclei with a small amount of cytoplasm surrounding it. These cells contain few mitochondria, endoplasmic reticulum and lysosomes (Hirsh *et al.*, 2007). The morphology observed for control MN cells in the present study was consistent with the literature. With SEM these cells displayed a rounded shape with numerous microvilli, while with TEM these

cells were observed to have large nuclei, a small amount of cytoplasm which contained few mitochondria, Golgi and RER and small microvilli on the cell surface. The more flattened cells with membrane ruffles observed with SEM may have been activated on contact with the polystyrene surface of the tissue culture plates.

Table 4.2. Summary of the morphological features associated with different types of cell death.

	Apoptosis	Oncosis/Necrosis	Autophagy
General	Cellular shrinking Chromatin condensation Nuclear blebbing Ruffling of membrane Apoptotic bodies Intact organelles Cytoplasm retains content / density	Cellular and organelle swelling Cellular and nuclear lysis Organelle damage Loss of cell content / density	Autophagosomes No chromatin condensation
Lymphocytes	Cytoplasmic vacuolation	Clumped chromatin	
Neutrophils	Vacuolation Rounding of cells	Homogeneous nuclei Nuclei lobules fuse	

PMN cells include neutrophils, eosinophils and basophils (Gartner and Hiatt, 2011). Resting PMN cells are typically rounded cells with ruffled membranes, multilobular nuclei, many diverse granules (primary and secondary), few mitochondria and scattered glycogen (Kapp *et al.*, 1988, Genestier *et al.*, 2005). Tomita *et al.* previously found that PMN cells spontaneously became activated upon contact with a glass surface (Tomita *et al.*, 1995). Contact of PMNs to a polystyrene surface has also been shown to lead to activation of neutrophils to produce large amounts of superoxide anion and H_2O_2 (Johnston and Lehmeyer, 1976). This effect was observed with SEM and TEM in the present study. Control PMN cells in the present study displayed some ultrastructural features associated with both activation and apoptosis. These include flattening of the cell with an increase in filopodia, chromatin condensation and vacuolisation. Neutrophils have a short lifespan and undergo apoptosis after 24 - 48 hours of leaving the circulation (Iba *et al.*, 2013). In an *in vitro* environment, neutrophils do not need an exogenous trigger to undergo apoptosis (Payne *et al.*, 1994). Savill and colleagues (1989) showed that ageing neutrophils eventually undergo apoptosis. Due to experimental requirements the PMN cells were incubated a total of 42 hours on tissue culture treated polystyrene plates before fixing. These conditions most probably led to activation of the PMN cells, and eventually the cells spontaneously started to undergo apoptosis. There were, however, still marked differences in ultrastructure between the PMN cells exposed to peptide and the control cells exposed only to water. Pre-treatment of a polystyrene surface with FBS was previously shown to suppress H_2O_2 production by PMNs for 60 minutes (Nathan, 1987). The FBS in the cell culture medium may have played

a role in decreasing the amount of contact-stimulated activation of the PMN cells in the control group.

A summary of the effects of Mel, Os and Os-C on leukocyte viability and the ultrastructural features observed with SEM and TEM is shown in Table 4.3.

Table 4.3. Summary of the effects of the peptides on peripheral blood cell viability and ultrastructure.

	Feature	Mel	Os	Os-C
Erythrocyte	Cytotoxicity	√	X	X
MN: Lymphocytes monocytes	Cytotoxicity	√	√ 100 µM	X
	Apoptosis	√	X	X
	Oncosis/necrosis	√	√	X
	Activation	X	X	√
PMN: Neutrophils basophils eosinophils	Cytotoxicity	√	X	X
	Apoptosis	√	√	√
	Oncosis/necrosis	X	√	X
	Activation	X	X	√

MN) mononuclear cells, PMN) polymorphonuclear leukocytes, √ effect observed, X no effect observed

The AB assay results showed that Mel caused a decrease in the dye reducing capabilities of peripheral MN cells at all concentrations tested. With SEM, 1 µM Mel caused large gaps in the cell membranes. For TEM at concentration of 1 µM Mel only a few cells remained after exposure and no sections containing cells could be visualised. Therefore, a concentration of 0.5 µM was used. However, at this concentration, not all the morphological features observed with SEM were observed. MN cells exposed to 1 µM Mel had large vacuoles not seen in the controls as well as dark bodies, presumed to be lipid bodies. Few lipid bodies are found in resting leukocytes, however, upon activation their numbers increase rapidly. Lipid bodies synthesise various inflammatory mediators such as eicosanoids (Melo and Weller, 2016). Several pathogenic bacteria have been shown to induce lipid body formation in leukocytes (Melo and Dvorak, 2012). Vacuolisation is one of the characteristics of apoptosis. Vacuoles in the present study often contained heterogeneous materials which could possibly be autophagosomes. As stated before, overstimulation of autophagocytosis could lead to apoptosis.

Abd-Elhakim *et al.* (2014) found that most rat lymphocytes underwent necrosis rather than apoptosis after exposure to whole bee venom. Mel occurs naturally in bee venom. Observed necrosis was confirmed with detection of released lactate dehydrogenase and lytic cell membranes observed with fluorescence microscopy (Abd-Elhakim *et al.*, 2014). The necrotic

cells most likely underwent oncosis prior to cell death. Peptides are thought to lyse cells through transmembrane pores which allow water to enter the cell leading to swelling and rupture, this is known as colloid-osmotic cell lysis or oncosis (Van Cruchten and Van Den Broeck, 2002, Fink and Cookson, 2005, Pratt *et al.*, 2005). Necrotic lymphocytes display ultrastructural features such as clumped chromatin (pyknosis) and an extreme decrease in cytoplasm electron density due to disintegration (Decker *et al.*, 2003). Apoptosis, on the other hand, results in separation of chromatin and nuclear blebbing while retaining electron density of the cytoplasm (Decker *et al.*, 2003). Other ultrastructural features of apoptotic lymphocytes include cytoplasmic vacuolation, chromatin condensation and margination, nuclear lobulation and membrane bound apoptotic bodies (Table 4.2) (Sun *et al.*, 2000). The SEM results of the present study indicated that MN cells were undergoing necrosis after Mel exposure. However, TEM revealed ultrastructural features associated with apoptosis. Gajski and colleagues (2016) found that Mel was cytotoxic to human peripheral blood lymphocytes and caused changes to the cell shape and membrane and caused lysis and granulation. These authors described cells with apoptotic features, however, the majority of the cells had undergone necrotic cell death (Gajski *et al.*, 2016). It has been suggested that Mel may have a dual mechanism, causing cell death via both apoptosis and membrane disruption (Lee and Lee, 2015). Apoptotic cell death is achieved through increased ROS generation, mitochondrial dysfunction and caspase activation (Lee and Lee, 2015). However, Mel is also capable of binding to the negative lipid membrane to form amphipathic α-helices, at threshold concentrations the peptide then inserts into the membrane forming pores. Pore formation leads to a collapse of the transmembrane electrochemical gradient, and ultimately membrane lysis as seen in necrosis (Lee and Lee, 2015, Gajski *et al.*, 2016).

Neutrophils undergoing apoptosis generally have condensed chromatin with fragmentation of nuclei while the nuclear envelope remains intact, the appearance of many vacuoles with intact organelles and rounding of cells (Savill *et al.*, 1989, Genestier *et al.*, 2005, Fuchs *et al.*, 2007). Necrotic neutrophils lose nuclei structure which appears homogeneous with no distinction of eu- or heterochromatin. The lobules fuse, the cell swells, lose membrane integrity and cellular content (Table 4.2) (Genestier *et al.*, 2005, Fuchs *et al.*, 2007). In the present study PMN cells were less sensitive to the effects of Mel on cell viability than MN cells. SEM showed similar results to MN cells after 1 µM Mel exposure with damaged cell membranes. TEM revealed that PMN cells exposed to Mel showed the same chromatin condensation seen in the control cells, but in some cases chromatin aggregation was observed. There was an increase in the number of vacuoles, with some inclusions not seen in the controls. The higher concentration of Mel led to a noticeable decrease in the number

of cells, and those remaining appeared to have undergone blebbing. It is therefore suggested that Mel caused a mixture of apoptosis and necrosis as with the MN cells.

Os caused a decrease in the cell viability of MN cells only at 100 µM. SEM results showed that Os caused damage to the cell membranes, especially at the 100 µM concentration. At 50 µM, SEM analysis showed that fewer cells were damaged and no toxicity was observed with the AB assay. TEM indicated a marked decrease in cytoplasmic electron density, with few organelles remaining and these were damaged. Some of these cells had large gaps in the cell membrane, and the nuclei had extreme chromatin condensation. These features are consistent with the described morphological characteristics of oncotic necrosis.

SEM analysis showed no changes in the surface morphology of PMN cells after exposure to 50 µM Os. However, a few damaged cells were observed with TEM. TEM also revealed that the 50 µM Os caused large intracellular inclusions and the marginalisation of condensed chromatin. At 100 µM Os, major cellular damage was observed with both SEM and TEM with large gaps in the cell membrane and a loss of intracellular content. Some PMN cells had lost their nuclei and no intact organelles could be observed. Some cells seemed to have undergone blebbing. The PMN ultrastructure suggested that these cells had undergone apoptotic necrosis. However, the AB results indicated that Os did not have a significant effect on the cell viability of PMN cells. A possibility for the difference between ultrastructural and AB results could be that the endogenous enzymes responsible for the reduction of the AB dye were released into the medium upon membrane damage of the PMN cells. Gonzalez and Tarloff (2001) previously demonstrated the ability of both mitochondrial and cytosolic fractions of rat liver to reduce AB. The AB assay does not require a washing step and the enzymes free in the culture medium may still be able to reduce the dye. This would then lead to a false indication of viable cells.

Os-C caused no changes in MN cellular viability. Even at 100 µM, SEM and TEM showed that Os-C caused no membrane damage. Os-C did cause a change in cell shape, associated with leukocyte activation to a larger degree than observed in the control samples. The 100 µM concentration of Os-C, especially, resulted in the formation of elongated cells. This is consistent with the cell shape observed when leukocytes migrate across a surface in response to a chemotactic substance. In a previous study, lymphocytes which were activated by CD3 presented with ultrastructural features such as indented nuclei, electron lucent vacuoles, abundant RER, free ribosomes, Golgi cisterns and electron dense lysosomes within a larger rim of cytoplasm (Hirsh *et al.*, 2007). CD3 antibodies stimulate lymphocytes via surface antigens to become metabolically active and to proliferate (Tsoukas

et al., 1985). MN cells exposed to Os-C in the present study were enlarged with elongated microvilli and pseudopodia. These cells also contained large vacuoles, either empty or containing heterogeneous material, increased amounts of RER and some nuclei had large indentations. These features are consistent with what was observed in the Hirsh study for activated lymphocytes (Hirsh *et al.*, 2007).

Granulocyte-macrophage colony-stimulating factor (GM-CSF) is a glycoprotein hormonal growth factor which stimulates granulocyte colony formation, increases oxidative metabolism and increases antibody-dependent cytotoxicity, phagocytosis and killing of pathogenic microorganisms (Kapp *et al.*, 1988). Kapp *et al.* (1988) found that stimulation of PMNs with GM-CSF led to cells with a flattened morphology and numerous filamentous filopodia, as well as an increase in the number and size of intracellular vesicles which is associated with a decrease in granules. The same morphological features were observed after stimulation with phorbol 12-myristate 13-acetate (PMA), which is known to activate neutrophils (Kapp *et al.*, 1988). These descriptions of activated PMN cells are similar to what was observed for cells exposed to Os-C. SEM showed cells with long filopodia, pseudopodia or cells which were elongated. Tomita and colleagues (1995) observed such elongated PMN leukocytes with differential interference contrast microscopy after exposure to platelet activating factor or fMet-Leu-Phe. TEM revealed a changed ultrastructure with features like vacuolisation and blebbing in some cases, and marginalisation of condensed chromatin, all features of apoptosis. It is possible that the ultrastructure seen with TEM which looks like apoptosis is in fact caused by activation of the cells by Os-C. This is corroborated by the toxicity results which indicated that Os-C did not cause significant cell death at any of the concentrations tested. The degradation of granules and intracellular inclusions seen after Os-C exposure could also be an indication of autophagy. Autophagy is known to counteract the negative effects of ROS production during neutrophil activation (You *et al.*, 2014). Therefore, it could be a protective measure of the granulocytes in the current study against over-activation of the cells. However, unregulated autophagy will lead to cell death.

In this study Mel was found to be cytotoxic to erythrocytes and leukocytes at concentrations similar to the reported MBC values of Mel (Issam *et al*. 2015, Lyu *et al.* 2016). In contrast, no erythrocyte haemolysis occurred at concentrations of 130x and 58x the MBC of Os and Os-C, respectively. Os caused MN cell toxicity only at 130x the MBC and morphological features associated with oncotic necrosis at 65x the MBC to both MN and PMN cells. In contrast, at 58x the MBC, Os-C caused activation of leukocytes. This implies that although toxic effects were observed for Os and activation was observed for Os-C these effects would only occur at concentrations several fold greater than the MBC of each peptide.

Though effects of the AMPs on platelets were not investigated in this study, some platelets remained in the MN cell suspension after separation and could be observed with SEM (Figure 4.5). All the peptides seemed to change the ultrastructure of the platelets which may indicate action on the coagulation system. The effect of the AMPs on platelets and the coagulation system needs to be investigated.

4.6) Conclusion

Neither Os nor Os-C caused erythrocyte haemolysis or ultrastructural changes at 100 µM, a concentration 130x and 58x the MBCs of Os and Os-C, respectively. Although Os at 100 µM altered MN and PMN cell ultrastructure, PMN cell metabolic activity was unaffected. Os caused both apoptotic and oncotic features in MN cells, and an increase in apoptosis of PMN cells. Os-C was not toxic to either group of cells, but caused a change in ultrastructural morphology associated with leukocyte activation. However, lower concentrations of both of these AMPs had no adverse effect on any of the peripheral blood cells tested. Os-C may have additional beneficial effects by activation of leukocytes at high concentrations.

Chapter 5: Antioxidant activity of Os and Os-C

5.1) Abstract

Multifunctional AMPs are peptides that besides antimicrobial activity, have additional beneficial effects such as anti-inflammatory and antioxidant activity. Infection is often associated with an increase in inflammation and associated increased levels of oxidants that are produced by immune cells to destroy pathogens, but in excess can cause cellular damage. Thus the aim of this study was to determine if Os and Os-C have antioxidant activity and can protect erythrocytes and leukocytes against ROS and/or induce ROS production in leukocytes.

With the TEAC assay the antioxidant activity of Os was greater than that of Os-C while with the ORAC assays both Os and Os-C had similar antioxidant activity. Os and Os-C did not enter erythrocytes and only created an extracellular environment that protected erythrocytes against oxidative damage. Os-C activation of PMN cells was found to be a result of increased ROS production. Os and Mel did induce ROS formation but levels were less than that observed for Os-C in PMN cells. The ability of each peptide to cross the cell membrane and protect MN and PMN cells against oxidative damage was then determined. Induction of cellular ROS formation in PMN was confirmed. Both the controls, GSH and caffeic acid protected PMN cells against oxidative damage and likewise Os at 50 µM and 100 µM protected PMN cells against oxidative damage.

In conclusion, Os and Os-C have antioxidant activity and in cellular systems protects erythrocytes by scavenging radicals in the extracellular environment. Os-C induces ROS formation in PMN cells which results in PMN activation while Os enters PMN cells and protects these cells against oxidative damage.

5.2) Introduction

AMPs have been shown to have multiple functionalities such as immunomodulatory, antitumor, antiparasitic, antiviral, antifungal or antioxidant properties (Sarmasik 2002, López-Expósito *et al.*, 2007, Matsuzaki, 2009, Kim and Wijesekara, 2010, Yeung *et al.*, 2011).

Persistent oxidative stress leads to chronic inflammation, which in turn could lead to chronic illnesses such as cancer, diabetes, cardiovascular, neurological and pulmonary disease.

ROS is a normal by-product of cellular respiration, and are important molecules for the stimulation of signalling pathways. Oxidative stress occurs when there is an imbalance between the production of ROS and their elimination by antioxidants. During prolonged environmental stress, this imbalance is maintained and causes damage to cellular structures and functions (Reuter *et al.*, 2010). Surplus amounts of hydroxyl radical and peroxynitrite may cause membrane damage through lipid peroxidation. ROS and reactive nitrogen species (RNS) can also cause structural changes to proteins which may lead to a loss of enzyme activity. DNA may undergo mutations which could lead to tumour formation (Pham-Huy *et al.*, 2008). Sources of oxidative stress and inflammation include microbial and viral infection, exposure to allergens, radiation, toxic chemicals, autoimmune and chronic diseases, obesity, overuse of alcohol, tobacco and a high-calorie diet. The longer the inflammation persists, the higher the chance of developing disease. AMPs with antioxidant activity can prevent oxidative stress associated infection (Reuter *et al.*, 2010).

Specific amino acid residues in proteins have been shown to possess antioxidant activity. The amino acid residues Trp and Tyr have previously been identified as antioxidants because of their respective indolic and phenolic groups that may function as hydrogen donors (Hernández-Ledesma *et al.*, 2005, Zheng *et al.*, 2012). Met can also act as an antioxidant by undergoing oxidation to Met-sulfoxide, and Cys by donating its sulfur hydrogen (Hernández-Ledesma *et al.*, 2005). Food derived peptides have been the most studied for a combination of antimicrobial and antioxidant activity. Dietary proteins are a source of biologically active peptides which are released during food processing or digestion (Gómez-Guillén *et al.*, 2010). For example, a hydrolysate of hen egg white lysozyme was shown to have antimicrobial activity against both Gram-positive *Leuconostoc mesenteroides* and Gram-negative *E. coli*, as well as antioxidant activity (Memarpoor-Yazdi *et al.*, 2012). Peptide fractions from the hydrosylates of tuna and squid gelatin were found to have both antioxidant and antimicrobial activity (Gómez-Guillén *et al.*, 2010). Insect defensins have not been widely studied for antioxidant activity. Os and Os-C are derived from insect defensins, and both contain three Tyr residues, while Os contains three Cys residues which indicate possible antioxidant activity.

Honzel *et al.* (2008) previously showed the advantage of interpreting the results of chemical antioxidant assays with erythrocyte and leukocyte assays. Chemical assays give results without cellular interference (Figure 5.1A) and provides preliminary data on possible benefical effects. Erythrocytes provide a clear picture of antioxidant capability *in vitro* without interference of inflammatory signals (Figure 5.1B). Leukocytes may react to potentially antioxidant compounds in three ways; 1) the test compound may enter the cytosol and neutralise the free radicals (Figure 5.1Ci); 2) the test compound may interact with receptors

on the leukocyte cell membrane, signalling the cell to reduce inflammatory behaviour and ROS production (Figure 5.1Cii); 3) or the test compound may interact with the leukocyte cell membrane receptors resulting in an increase in inflammatory behaviour and ROS production (Figure 5.1Ciii) (Honzel *et al.*, 2008).

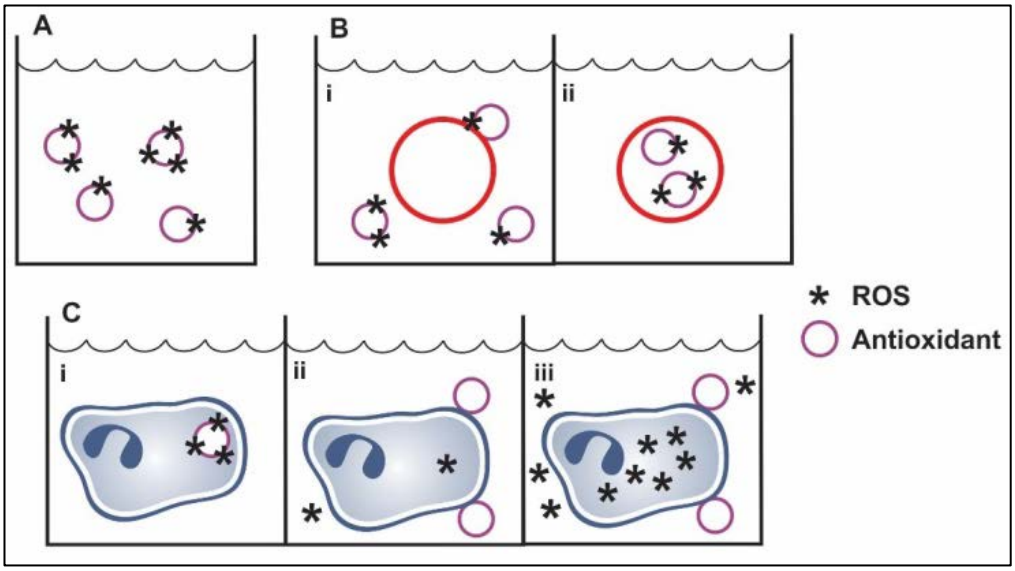

Figure 5.1. Strategies used in this study to evaluate antioxidant properties (adapted from Honzel *et al.*, 2008). A) **Chemical assays** measure direct scavenging capability. B) **Erythrocyte assays,** i) measure external antioxidant scavenging capability, ii) measure whether an antioxidant enters and protects a cell from ROS. C) **Leukocyte assays**, i) measure whether an antioxidant enters the cell and neutralises free radicals, ii) measure whether the antioxidant mediates inflammatory cell signalling to reduce ROS production, iii) measure whether the antioxidant mediates cell signalling to increase ROS production.

Thus the aim of this study was to determine if Os and Os-C have antioxidant activity and can protect erythrocytes and leukocytes against ROS and/or induce ROS production in leukocytes.

5.3) Materials and methods

5.3.1) Chemical antioxidant assays

Trolox equivalent antioxidant capacity assay

The TEAC assay (Figure 5.1A) is an electron transfer assay, used to measure antioxidant activity. The method used was based on the modified method of Awika *et al.* (2003) and was used to evaluate the reducing capacity of Os and Os-C compared to Mel and GSH (Miller *et al.*, 1993). A stock solution of ABTS was prepared by adding 3 mM of potassium peroxodisulfate ($K_2S_2O_8$) solution to 8 mM ABTS. The $ABTS^{\bullet+}$ was freshly generated for

each experiment by preparing an ABTS stock solution prior to experimentation. The mixture was incubated at room temperature in the dark for a minimum of 12 hours and used within 16 hours. The ABTS stock solution was diluted with 0.1 M PBS[b] (81 mM $Na_2HPO_4.2H_2O$, 19 mM $NaH_2PO_4.H_2O$, 0.15 M NaCl, pH 7.4), before use to obtain a working solution of 0.26 mM ABTS. A concentration range of 0.5 - 20 µM of Mel, Os and Os-C was used. Trolox (an analogue of vitamin E) was used as the standard at a concentration range of 0 - 1000 µM, with $dddH_2O$ as the blank (and negative control for antioxidant activity). GSH served as a positive control for antioxidant activity. A volume of 290 µL of the ABTS working solution was added to 10 µL of each peptide concentration or Trolox, incubated at room temperature for 15 minutes and the absorbance measured at 630 nm with the Emax Plus spectrophotometer (Molecular Devices, California, USA). The results were expressed as µM Trolox equivalent (TE).

Oxygen radical absorbance capacity assay

The ORAC assay (Figure 5.1A) is considered to be physiologically relevant as hydrogen atom transfer (HAT) reactions are an important step in the radical chain reaction in cells and tissue. The method used was based on the procedure described by Serem and Bester (2012) and modified from Ou *et al.* (2002) . A serial dilution of Trolox (0 - 800 µM) was used as the standard, with $dddH_2O$ as the blank (and negative control for antioxidant activity). Fluorescein was used as the fluorescent probe and 2,2'-azobis(2-amidinopropane) dihydrochloride (AAPH) was added to generate peroxyl radicals. A concentration range of 0.5 - 20 µM Mel, Os and Os-C peptides was used. GSH is a known antioxidant tripeptide that offers protection against peroxides and was thus used as a positive control for antioxidant activity (Zheng *et al.*, 2012). A volume of 160 µL of 0.139 nM fluorescein, 10 µL of either $dddH_2O$ or the various concentrations of Trolox or the three peptides were added in separate wells of a 96-well plate. Following this, 40 µL of a 0.11 µM AAPH solution was added to each well. The microplate was placed in a FLUOstar OPTIMA plate reader (BMG Labtechnologies, Offenburg, Germany) and the fluorescence measured every 5 min for 4 hours. The fluorescein was excited at a wavelength of 485 nm and the emission measured at 520 nm. The net area under the decay curve for each sample was calculated, and the final results were expressed as µM TE.

5.3.2) Erythrocyte antioxidant assays

Erythrocyte membrane protection assay

To determine if Os and Os-C protects erythrocyte membranes against oxidative damage (Figure 5.1B (i and ii)), erythrocytes were collected and processed as described previously in

Chapter 4, Section 4.2.1. A volume of 90 µL of 5% erythrocytes was incubated with 15 µL Mel, Os or Os-C (final concentrations 20 µM, 50 µM, 100 µM) for 30 min at 37°C. A volume of 15 µL AAPH (final concentration of 100 mM) was then added to generate peroxyl radicals, and incubated for a further 3 hours at 37°C. Two controls were included that were incubated with no peptide or Trolox, the first was not exposed to AAPH, the second was exposed to AAPH. Each sample was then centrifuged at 400 x*g*, 100 µL of the resulting supernatant was transferred to a 96-well plate and the absorbance measured at 570 nm with the Emax Plus spectrophotometer (Molecular Devices, California, USA). The % haemolysis was calculated as in Chapter 4, Section 4.2.2.

Cell-based antioxidant protection in an erythrocyte model (CAP-e) assay

The CAP-e assay (Figure 5.1B ii) was used to determine if Os and Os-C are able to enter erythrocytes and protect these cells against oxidative damage. Erythrocytes were collected and diluted to a 5% (*v/v*) suspension in isoPBS (0.137 M NaCl, 3 mM KCl, 1.9 mM NaH_2PO_4, 8.1 mM Na_2HPO_4, pH 7.4) as described in Chapter 4, Section 4.2.1. The method used was an adaption of the method described by Honzel *et al.* (2008). Instead of using H_2O_2, AAPH was used to generate radicals. A volume of 90 µL of 5% erythrocytes in isoPBS was added to 15 µL of each peptide (final concentrations 20 µM, 50 µM, 100 µM) in a 96-well plate and incubated for 60 min at 37°C. Two controls were included that were incubated with no peptide or Trolox, the first was not exposed to AAPH, the second was exposed to AAPH. A volume of 15 µL of a 75 µM solution of DCFH-DA was then added and incubated for a further 60 min. After incubation the erythrocytes were washed with isoPBS to remove all extracellular DCFH-DA and peptide. After washing, the erythrocytes were exposed to 15 µL AAPH (final concentration of 3 mM). The change in fluorescence was measured immediately for 60 min in 2 min intervals using an excitation wavelength of 485 nm and an emission wavelength of 520 nm with the FLUOstar OPTIMA plate reader (BMG Labtechnologies, Offenburg, Germany). The net area under the curve for each sample was calculated and used to calculate the % damage, where AAPH alone causes 100% damage.

5.3.3) Leukocyte antioxidant assays

Leukocyte separation

Venous blood was collected in the same manner as in Chapter 4, Section 4.2.1 for the haemolysis assay. The MN and PMN cells were separated and the cell concentration

adjusted to 1x10^6 cells/mL in RPMI containing 2% FBS in the same manner as in Chapter 4, Section 4.2.4.

Leukocyte ROS production

To determine if Os and Os-C induces ROS formation (Figure 5.1C iii) the method of Honzel and colleagues (2008) was adapted. MN and PMN cells were incubated separately in a concentration range (0.25 - 100 µM) of Os and Os-C for 90 min at 37°C and 5% CO_2. A control with the same volume of dddH_2O was included. The cell suspension was then rinsed twice with isoPBS to remove all extracellular peptide, and the cells incubated with 25 µM DCFH-DA in 0.1 M PBS[b], pH 7.4. The amount of ROS production by the leukocytes was detected by measuring the fluorescence intensity with the FLUOstar OPTIMA plate reader from BMG Labtechnologies (Offenburg, Germany) for 1 hour at 37°C. An excitation wavelength of 485 nm and an emission wavelength of 520 nm were used. The net area under the decay curve for each sample was calculated, and the final results were expressed as a percentage of the control by using the formula below:

$$\%\ ROS\ production = \frac{(sample\ fluorescence) - (background\ fluorescence)}{(maximum\ fluorescence) - (background\ fluorescence)} \times 100$$

Background fluorescence was taken as cells exposed only to water, and maximum fluorescence as cells exposed to 1.25 mM AAPH.

Leukocytes cellular protection assay

The ability of Os and Os-C to protect leukocytes against oxidative damage (Figure 5.1C i and ii) was then investigated. MN and PMN cells were exposed to a concentration range of 0.25 – 100 µM Os and Os-C for 90 min at 37°C and 5% CO_2. This was followed by incubation with 25 µM DCFH-DA in 0.1 M PBS[b], pH 7.4 for 1 hour. The leukocytes were then exposed to 1.25 mM AAPH for 45 min. The amount of ROS production by the leukocytes was detected by measuring the fluorescence intensity with the FLUOstar OPTIMA plate reader from BMG Labtechnologies (Offenburg, Germany) for 1 hour at 37°C. An excitation wavelength of 485 nm and an emission wavelength of 520 nm were used. The net area under the decay curve for each sample was calculated. The results were expressed as a percentage of the control and were calculated in the same manner as for the ROS production assay.

5.3.4) Data analysis

Each experiment consisted of three repeats of each concentration, and the experiment was repeated three times. Multiple comparisons were tested by one-way ANOVA followed by the Tukey post hoc test for significant difference between the different peptides. Linear regression fit and comparison of the slopes for statistical significance was done on a scatterplot for the TEAC, ORAC, erythrocyte membrane protection and leukocyte ROS production assays (Graphpad Prism v6.01, California, USA). Significance was set at $p < 0.05$.

5.4) Results

5.4.1) Chemical antioxidant activity

The antioxidant activity of the peptides was evaluated using the TEAC assay. This assay is based on a single electron transfer, where the oxidant probe is reduced by the transfer of an electron from the antioxidant molecule, resulting in a colour change that is measured. The change in colour is directly proportional to the concentration of antioxidant present (Huang *et al.*, 2005). The results indicated a dose-dependent increase, with Os showing significantly higher antioxidant capability than both Mel and GSH at all concentrations tested (Figure 5.2A). Os-C showed significantly higher antioxidant activity at the 50 µM and 100 µM concentrations. A dose-dependent increase in activity was confirmed by linear regression analysis with R^2 values of 0.9972 and 0.9974 for Os and Os-C, respectively (Figure 5.2B). Os showed more activity than Os-C, as indicated by the significant difference at the 100 µM concentration (Figure 5.2A) and the steeper slope (10.577 compared to 8.331, Figure 5.2B). However, there was no statistically significant difference ($p > 0.05$) observed between the slopes in Figure 5.2B.

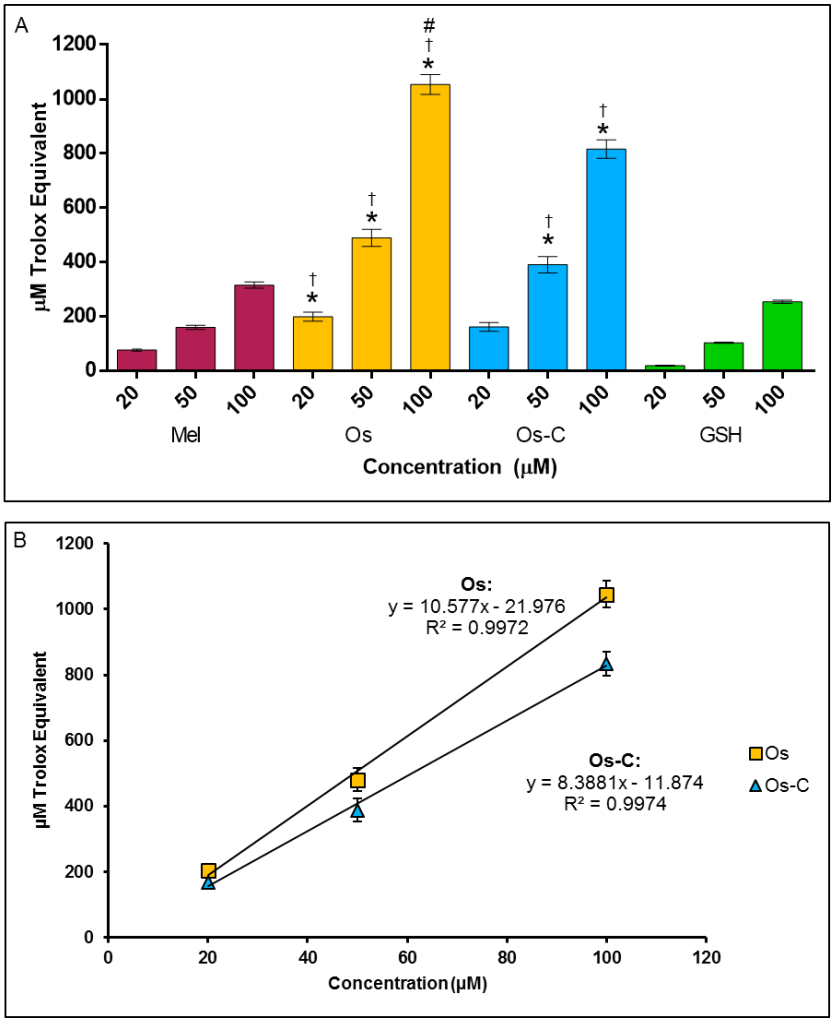

Figure 5.2. Antioxidant activity (TEAC assay) of Os and Os-C compared to Mel and GSH. A) Bar chart comparison, B) Dose response comparison of Os and Os-C. Asterisks indicated significant difference to the same Mel concentration, crosses indicate significant difference to the same GSH concentration and the hash indicates significant difference to Os-C of the same concentration ($p < 0.05$, $n = 9$).

The antioxidant ability of the peptides was also investigated using the ORAC assay. This assay measures hydrophobic and lipophilic chain-breaking antioxidant activity and is therefore more biologically relevant than the TEAC assay (Huang *et al.*, 2005). It also measures antioxidant capacity over time, which allows detection of activity of slow acting compounds (Schaich *et al.*, 2015). The ORAC assay is a HAT assay, meaning that the antioxidant donates a hydrogen atom to the free radical in the same manner as the substrate (in this case it was a probe that fluoresces upon binding the free radical). This results in the antioxidant competing with the substrate for free radicals (Ou *et al.*, 2002, Huang *et al.*, 2005). A dose-dependent increase in ORAC activity was observed with the two synthetic peptides Os and Os-C (Figure 5.3). The dose-effect was confirmed by a linear fit with R^2-values of 0.9985 (slope 21.682) and 0.9826 (slope 22.956) for Os and Os-C, respectively (Figure 5.3B). At the 20 µM concentration, Os had an ORAC value of 456.59 µMTE, and Os-C an ORAC value of 478.06 µMTE, whereas Mel showed little antioxidant activity with an

ORAC value of 31.15 µMTE (Figure 5.3A). GSH is a known antioxidant tripeptide that offers protection against peroxides (Zheng *et al.*, 2012). The peptides Os and Os-C showed approximately six times higher Trolox equivalence at 20 µM than GSH. There were no significant differences observed between Os and Os-C at any of the concentrations tested. Linear regression analysis showed no significant difference between the slopes (Figure 5.5, $p > 0.05$).

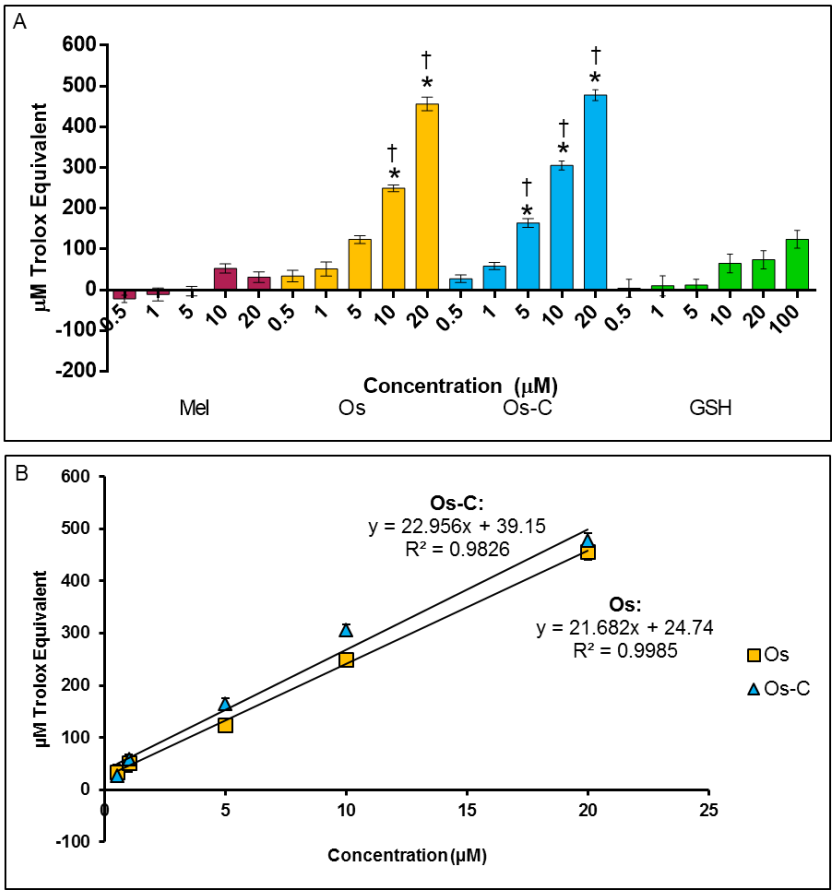

Figure 5.3. Antioxidant activity (ORAC assay) of Os and Os-C compared to Mel and GSH. A) Bar chart comparison, B) dose response comparison of Os and Os-C. Data is the average of two experiments with three repeats each ± SE. Asterisks indicated significant difference to the same Mel concentration and crosses indicate significant difference to the same GSH concentration ($p < 0.05$, $n = 6$).

5.4.2) Protection of erythrocytes against oxidative damage

The erythrocyte cell membrane is a typical bilayer that can be used to determine the ability of antioxidants to protect this membrane against oxidative damage (Tabart *et al.*, 2009, Ximenes *et al.*, 2010). With the erythrocyte membrane protection assay, human erythrocytes are exposed to peroxyl radicals generated by AAPH that cause oxidative damage. Oxidation of the membrane proteins and lipids results in a loss of membrane integrity and subsequently the leakage of Hb, that can be quantified at 450 nm. Peptides with antioxidant activity would protect the erythrocytes from ROS induced damage, thus reducing the amount

of Hb released (Tabart *et al.*, 2009, Ximenes *et al.*, 2010). Results indicated that both Os and Os-C offered protection against AAPH induced oxidative damage (Figure 5.4). At 100 µM, Os offered 87.3% protection, whereas Os-C showed 67.9% protection. However, there was no statistical difference found with the Tukey multiple comparison test. Both Os and Os-C offered significantly greater protection than GSH at both 50 µM and 100 µM concentrations (Figure 5.4A). Both peptides also showed a dose-dependent increase in membrane protection as can be seen by the linear fit in Figure 5.4B. Os had an R^2-value of 0.9506, and Os-C an R^2-value of 0.9965. No significant difference was observed between the slopes of Os and Os-C in Figure 5.7 ($p > 0.05$).

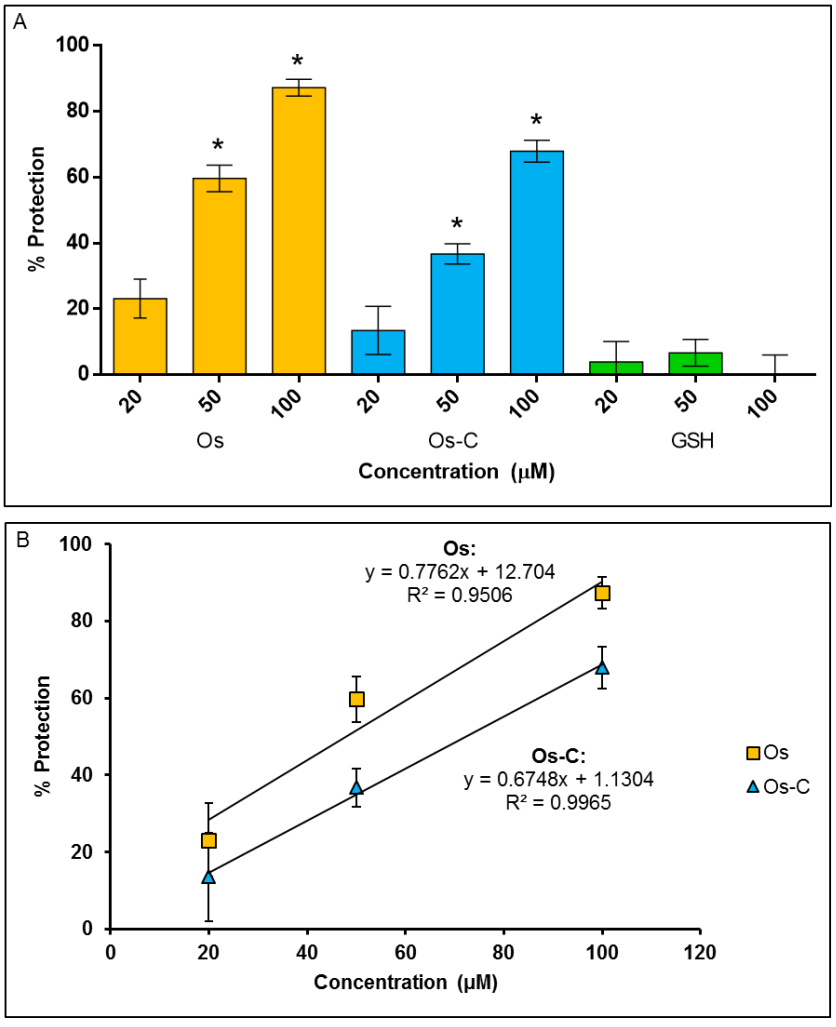

Figure 5.4. Antioxidant protective effects of Os, Os-C and GSH against AAPH induced erythrocyte membrane damage. A) Bar chart comparison, B) Dose response comparison of Os and Os-C. Data is the average of six experiments ± SE. Asterisks indicate significant difference to same concentration of GSH ($p < 0.05$, $n = 18$).

The CAP-e assay determines whether antioxidants cross the cell membrane and from the intracellular environment protect erythrocytes from oxidative damage. In the CAP-e assay,

erythrocytes are incubated with Os, Os-C, GSH and caffeic acid. Excess peptide is then removed and then the cells are incubated with DCFH-DA which rapidly crosses the cell membrane. Intracellularly DCFH-DA is cleaved to DCFH by intracellular esterase, which cannot cross the membrane. Excess DCHF-DA is removed and then the erythrocytes are exposed to an oxidant such as AAPH. With oxidation, DCFH is converted to fluorescent DCF which is quantified. Antioxidants will prevent the conversion of DCFH to DCF resulting in lower fluorescence compared with the controls exposed to AAPH. The positive control caffeic acid was included in these experiments as this small phenolic acid is capable of increasing intracellular antioxidant activity (Jeong *et al.*, 2011). GSH was used as a peptide antioxidant control. Caffeic acid showed the most intracellular protection and illustrated the sensitivity of this assay (Figure 5.5). Os, Os-C and GSH showed significantly lower antioxidant capability than caffeic acid at all concentrations tested. GSH showed only 10% protection at both 50 µM and 100 µM. Neither Os nor Os-C showed significant intracellular protection of erythrocytes against AAPH induced ROS.

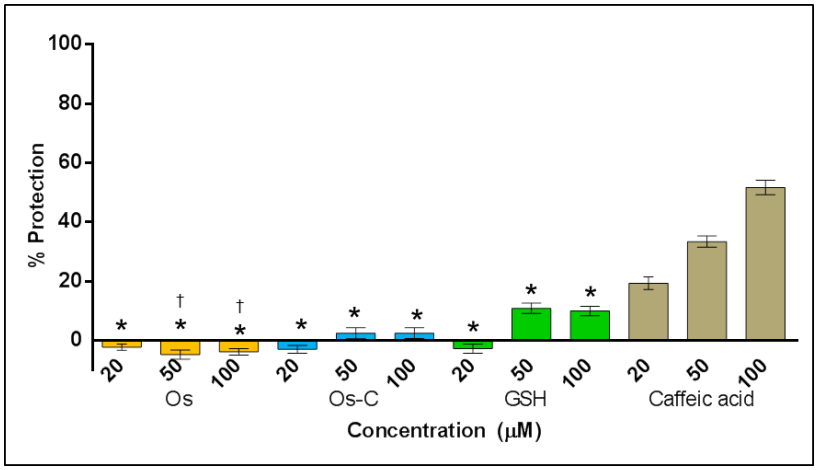

Figure 5.5. Intracellular antioxidant activity of Os and Os-C in erythrocytes. Data is the average of three experiments ± SE. Asterisks indicated significant difference to the same caffeic acid concentration, crosses indicate significant difference to the same GSH concentration ($p < 0.05$, $n = 9$).

5.4.3) Protection of leukocytes against oxidative damage

Leukocytes were used in order to study the effects of Os and Os-C on a more complex cell than the erythrocyte. The peptides may affect leukocytes in two different ways. As pro-oxidants, peptides can increase cellular function and consequently the formation of ROS and as antioxidants, these peptides can protect cells from oxidative damage by reducing intracellular ROS levels.

H_2O_2 is a secondary messenger in leukocyte activation and this process is an important component of innate immunity. Intracellular H_2O_2 is converted to ROS and these levels can

be quantified using DCFH-DA (Honzel *et al.*, 2008). All peptides tested caused a slight increase in the production of ROS by MN cells, in a dose-dependent manner (Figure 5.6). Mel and Os-C caused 14.1% and 15.7% ROS production at 100 µM, respectively. Os caused 9.3% ROS production which is significantly lower than Os-C at 100 µM. Figure 5.6B shows the dose-dependent increase in ROS production by Os and Os-C exposed MN cells. Os-C had a significantly higher slope than Os ($p < 0.01$) indicating a higher dose response.

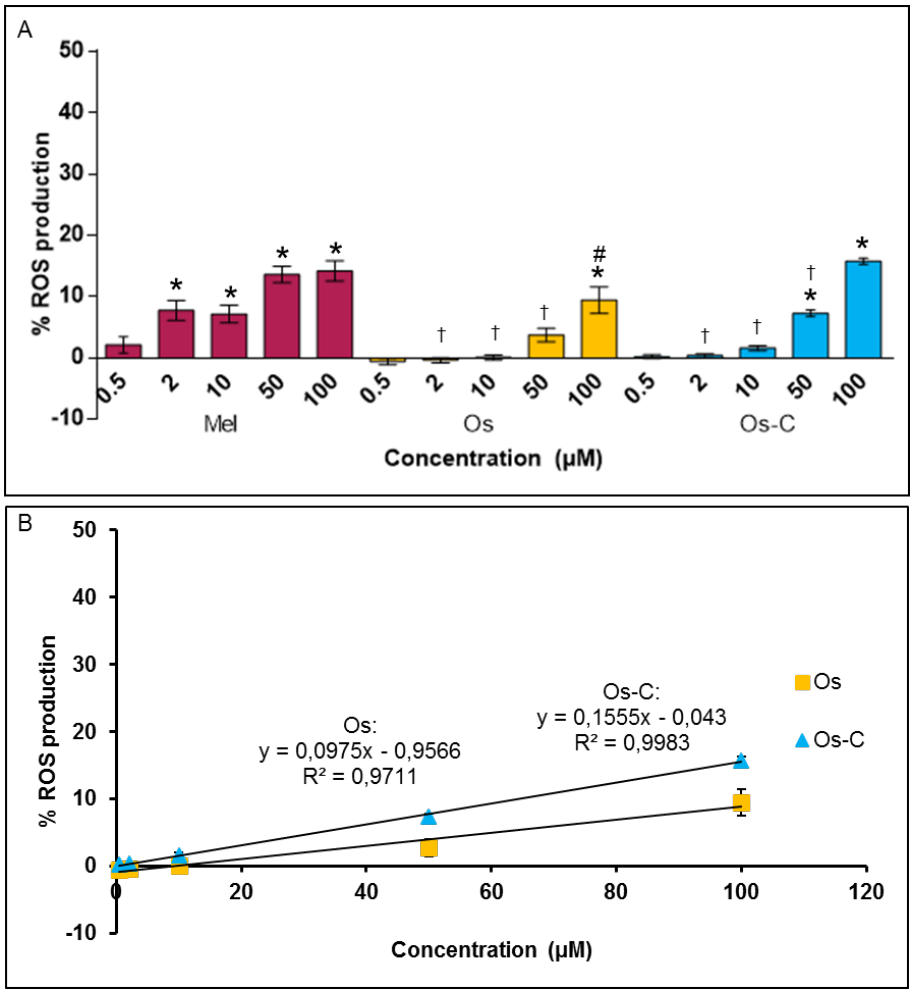

Figure 5.6. ROS production in MN leukocytes stimulated by Os, Os-C and Mel. A) Bar chart comparison, B) dose response comparison of Os and Os-C. Data is the average of two experiments ± SE. Asterisks indicate significant difference to the control (0% ROS production), crosses indicate significant difference the same Mel concentration and hash indicate significant difference between Os and Os-C at the same concentration ($p < 0.05$, $n = 6$).

Os-C caused a marked increase in ROS production by PMN cells, as compared with the other peptides at 50 µM and 100 µM (Figure 5.7). At 100 µM Os-C led to 31% ROS production, whereas Mel caused only 4.1%. Exposure to Os resulted in a small decrease in ROS production at all concentrations, as compared with the control exposed only to water. Mel also caused a decrease in ROS production at concentrations below 10 µM. Os-C

exposed PMN cells showed a dose-dependent increase in ROS production, with a significant difference to Os ($p < 0.01$ between slopes, Figure 5.7B).

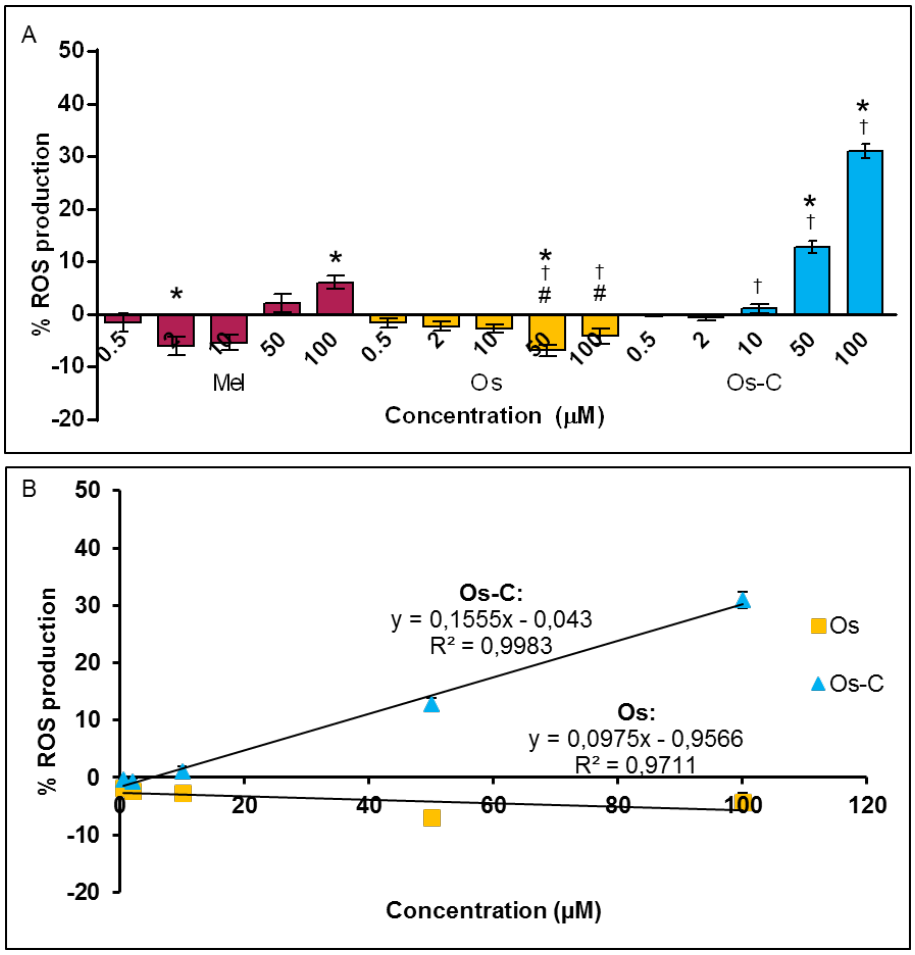

Figure 5.7. ROS production in PMN leukocytes stimulated by Os, Os-C and Mel. A) Bar chart comparison, B) dose response comparison of Os and Os-C. Data is the average of two experiments ± SE. Asterisks indicate significant difference to the control (0% ROS production), crosses indicate significant difference the same Mel concentration and hash indicate significant difference between Os and Os-C at the same concentration ($p < 0.05$, $n = 6$).

Antioxidant peptides may penetrate into leukocytes and neutralise intracellular or endogenous sources of ROS, either by direct scavenging or by inhibition of the associated pathways. A dosage dependent increase in the % protection indicates antioxidant activity while a decrease < 0% indicates no scavenging activity but rather that ROS formation was induced. Caffeic acid was used as a positive control, and showed maximal ROS scavenging at concentrations 10 µM and higher for both MN and PMN cells (Figure 5.8B & D). Mel and Os-C showed no scavenging activity but a dosage dependent increase in ROS formation was observed in MN cells (Figure 5.8A), which confirms the findings presented in Figure 5.6. No dosage effect was observed for Os or GSH although the range for Os was 2.7% - 13.5% and for GSH 9.8% - 16.7% which implies some degree of protection.

In contrast to MN cells, Mel had an increased scavenging effect at low concentrations in PMN cells (Figure 5.8C). The intracellular scavenging or antioxidant effect of both GSH and Os was greater than that observed for MN cells. A dosage effect was observed for GSH while Os caused a statistically significant increase in activity of 23.4% at 50 µM and 25.5% at 100 µM. Os-C caused and increase in ROS formation in PMN cells at 50 and 100 µM and this confirmed the findings in Figure 5.6.

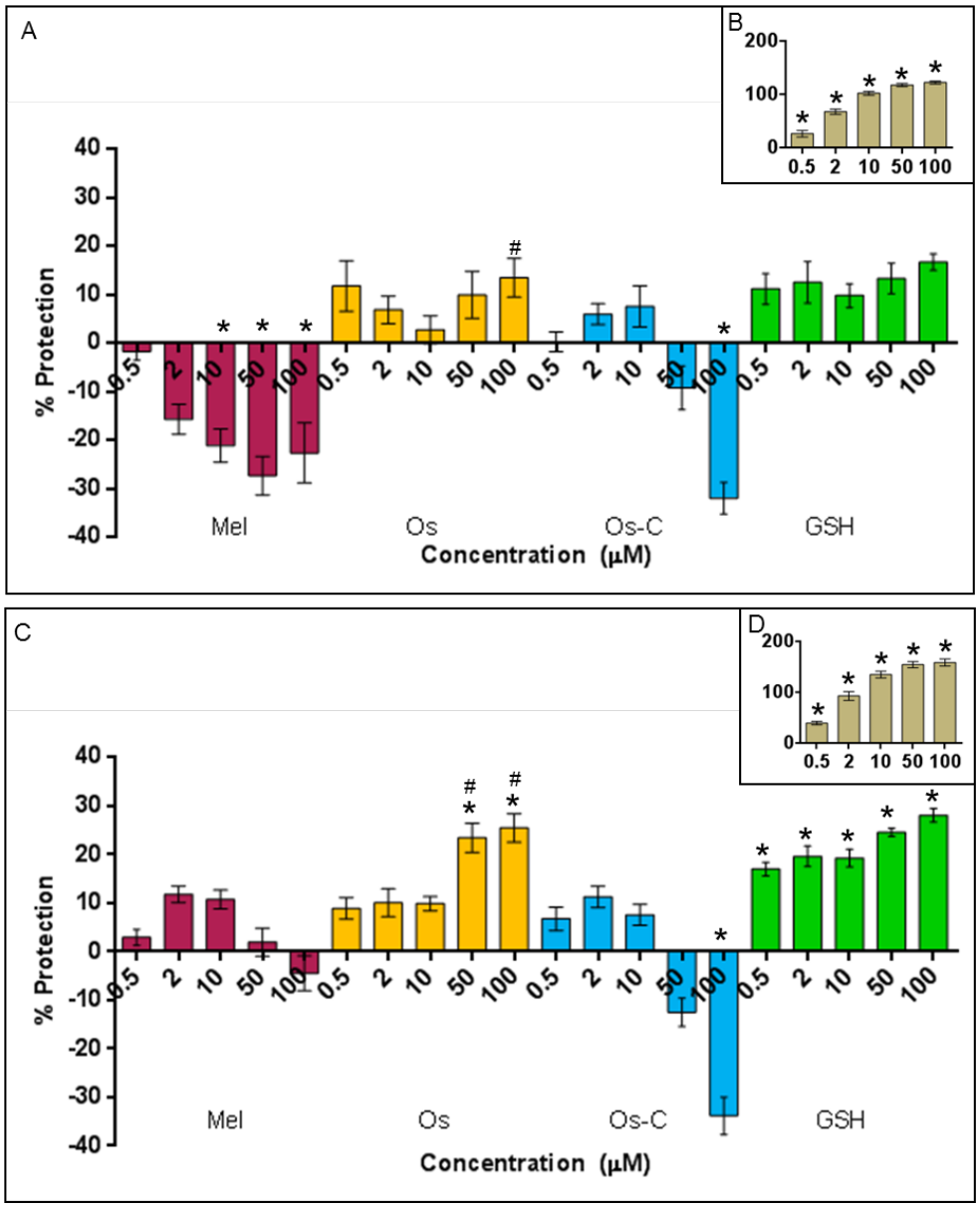

Figure 5.8. Protection against AAPH induced oxidative damage in leukocytes by Mel, Os, Os-C, GSH and caffeic acid. A) MN leukocytes, B) caffeic acid insert, C) PMN leukocytes, D) caffeic acid insert. Data is the average of two experiments ± SE. Asterisks indicate significant difference to AAPH (0% ROS protection), number signs indicate significance between to Os-C of the same concentration ($p < 0.05$, $n = 6$).

5.5) Discussion

Os and Os-C were previously found to effectively kill bacteria and not to be cytotoxic to eukaryotic cells at concentrations that cause bacterial killing (Prinsloo *et al.*, 2013). At high concentrations Os-C was found to cause morphological features associated with leukocyte activation (Chapter 4). Many AMPs have multifactorial bioactivity and therefore the aim of this study was to determine the ROS scavenging i.e. antioxidant activity of both peptides and at the same time confirm whether Os-C PMN activation is mediated by ROS formation.

Using chemical based assays, the antioxidant activity of the peptides was determined. The first assay used was the TEAC assay which is based on single electron transfer (ET). The antioxidant capacity is an actual measurement of reducing capacity since there are no oxygen radicals involved in the reaction (Huang *et al.*, 2005, Serem, 2012). A disadvantage of using an ET reaction based assay, is that they are sensitive to pH. The reducing capacity of ET reactions may be inhibited in acidic conditions due to protonation of antioxidant compounds, while basic conditions could enhance reducing capacity of the sample tested due to proton dissociation (Huang *et al.*, 2005).

The ORAC assay was also used which is based on a HAT reaction (Schaich *et al.*, 2015). The ORAC assay measures hydrophobic and lipophilic chain-breaking antioxidant activity and is therefore more biologically relevant than the TEAC assay (Huang *et al.*, 2005). This assay also measures antioxidant capacity over time, which allows detection of activity of slow acting compounds (Schaich *et al.*, 2015). In this type of assay, the antioxidant and substrate compete for free radicals (Huang *et al.*, 2005). HAT assays follow the reaction:

$$ROO^{\bullet} + AH \rightarrow ROOH + A^{\bullet}$$

The antioxidant (AH) donates a hydrogen atom (H) to reduce the free radical ($ROO^{\bullet}$) (Huang *et al.*, 2005). In the ORAC assay peroxyl radicals are generated by AAPH. An indicator molecule (fluorescein) is also present that loses fluorescence upon binding to the free radical. The ability of the antioxidant to protect the indicator molecule is thus measured (Ou *et al.*, 2002).

Both the TEAC and ORAC assays showed that Os and Os-C have much greater antioxidant activity than the positive control tripeptide GSH. Os showed significantly higher antioxidant activity than Os-C, as measured with the TEAC assay. As mentioned before, the amino acid composition of a peptide could influence its antioxidant activity. Both Os and Os-C have the same number of Trp and Tyr residues and the sequence IR. In addition, Os contains three

Cys residues which also contributes to antioxidant activity (Hernández-Ledesma *et al.*, 2005). The additional Cys residues in Os may contribute to the observed antioxidant effect as the mechanism of Cys antioxidant activity is the donation of a hydrogen atom from its thiol group (Elias *et al.*, 2005). As the latter process involves HAT, a difference in antioxidant activity is expected between Os and Os-C when quantified with the ORAC assay. However, no differences were observed between Os and Os-C.

Yang and colleagues (2009) identified 14 groups of peptides containing 36 peptides in total from the skin of the frog *Rana pleuraden*. Eleven of these groups showed antioxidant activity and all peptides contained Pro. The researchers found that replacement of Pro, Cys and Tyr with glycine (Gly) caused a marked decrease in antioxidant activity. Placement of Pro at different positions also resulted in differences in antioxidant activity which indicated that peptide antioxidant activity is sequence-specific (Yang *et al.*, 2009). The difference in peptide sequence of Os-C could therefore be the cause for the decreased antioxidant activity observed in the TEAC results, and not necessarily just the absence of Cys.

The next step was to evaluate antioxidant activity using a cellular model which is more physiologically relevant. In this study the effect of both peptides on erythrocytes and leukocytes was determined as both cell types play important roles in protecting other cells such as the endothelium of blood vessels against oxidant damage as well as maintaining the antioxidant status of the blood (Honzel *et al.*, 2008). Erythrocytes represent the most abundant cell type in blood and these cells have a well-developed antioxidant system consisting of GSH and several antioxidant enzymes (Chapter 2, Table 2.3). Endogenous dietary antioxidants also contribute to this antioxidant capacity of erythrocytes. With infection, these systems are compromised and consequently an AMP with antioxidant activity can re-establish and/or improve the antioxidant capacity of blood. Erythrocytes are suitable for membrane damage studies as these cells contain no DNA and have a typical bilayer membrane and due to the absence of mitochondria the assays used are not affected by cellular ROS formation. In many studies H_2O_2 is used to generate ROS, however, in the present study AAPH is used as a radical generator. H_2O_2 degrades rapidly while AAPH provides a constant time dependent release of peroxyl radicals (Wolfe & Liu, 2007). AAPH is also the radical generator used in the ORAC assay, so use of AAPH in the cellular assays allows for more direct comparison.

Although erythrocytes have well developed GSH and enzyme mediated antioxidant capacity, excessive oxidant levels cause haemolysis. For this reason, the ability of peptides to protect against this oxidative effect to reduce the levels of haemolysis can be quantified (Tabart *et al.*, 2009, Ximenes *et al.*, 2010). Both peptides effectively protected erythrocytes against

oxidative damage with the membrane protection assay. The CAP-e assay was used to determine whether the peptides can cross the cell membrane, and from an intracellular milieu, protect erythrocytes against oxidative damage (Honzel *et al.*, 2008). Neither Os nor Os-C were able to protect erythrocytes against oxidative damage, suggesting that the peptides were unable to enter these cells. GSH offered little protection in both erythrocyte assays. GSH is a physiological antioxidant tripeptide found in healthy erythrocytes and unless the blood has already been compromised before donation it would contain sufficient GSH. The addition of extra GSH is therefore unlikely to greatly increase the amount of protection offered by this molecule.

Mel, Os and Os-C caused an increase in ROS production by MN cells. However, at concentrations at 1 µM and above, Mel was found to be cytotoxic and induced leukocyte apoptosis. During apoptosis, cytochrome c is released from the mitochondria, and is able to oxidise DCFH directly or indirectly to form the fluorescent DCF (Kalyanaraman *et al.*, 2012). Consequently, an artefactual increase in fluorescence occurs which is unrelated to ROS production.

The cytotoxicity and ultrastructural results (Chapter 4) showed that Os but not Os-C had a cytotoxic effect on MN and PMN cells. Necrosis is associated with increased levels of ROS, which would be reflected in the DCFH-DA assay (Friers *et al.*, 1999). The slight increase in ROS observed for MN cells exposed to Os or Mel could therefore be attributed to an increase in DCF fluorescence due to cell death. However, the cytotoxicity results and ultrastructural features observed for Os-C serve as confirmation that the increase in fluorescence observed with the leukocyte antioxidant assays was due to an increase in ROS produced by the cells, and is not an artefact due to cell death. Phagocytes are known to kill pathogens by production of ROS during the respiratory burst after activation (Male *et al.*, 2013). It is therefore possible that Os-C caused activation of peripheral leukocytes which lead to an increase in ROS production. This is supported by the ultrastructural observations presented in Chapter 4. NADPH oxidase catalyses the production of O_2^- and H_2O_2 in stimulated phagocytes with the concurrent consumption of oxygen. Both O_2^- and H_2O_2 are used during the destruction of microbes in phagocytic cells (Robinson, 2008). Zughaier *et al.* (2005) found that various AMPs caused a slight increase in ROS generation by macrophages. The AMPs were able to neutralise endotoxin induced nitric oxide and tumour necrosis factor (TNF)-α release in human and murine macrophages in a toll-like receptor 4 (TLR4)-dependent manner. However, the researchers also found that LPS and AMPs synergistically increased ROS release by macrophages to a much greater level than AMP or LPS alone. This increase in ROS production was TLR4-independent, which suggested that the combination increased NADPH oxidase catalysis (Zughaier *et al.*, 2005). Malan *et al.*,

(2016) showed that Os and Os-C possess anti-endotoxin activity. Both peptides were able to reduce LPS/IFN-γ induced NO and TNF-α production in murine macrophages (Malan *et al.*, 2016). The low level of increased ROS production seen in leukocytes exposed to Os-C in the present study indicate activation of the respiratory burst mechanism in these cells which may work synergistically with LPS as in the Zughaier *et al.* (2005) study. Further studies are necessary to determine whether Os-C directly affects NADPH oxidase, and/or whether it is a synergistic effect with LPS. Another possible pathway for leukocyte stimulation by AMPs is the complement receptors. If the peptides bind to the C3a and C5a complement receptors of polymorphs and macrophages, it will lead to an increase in pro-inflammatory molecules, including reactive oxygen intermediates (Male *et al.*, 2013). It must also be considered that although up-regulation of the amount of ROS production by leukocytes could lead to more effective killing of infectious agents, uncontrolled ROS production could lead to an unwanted inflammatory response and sepsis (Zughaier *et al.*, 2005).

The ability of Os and Os-C to protect leukocytes against oxidative damage was then determined. GSH showed limited antioxidant activity in erythrocytes and this was probably due to high intracellular GSH levels. For this reason, the polyphenol, caffeic acid, was used as a positive control. Caffeic acid protected MN and PMN cells against the oxidative effects of AAPH in a dose-dependent manner. Possible peptide effects are: dosage dependent increase in antioxidant activity, no effect or a pro-oxidant effect i.e. the observed levels of ROS are greater than that of AAPH. In MN cells, caffeic acid was found to have antioxidant activity, Os and GSH had no effect and Mel as well as Os-C at the highest concentration had a pro-oxidant effect. In PMN cells, caffeic acid and GSH had antioxidant activity, Os had activity at 50 and 100 µM and Os-C had a pro-oxidant effect.

Malan *et al.* (2016) found that Os and Os-C protected RAW 246.7 mouse macrophage cells against AAPH induced oxidative damage to a greater degree than found in the present study. The experimental design was similar to that of the haemolysis assay and it is unknown if the peptides cross the cell membrane and thereby directly protect these cells against oxidative damage. Interestingly, Malan *et al.* (2016) also found that Os and Os-C could scavenge NO and reduce levels of LPS-induced NO formation. The mechanism/s involved are unknown, however, it was found that there were differences in the mode of action of Os and Os-C related to anti-inflammatory effects. In addition, the present study showed that Os and Os-C have additional beneficial effects related to creating a cellular environment free of ROS and the ability of Os-C to induce ROS formation.

Many endogenous and food derived peptides have been studied for antioxidant potential. However, very few studies could be found concerning antioxidant activity of insect derived

defensins and none on tick defensins. Therefore, this study is the first to determine antioxidant potential of a tick derived defensin.

5.6) Conclusion

In conclusion, both Os and Os-C showed antioxidant activity with the chemical based assays and protected erythrocyte membranes from oxidative damage. Os did not cause ROS production, whereas Os-C caused increased ROS production especially by PMN cells and this confirms PMN activation by Os-C. Os did provide some protection of PMN cells against oxidative damage.

Chapter 6: Concluding discussion

In a world with no working antibiotics, major surgery, organ transplants and chemotherapy among other things would not be possible (Schaich *et al.*, 2015). Many factors contribute toward the development of antibiotic resistance, including high rates of antibiotic use in hospitals, the community and agriculture, misdiagnosis of infection, inappropriate treatments and improper dosage. Resistance arises as a result of mutations in microbes and selection pressure which benefits mutated strains (Schaich *et al.*, 2015). In order to combat antibiotic resistance, a multifaceted global strategy is necessary. These interventions are to prevent infection, to promote investments into developing new antimicrobial treatments from both private and state sectors, to slow the spread of resistant strains to prolong the usefulness of current antibiotics, to find new direct killing targets which will not promote resistance, and lastly to modify host-microbe interactions without directly killing the microbes (Rai *et al.*, 2016).

The present study of AMPs was undertaken with the aim to further investigate alternative antibiotic treatment options. Because AMPs are relatively new molecules in the research of antimicrobials, many aspects such as mode of bacterial killing, the effect on eukaryotic cells needs to elucidated long before these peptides can be considered as therapeutic agents. Furthermore, immunomodulatory peptides need to be carefully evaluated. Overstimulation or suppression of the immune response may lead to a disruption in homeostasis, which in turn may lead to overproduction of cytokines or sepsis. Most clinical trials have focused on the use of AMPs as topical treatment, consequently there exists a lack of systemic data (Yeung *et al.*, 2011).

Besides having antibacterial activity, Os and Os-C were found to possess antioxidant and anti-inflammatory activities (Prinsloo *et al.*, 2013, Malan *et al.*, 2016). Additional positive attributes such as these identifies these AMPs as multifunctional peptides that can target several aspects of infection. A limitation of these studies are that evaluation of activity has been done using cell lines. In a first step toward the study of systemic effects of the peptides, the effects on peripheral blood cells was investigated. Therefore, the aims of the study were to investigate the effects of the synthetic peptides Os and Os-C both on bacteria and on human peripheral blood cells. A summary of all the effects observed and types of activity confirmed by results is presented in Table 6.1.

Table 6.1. Summary of peptide effects and activities found in this study

	Activity	Mel	Os	Os-C
Bacterial effects	Membrane permeabilisation	√	√*	√
	DNA binding capability	√	√*	√
	Intracellular effects (TEM)	√	√	√
	Membrane blebbing	√	X	X
	Other membrane effects (TEM)	√	√	√
	Cross membrane	-	√	√[1]
Cytotoxicity	Erythrocytes	√	X	X
	Mononuclear leukocytes (AB)	√	√ (100 µM)	X
	Polymorphonuclear leukocytes (AB)	√	X	X
	Mononuclear leukocytes (EM)	√	√	X
	Polymorphonuclear leukocytes (EM)	√	√	√[2]
Antioxidant activity	TEAC	-	√*	√
	ORAC	-	√	√
	Erythrocytes extracellular	-	√	√
	Erythrocytes intracellular	-	X	X
	Mononuclear leukocytes	-	√*	√ (< 10 µM)
	Polymorphonuclear leukocytes	-	√	X
Activation	Mononuclear ROS production	-	X	√
	Polymorphonuclear ROS production	-	X	√
	Mononuclear morphology (EM)	-	X	√
	Polymorphonuclear morphology (EM)	-	X	√

√ Effect observed, * higher activity between Os and Os-C, X effect not observed, - not tested
[1]Unable to cross stationary phase *E. coli*, stain septa of *B. subtilis,* [2]associated with activation

Using electron microscopy, the ultrastructural features of bacteria were very different to the effects observed with Mel. TEM studies revealed that not only was the structure of the cell membrane altered but changes to intracellular morphology indicated additional intracellular targets. Fluorescently labelled Os and Os-C were both able to enter stationary and exponential growth phases of the bacteria. The exception was Os-C, which was unable to cross the membranes of *E. coli* in the stationary phase. SYTOX green and the fluorescence triple stain results indicated that both peptides were able to permeabilise the bacterial membranes at low concentrations. However, the degree of permeabilsation was less than Mel. A decrease in SYTOX fluorescence, the capability to bind DNA, and the ability of peptides to enter bacterial cells indicated possible intracellular action. It is therefore suggested that Os and Os-C have a dual mechanism of action on bacteria which include

both membrane and intracellular targets. Differences such as differences in killing time, the inability of Os-C to enter stationary *E coli* cells and the localisation of Os-C to the septa of *B. subtilis* indicates differences in the mode of action. Ultrastructure analysis following exposure indicates that although the mechanism of killing may differ the consequence of exposure results in similar cellular effects.

Pexiganan is undergoing phase 3 testing in a clinical trial for the topical treatment of diabetic foot ulcers. The concentration used in the clinical trial was 8 mg/mL or 3 mM. Pexiganan was previously shown to inhibit the growth of bacteria between 3 – 30 µM, depending on the bacterial strain (Flamm *et al.*, 2015). Os and Os-C had MBC values ranging between 0.38 – 6.98 µM depending on the bacterial strain (Prinsloo *et al.*, 2013). Because Os and Os-C are able to kill bacteria at these low concentrations, they are good candidates for further development as antibiotic agents.

Often the clinical application of AMPs is limited due to the cytotoxicity of the peptides. An example of such a peptide is Mel. For this reason Mel was used as a control. Both Os and Os-C at all concentrations evaluated did not cause damage to erythrocytes, and no change to their ultrastructure was observed. Mel, on the other hand caused haemolysis of erythrocytes and the formation of echinocytes at concentrations above 10 µM.

At the highest concentrations Os caused loss of MN cellular viability while no change in PMN cell viability was measured. Ultrastructural damage could be observed in both MN and PMN cells exposed to 50 µM and 100 µM Os which displayed a mixture of apoptotic and necrotic features. The discrepancy in damage to cells between erythrocytes and leukocytes can be explained by the difference in cell numbers and exposure time used in the different assays, the difference in cell membrane structure and cell function or response to activation. Even though the same concentration of peptide was used, a larger number of cells were used in the erythrocyte assay as compared with the leukocyte assays. The cell concentration used for the leukocyte assays was $1x10^6$ cells/mL. A 5% *v/v* dilution of erythrocytes was used for the haemolysis assay, and the cell concentration of a 5% dilution was determined to be $4.65x10^8$ cells/mL. Thus there was a much lower ratio of peptide to cells in the haemolysis assay. Erythrocytes in circulation outnumber leukocytes roughly by 43%, as such the difference in cell numbers used in the respective assays correlates with the *in vivo* environment. In addition, the haemolysis assay measured immediate effects as the cells are exposed for 30 min before measurement. The leukocyte cytotoxicity assay measured long term effects by exposing the cells for 24 hours before measurement.

Leukocyte ROS production was measured over a short time of 2 hours. Fluorescence studies showed that Os-C caused an increase in ROS production by leukocytes at high concentrations. Longer exposure to Os-C of between 18 – 24 hours did not cause any damage to leukocytes but resulted in ultrastructural changes associated with cell activation observed in both MN and PMN cells. This indicates initial stimulation of leukocytes to produce ROS which does not lead to cell death but rather prolonged activation.

Chemical and erythrocyte antioxidant assays indicated that both Os and Os-C are good antioxidants. Os and Os-C created an extracellular environment that protected erythrocytes from oxidative damage. Os and Os-C did not cross the cell membrane of erythrocytes and protect the intracellular environment against oxidative damage.

Os-C was also able to stimulate leukocytes to produce ROS, which indicated an immunomodulatory function. A previous study demonstrated the anti-inflammatory activity of Os and Os-C by showing their ability to bind to LPS, and the ability of Os but not Os-C to scavenge NO (Malan *et al.*, 2016). These results further support the immunomodulatory activity of these peptides although the mechanism as for antibacterial activity may differ. Immunomodulatory peptides may serve as alternative therapies for the treatment of chronic inflammatory diseases (Schall *et al.*, 2012). Os crossed the cell membrane of PMN cells and protected these cells against oxidative damage. A limitation of the DCFH-DA assay is that it only evaluates short term antioxidant effects. Longer time studies such as that used for the AB assay and electron microscopy showed cellular toxicity. Observed effects are a function of cell density, concentration and incubation times as well as the type of assays and techniques used. As such, extrapolation of findings is often difficult.

In conclusion, the results of the study indicated that both Os and Os-C have dual mechanisms of action for bacterial killing, which include membrane and intracellular targets. This decreases the possibility of microbes to develop resistance to the peptides. Os-C caused no cellular toxicity to human blood cells, and Os caused toxicity only at the highest concentration evaluated. This suggests that both the peptides would be safe to use at concentrations close to the MBCs. Both peptides were good extracellular antioxidants, and would prove beneficial in a wound healing environment where there is an excess of radicals due to infection. Some intracellular protection was observed for Os. Os-C caused activation of peripheral leukocytes, which could be useful in the initial immune defence against invading pathogens. However, excess amounts of Os-C may lead to overstimulation and inflammation.

6.1) Limitations and future perspectives

In order to plan for future research, it is important to evaluate the limitations of the present study. Firstly, the type of bacteria used in experimentation needs to be clinically relevant. As stated in Chapter 3 a relapse of infection may occur if all non-dividing bacteria are not eliminated (Coates *et al.*, 2002). Therefore, measured antibacterial activity need to be confirmed in a stationary phase bacteria population. Furthermore, the activity of the peptides needs to be evaluated against drug resistant or even multidrug resistant strains of bacteria and biofilms. This includes MRSA, vancomycin-resistant enterococci, extended-spectrum-beta-lactamase producing *E. coli* and multidrug-resistant *Mycobacterium tuberculosis* (Issam *et al*. 2015).

The mechanism of bacterial killing needs to be further evaluated, especially the differences observed between Os and Os-C. There are many ways in which to study the mode of bacterial killing. One technique used in the present study was to observe the effect of the peptides on the bacterial cell surface by the use of SEM. For further surface studies atomic force microscopy (AFM) would give more insights into the effect of Os and Os-C on surface tension and roughness. The biggest advantage of using AFM over TEM and SEM is that the sample remains *in situ* without fixing. This allows for observations which are lost during sample preparation for electron microscopy. Meincken and colleagues (2005) used AFM to study the effect of the AMPs, magainin II, PGLa and Mel on *E. coli*. Various changes in cell envelope morphology were described such as an increase in surface roughness and the formation of lesions on the cell wall, formation of vesicles and the collapse of the cell structure at the apical ends.

In the current study, TEM results indicated that Os and Os-C affected the outer membrane of *E. coli* cells, and possibly caused permeabilisation. To measure outer membrane permeabilisation of Gram-negative bacteria, the fluorescent dye 1-N-phenylnaphthylamine (NPN) may be used. NPN is a hydrophobic fluorescent molecule which shows weak fluorescence in an aqueous environment and cannot cross an intact outer membrane. If the membrane is disrupted, NPN inserts into the membrane, and the fluorescence increases significantly (Yi *et al.*, 2015, Mohanram and Bhattacharjya, 2016). AN5-1 is an AMP isolated from the fermentation broth of *Paenibacillus alvei* AN5. The fluorescence of NPN was found to increase after incubation of *E. coli* with AN5-1, indicating that this peptide permeabilised the outer membrane (Yi *et al.*, 2015).

Exposure of *E. coli* and *B. subtilis* to Mel caused characteristic ultrastructural changes associated with apoptosis. However, this needs to be confirmed using biochemical assays. In bacterial apoptosis, calcium dependent depolarisation of membranes occurs and this effect can be measured using the membrane potential-sensitive fluorescent dye $DiBAC_4$. DNA fragmentation may be measured with the terminal deoxynucleotidyl transferase dUTP nick end labelling (TUNEL) assay. DNA condensation may be observed by fluorescence microscopy using DAPI. Annexin-V labelling can be used with flow cytometry to quantify phosphatidylserine levels on the outer cell surface (Dewachter *et al.*, 2015). Likewise the same methods may be used to determine whether Os and Os-C induces bacterial death via apoptosis or necrosis.

In this study an end-point assay was used to evaluate bacterial membrane permeabilisation. Over the past few years, valuable information was gained on AMP mechanisms by using real-time methods. Sochacki *et al.* (2011) used SYTOX green and *E. coli* strains which synthesise green fluorescent protein (GFP) which either stays in the cytoplasm or translocates to the periplasmic space. Together with time-lapse imaging the sequence of events that lead to bacteria killing by fluorescently labelled LL-37 was studied. Firstly, LL-37 was found to be concentrated on the septal regions of dividing cells and then slowly spread over the whole cell surface. Taking into account the timing of permeabilisation to periplasmic GFP, it was inferred that LL-37 enters the periplasmic space at the septal region. After this, LL-37 penetrated the cytoplasmic membrane with concurrent permeabilisation to both cytoplasmic GFP and the smaller SYTOX green molecules. It was observed that cell growth was halted before the LL-37 permeabilised either the outer or cytoplasmic membranes. It was therefore concluded that LL-37 did not kill through membrane permeabilisation (Sochacki *et al.*, 2011). Barns and Weisshaar (2013) also used a time-course study with fluorescent probes to study the effects of different concentrations of LL-37 on *B. subtilis*. These researchers found that 2 µM LL-37 caused a decrease in growth rate, while 4 µM caused shrinkage in cell size. Furthermore, the cells were able to recover from the effects of 2 µM LL-37, but were unable to recover from the shrinkage caused by 4 µM (Barns and Weisshaar, 2013). In the present study differences in membrane permeabilisation, DNA binding and septal accumulation were found between Os and Os-C. A fluorescence time-course study would give valuable additional information and most probably clarify differences in the mechanisms of the two peptides.

The results of this study indicated that the peptides may have intracellular bacterial targets. However, further assays need to be done to confirm specific intracellular targets in bacteria. In the present study it was seen by fluorescently labelling the peptides that they were able to

cross the membranes of the bacteria. To determine the exact location of the peptides after entering the cells TEM with immunogold labelled peptides would give more clarification on the intracellular targets. Nanogold particles of between 5 – 10 nm can be covalently linked to streptavidin which is then conjugated with the N-terminal of the peptide of interest (Leptihn *et al.*, 2009). Leptihn and colleagues (2009) were able to locate nanogold labelled S1 peptide on the inner and outer leaflets of the inner and outer membranes of *E. coli* cells. The peptide was observed in the periplasmic space and within the cytosol of the bacteria. Other assays may also be employed to identify possible intracellular targets such as the stimulation of autolytic enzymes or inhibition of other proteins essential to the bacterial life cycle.

Limitations concerning the leukocyte assays are the inability to confirm apoptotic or necrotic cell death, cell activation and spontaneous leukocyte activation. For future studies the experimental conditions need to be changed to minimise spontaneous activation of leukocytes following attachment to culture plates. One solution is to use ultra-low adhesion plates to keep the leukocytes in suspension during experimentation. Ultrastructural results served as indication that Os caused a mixture of apoptosis and oncotic necrosis in leukocytes. Biochemical assays can be used to identify the mode of cellular death and these include the detection and quantification of caspase levels, lactate dehydrogenase release, DNA fragmentation with TUNEL and flow cytometry to identify the phase of cell cycle arrest.

Other effects must be studied before AMPs can be considered for pharmaceutical use. These are stability of peptides to proteolysis, haemolytic activity, sensitivity to salts, and possible effects on the coagulation system (Aoki and Ueda, 2013). The current study confirmed that the peptides did not cause haemolysis, and that leukocyte viability was only affected at the highest concentration of Os tested. However, the loss of activity of peptides in an environment high in salt, proteolytic degradation of peptides and lastly, effect of the peptides on the coagulation system all need to be evaluated.

It has been experimentally observed that many peptides lose antimicrobial activity in a high salt environment such as blood serum (Kandasamy and Larson, 2006). Molecular dynamic simulations have shown that monovalent Na^+ cations bind deeply to lipid ester oxygen which causes a decrease in the average area available per lipid head group in a bilayer. AMPs with overall cationic residues therefore compete with the salt cations for favourable binding sites, which lead to a decrease in bilayer destabilisation (Kandasamy and Larson, 2006). It was previously shown that Os-C lost half of its activity against *E. coli* in the presence of 100 mM NaCl, possibly due to its lower percentage of hydrophobic amino acid residues, but that Os retained activity. Both peptides lost activity against *S. aureus* in salt (Prinsloo, 2013). It is

therefore necessary to develop strategies to overcome salt sensitivity. There are various options for peptide modification which have the possibility of forming a salt-insensitive peptide while retaining antimicrobial activity. Most of these strategies focus on structure modification, for example increasing structure rigidity, helix stability, hydrophobicity and amphipathicity (Yu *et al.*, 2011). Yu *et al.* (2011) described a relatively simple method to increase AMP salt resistance by replacing His or Trp residues with β-naphthylalanine or β-(4,4'-biphenyl)alanine. The authors found that the modified peptides remained active in high salt concentrations (150 mM NaCl) with a slight increase in haemolytic activity (Yu *et al.*, 2011). It was previously found that adding certain tags to the ends of peptides (e.g. Trp, Phe or vit E) increased salt resistance. The same research group therefore decided to investigate the effect of adding the previously used β-naphthylalanine or Trp on the termini of short AMPs (Chu *et al.*, 2013). Peptides with β-naphthylalanine showed higher salt resistance over those with Trp, whereas the Trp peptides showed low haemolytic activity when compared to the β-naphthylalanine peptides. A peptide with both Trp and β-naphthylalanine end tags could possibly have lower haemolytic activity while remaining active in a salt environment (Chu *et al.*, 2013).

AMPs are susceptible to proteolytic degradation by enzymes in the digestive tract or proteases in blood if administered orally or intravenously. Some microbes are capable of producing proteases, which would lead to resistance to a peptide susceptible to proteolysis (Haney and Hancock, 2013). Research on the modification of peptides to increase stability against both host and microbe proteolysis (Haney and Hancock, 2013) has been undertaken. Acetylation of the N-terminus will block the activity of aminopeptidases, while incorporation of non-natural D-isomers of amino acids alters the peptide backbone to protect against proteolysis (Aoki and Ueda, 2013, Haney and Hancock, 2013). Previous research has found D-isomerisation provides the most protection against proteolysis, however, this strategy is expensive (Stromstedt *et al.*, 2009). N-terminus acetylation decreased proteolytic sensitivity, but also decreased antimicrobial activity. Cyclisation was shown to increase peptide stability and microbial activity (Nguyen *et al.*, 2010, Aoki and Ueda, 2013). Another method is to develop peptidomimetics which are polymers that mimic the AMP structure, but have altered backbone structures. Peptidomimetics do not have peptide bonds and cannot undergo proteolysis, and are relatively easy to prepare from inexpensive monomers (Nguyen *et al.*, 2010, Aoki and Ueda, 2013).

The cost of AMP production remains one of the biggest disadvantages to using AMPs pharmaceutically. Chemical modifications to AMPs mostly result in more expensive production costs. Recombinant expression is the best method to produce large quantities of

AMP at low cost. However, no synthetic amino acids can be used with this method. The AMPs produced would also be toxic to the producing microbe, so the peptide needs to be produced with a fusion partner protein which would prevent host toxicity. The recombinant fusion proteins can then be cleaved from the AMP after purification (Kim *et al.*, 2014). Kim *et al.* (2014) developed novel AMPs consisting entirely of unmodified natural amino acids which showed good antimicrobial activity, low human cytotoxicity and stability in the presence of 150 mM NaCl, 10% serum and proteases. Peptide design were based on three criteria; hydrophobic and polar residues were arranged to be on either side of the helical axis, structural features which enhance antimicrobial activity and selectivity were maintained, and lastly amino acids were arranged to avoid protease-scissile sites (Kim *et al.*, 2014). Similar criteria could be applied to Os and Os-C to optimise the stability of these peptides in physiological conditions while retaining antimicrobial activity. Possible protease-scissile sites in both Os and Os-C were predicted *in silico* with PROSPER (Song *et al.*, 2012). Os has two and Os-C has three possible cleavage sites by elastase-2 and matrix metallopeptidase-9 (Table 6.2). Elastase-2 is in the serine protease family and the MEROPS database indicates that Ile and Val residues are the most frequently found in the P1 scissile position (Rawlings *et al.*, 2014). Both Os and Os-C has Ile on the P1 position of the first scissile site. The second elastase-2 scissile site has a Thr on P1 and Lys on P1'. MEROPS indicated a probability of cleavage with Thr on either the P1 or P1' site (Rawlings *et al.*, 2014). Matrix metallopeptidase-9 often cleaves when Gly is on P1, P3' or P4 and Leu on P1', and also when there is a Pro on P3 (Rawlings *et al.*, 2014). In the case of Os and Os-C, there is a Gly on the P1 position of this scissile site. To stabilise the peptides, the Ile, Gly and Thr may be replaced by another amino acid to prevent proteolysis while still using only natural residues. This will ensure that the possibility of producing these peptides with recombinant expression. Another solution would be use the end-capping method of Chu *et al.* (2103) with Trp and β-naphthylalanine. However, the proteolytic sensitivity of Os and Os-C should be confirmed experimentally before decisions are made on peptide modification. Furthermore, the fragments that form following digestion may also still have bioactivity.

Table 6.2. Predicted protease-scissile sites on Os and Os-C (Song *et al.*, 2012).

Peptide	Sequence and cleavage sites	Protease	Probability score
Os	KGI | RGYKGGYCKGAFKQTCKCY	Elastase-2	0.98
	KGIRG | YKGGYCKGAFKQTCKCY	Matrix metallopeptidase-9	1.00
Os-C	KGI | RGYKGGYKGAFKQTKY	Elastase-2	0.98
	KGIRG | YKGGYKGAFKQTKY	Matrix metallopeptidase-9	1.00
	KGIRGYKGGYKGAFKQT | KY	Elastase-2	0.98

Red line in sequence indicates predicted cleavage site

The current study did not take possible effects of blood plasma on the peptides into account. This may be done by exposing the peptides to individual plasma factors, or to peripheral *ex vivo* plasma and consequently evaluating bacterial killing. Many coagulation factors are themselves peptides, so it is possible that an AMP may affect this system. Furthermore, platelets have recently been shown to play an important role in host defence by detecting pathogens, releasing AMPs and recruiting leukocytes (Yeaman, 2014). The effects of a possible therapeutic peptide on the coagulation system thus need to be investigated. Bosch-Marcé *et al.* (2014) investigated the effect of two peptides (RW3 and RW4), which was previously shown to have antimicrobial activity with low haemolytic activity, on human platelets. The authors reported no change from the control concentration, volume, shape change, hypotonic shock response, activation, aggregation and morphology after storage for 5 and 7 days (Bosch-Marcé *et al.* 2014). To investigate the possible effect of Os and Os-C on the coagulation system, platelet activation, fibrin network formation, clot formation or lysis should be evaluated.

The immunomodulatory effects of the peptides also need to be investigated further. There are *in vitro* assays which may give an initial indication of the effects of AMPs on inflammatory factors to predict *in vivo* effects. Some of these studies have already been performed on Os and Os-C, and showed that both peptides have the ability to bind LPS and reduce LPS-induced nitric oxide (NO) production in mouse macrophage cells, thereby possibly limiting excessive LPS-induced inflammatory effects of Gram-negative bacterial infection associated with sepsis (Malan *et al.*, 2016). An *in vivo* model would provide a more accurate indication of systemic effects. Most *in vivo* studies have focused on topical administration of peptides to circumvent the effects of proteolytic enzymes on the AMPs. However, a recent study by Rai and colleagues (2016) devised a one-step method to conjugate the AMP, cecropin-melittin (CM), to a gold nanoparticle (NP) to reduce proteolytic effects and mammalian toxicity, while increasing bacterial activity. The researchers tested CM-NP *in vivo* on C57/BL6 mice. Results showed no significant damage to liver, kidney or lungs of control mice that received the peptide treatment. Topical administration of CM-NP to wounds infected with a mixture of Gram-positive *P. aeruginosa* and methillin-resistant *S. aureus* caused a reduction in the microorganisms. The systemic effects of CM-NP were also tested using the cecal ligation and puncture mouse model of experimental sepsis. The peptide suspension was administered via intraperitoneal injection. The amount of bacteria in the blood stream was significantly reduced. There was no reduction in the pro-inflammatory marker interleukin (IL)-1β. However, CM-NP caused a significant decrease in TNF-α, another pro-inflammatory molecule. The peptide also caused a decrease in the anti-

inflammatory molecule IL-10. Low levels of CM-NP accumulated in the spleen, liver, lung and kidney. Multiple administrations of CM-NP did not cause a significant increase in organ accumulation of the peptide. However, the results did not eliminate the possibility that CM-NP may be phagocytosed by macrophages in lymph nodes (Rai *et al.*, 2016). Once salt and proteolytic stability of the peptides have been achieved, this type of *in vivo* study would give valuable insights into the systemic effects of the peptide, and the suitability of these AMPs to be used in a clinical setting.

References

Abbas AK, Lichtman AH & Pillai S, 2015. *Cellular and molecular immunology*. 8th ed, e-book, Philadelphia, Pennsylvania. Elsevier Saunders. https://www-clinicalkey-com.uplib.idm.oclc.org/#!/browse/book/3-s2.0-C20130013230 [Viewed 03 Aug 2016].

Abd-Elhakim YM, Khalil SR, Awad A & Al-Ayadh LY, 2014. Combined cytogenotoxic effects of bee venom and bleomycin on rat lymphocytes: An *in vitro* study. *Biomed Res Int,* 2014: 1-9.

Actor JK, 2012. *Elsevier's integrated review. Immunology and microbiology*. 2nd ed, e-book. Philadelphia, Pennsylvania. Elsevier's integrated series. https://www-clinicalkey-com.uplib.idm.oclc.org/#!/browse/book/3-s2.0-C20090327166 [Viewed 03 Aug 2016].

Alanis AJ, 2005. Resistance to antibiotics: Are we in the post-antibiotic era? *Arch Med Res,* 36(6): 697-705.

Aoki W & Ueda M, 2013. Characterization of antimicrobial peptides toward the development of novel antibiotics. *Pharmaceuticals*, 6(8): 1055-1081.

Aragão EA, Chioato L & Ward RJ, 2008. Permeabilization of *E. coli* K12 inner and outer membranes by bothropstoxin-I, A LYS49 phospholipase A2 from *Bothrops jararacussu*. *Toxicon,* 51(4): 538-546.

Awika JM, Rooney LW, Wu X, Ronald L & Cisneros-Zevallos L, 2003. Screening methods to measure antioxidant activity of sorghum (sorghum bicolor) and sorghum products. J *Agric Food Chem*, 51(23): 6657-6662.

Barns KJ & Weisshaar JC, 2013. Real-time attack of ll-37 on single *Bacillus subtilis* cells. *BBA Biomembranes,* 1828(6): 1511-1520.

Bayer M, 1967. Response of cell walls of *Escherichia coli* to a sudden reduction of the environmental osmotic pressure. *J Bacteriol,* 93(3): 1104-1112.

Bechinger B & Lohner K, 2006. Detergent-like actions of linear amphipathic cationic antimicrobial peptides. *BBA Biomembranes*, 1758(9): 1529-1539.

Black JG & Black LJ, 2008. *Microbiology: Principles and explorations.* 7th ed. Hoboken, New Jersey, John Wiley & Sons, p. 81.

Blasa M, Angelino D, Gennari L & Ninfali P, 2011. The cellular antioxidant activity in red blood cells (CAA-RBC): A new approach to bioavailability and synergy of phytochemicals and botanical extracts. *Food Chem,* 125(2): 685-691.

Blondelle SE & Houghten RA, 1991. Hemolytic and antimicrobial activities of the twenty-four individual omission analogs of melittin. *Biochem,* 30(19): 4671-4678.

Boman H, 2003. Antibacterial peptides: Basic facts and emerging concepts. *J Intern Med,* 254(3): 197-215.

Bosch-Marcé M, Seetharaman S, Kurtz J, Mohan KV, Wagner SJ & Atreya CD, 2014. Leukoreduced whole blood–derived platelets treated with antimicrobial peptides maintain *in vitro* properties during storage. *Transfusion*, 54(6): 1604-1609.

Bouayed J & Bohn T, 2010. Exogenous antioxidants - double-edged swords in cellular redox state: Health beneficial effects at physiologic doses versus deleterious effects at high doses. *Oxid Med Cell Longev,* 3(4): 228-237.

Boucher HW, Talbot GH, Benjamin DK, Bradley J, Guidos RJ, Jones RN, Murray BE, Bonomo RA & Gilbert D, 2013. 10 × '20 progress - development of new drugs active against gram-negative bacilli: An update from the Infectious Diseases Society of America. *Clin Infect Dis,* 2013: 1-10.

Bratosin D, Mazurier J, Debray H, Lecocq M, Boilly B, Alonso C, Moisei M, Motas C & Montreuil J, 1995. Flow cytofluorimetric analysis of young and senescent human erythrocytes probed with lectins. Evidence that sialic acids control their life span. *Glycoconj J,* 12(3): 258-267.

Brogden KA, 2005. Antimicrobial peptides: Pore formers or metabolic inhibitors in bacteria? *Nat Rev Microbiol,* 3(3): 238-250.

Buranasompob A, 2005. *Kinetics of the inactivation of microorganisms by water insoluble polymers with antimicrobial activity.* PhD, Technischen Universität Berlin, p. 41.

Catrina SB, Refai E & Andersson M, 2009. The cytotoxic effects of the anti-bacterial peptides on leukocytes. *J Pept Sci,* 15(12): 842-848.

Chambers HF & Deleo FR, 2009. Waves of resistance: *Staphylococcus aureus* in the antibiotic era. *Nat Rev Micro,* 7(9): 629-641.

Chu H-L, Yu H-Y, Yip B-S, Chih Y-H, Liang C-W, Cheng H-T & Cheng J-W, 2013. Boosting salt resistance of short antimicrobial peptides. *Antimicrob Agents Chemother,* 57(8): 4050-4052.

Coates A, Hu Y, Bax R & Page C, 2002. The future challenges facing the development of new antimicrobial drugs. *Nat Rev Drug Discov,* 1(11): 895-910.

Cole AM, Hong T, Boo LM, Nguyen T, Zhao C, Bristol G, Zack JA, Waring AJ, Yang OO & Lehrer RI, 2002. Retrocyclin: A primate peptide that protects cells from infection by T-and M-tropic strains of HIV-1. *Proc Natl Acad Sci,* 99(4): 1813-1818.

Collins L & Franzblau SG, 1997. Microplate Alamar blue assay versus Bactec 460 system for high-throughput screening of compounds against *Mycobacterium tuberculosis* and *Mycobacterium avium*. *Antimicrob Agents Chemother,* 41(5): 1004-1009.

Cornet B, Bonmatin JM, Hetru C, Hoffmann JA, Ptak M & Vovelle F, 1995. Refined three-dimensional solution structure of insect defensin A. *Structure,* 3(5): 435-448.

Cota-Robles EH, 1963. Electron microscopy of plasmolysis in *Escherichia coli*. *J Bacteriol,* 85(3): 499-503.

Crowther-Gibson P, Govender N, Lewis D, Bamford C, Brink A, Von Gottberg A, Klugman K, Du Plessis M, Fali A & Harris B, 2011. Part IV. Human infections and antibiotic resistance. *S Afr Med J,* 101(8): 567-578.

Cudic M & Otvos JL, 2002. Intracellular targets of antibacterial peptides. *Curr Drug Targets,* 3(2): 101-106.

Decker P, Wolburg H & Rammensee HG, 2003. Nucleosomes induce lymphocyte necrosis. *Eur J Immunol,* 33(7): 1978-1987.

Dewachter L, Verstraeten N, Monteyne D, Kint CI, Versées W, Pérez-Morga D, Michiels J & Fauvart M, 2015. A single-amino-acid substitution in Obg activates a new programmed cell death pathway in *Escherichia coli*. *mBio,* 6(6): E01935-E01941.

Ehrenfeld GM, Shipley JB, Heimbrook DC, Sugiyama H, Long EC, Van Boom JH, Van Der Marel GA, Oppenheimer NJ & Hecht SM, 1987. Copper-dependent cleavage of DNA by bleomycin. *Biochem,* 26(3): 931-942.

Ehrenstein G & Lecar H, 1977. Electrically gated ionic channels in lipid bilayers. *Q Rev Biophys*, 10(1): 1–34.

Elias RJ, Kellerby SS & Decker EA, 2008. Antioxidant activity of proteins and peptides. *Crit Rev Food Sci Nutr,* 48(5): 430-441.

Elias RJ, Mcclements DJ & Decker EA, 2005. Antioxidant activity of cysteine, tryptophan, and methionine residues in continuous phase β-lactoglobulin in oil-in-water emulsions. *J Agric Food Chem*, 53(26): 10248-10253.

English D & Andersen BR, 1974. Single-step separation of red blood cells, granulocytes and mononuclear leukocytes on discontinuous density gradients of Ficoll-Hypaque. *J Immunol Methods,* 5(3): 249-252.

Fink SL & Cookson BT, 2005. Apoptosis, pyroptosis, and necrosis: Mechanistic description of dead and dying eukaryotic cells. *Infect Immun,* 73(4): 1907-1916.

Finlay BB & Hancock REW, 2004. Can innate immunity be enhanced to treat microbial infections? *Nat Rev Microbiol,* 2(6): 497-504.

Flamm RK, Rhomberg PR, Simpson KM, Farrell DJ, Sader HS & Jones RN, 2015. *In vitro* spectrum of pexiganan activity when tested against pathogens from diabetic foot infections and with selected resistance mechanisms. *Antimicrob Agents Chemother*, 59(3): 1751-1754.

Fletcher C, 1984. First clinical use of penicillin. *Br Med J (Clin Res Ed),* 289(6460): 1721-1723.

Fox JL, 2013. Antimicrobial peptides stage a comeback. *Nat Biotechnol,* 31(5): 379-382.

Fiers W, Beyaert R, Declercq W & Vandenabeele P, 1999. More than one way to die: Apoptosis, necrosis and reactive oxygen damage. *Oncogene*, 18(54): 7719-7730.

Fuchs TA, Abed U, Goosmann C, Hurwitz R, Schulze I, Wahn V, Weinrauch Y, Brinkmann V & Zychlinsky A, 2007. Novel cell death program leads to neutrophil extracellular traps. *J Cell Biol,* 176(2): 231-241.

Gajski G, Domijan A-M, Žegura B, Štern A, Gerić M, Jovanović IN, Vrhovac I, Madunić J, Breljak D & Filipič M, 2016. Melittin induced cytogenetic damage, oxidative stress and changes in gene expression in human peripheral blood lymphocytes. *Toxicon,* 110:56-67.

Ganz T, 2003. Defensins: Antimicrobial peptides of innate immunity. *Nat Rev Immunol,* 3(9): 710-720.

Gartner LP & Hiatt JL, 2011. *Concise histology.* E-book. Philadelphia, Pennsylvania, Saunders/Elsevier. https://www-clinicalkey-com.uplib.idm.oclc.org/#!/browse/book/3-s2.0-C20090388820 [Viewed 03 Aug 2016].

Geall AJ & Blagbrough IS, 2000. Rapid and sensitive ethidium bromide fluorescence quenching assay of polyamine conjugate–DNA interactions for the analysis of lipoplex formation in gene therapy. *J Pharm Biomed Anal*, 22(5): 849-859.

Genestier A-L, Michallet M-C, Prévost G, Bellot G, Chalabreysse L, Peyrol S, Thivolet F, Etienne J, Lina G & Vallette FM, 2005. *Staphylococcus aureus* panton-valentine leukocidin directly targets mitochondria and induces bax-independent apoptosis of human neutrophils. *J Clin Invest,* 115(11): 3117.

Goering RV & Mims CA, 2013. *Mims' medical microbiology.* 5th ed, e-book. Philadelphia, Pennsylvania, Mosby Elsevier.
https://www-clinicalkey-com.uplib.idm.oclc.org/#!/browse/book/3-s2.0-B9780323044752X50018 [Viewed 03 Aug 2016].

Gómez-Guillén MC, López-Caballero ME, Alemán A, López de Lacey A, Giménez B, & Montero P, 2010. Antioxidant and antimicrobial peptide fractions from squid and tuna skin gelatin. In: *Sea by-products as real material: New ways of application.* Trivandrum, India: Transworld Research Network, p.85-115.

Gonzalez R & Tarloff J, 2001. Evaluation of hepatic subcellular fractions for Alamar blue and MTT reductase activity. *Toxicol In Vitro*, 15(3): 257-259.

Graumann, P, 2012. *Bacillus: Cellular and molecular biology.* 2nd ed. Norfolk, Caister Academic Press, p.86.

Guarna M, Coulson R & Rubinchik E, 2006. Anti-inflammatory activity of cationic peptides: Application to the treatment of acne vulgaris. *FEMS Microbiol Lett,* 257(1): 1-6.

Hallock KJ, Lee D-K & Ramamoorthy A, 2003. Msi-78, an analogue of the magainin antimicrobial peptides, disrupts lipid bilayer structure via positive curvature strain. *Biophys J*, 84(5): 3052-3060.

Hamid R, Rotshteyn Y, Rabadi L, Parikh R & Bullock P, 2004. Comparison of Alamar blue and MTT assays for high through-put screening. *Toxicol In Vitro*, 18: 703-710.

Hancock RE & Rozek A, 2002. Role of membranes in the activities of antimicrobial cationic peptides. *FEMS Microbiol Lett,* 206(2): 143-149.

Hancock REW & Sahl HG, 2006. Antimicrobial and host-defense peptides as new anti-infective therapeutic strategies. *Nat biotechnol,* 24(12): 1551-1557.

Haney EF & Hancock RE, 2013. Peptide design for antimicrobial and immunomodulatory applications. *Biopolymers*, 100(6): 572-583.

Hartmann M, Berditsch M, Hawecker J, Ardakani MF, Gerthsen D & Ulrich AS, 2010. Damage of the bacterial cell envelope by antimicrobial peptides Gramicidin S and PGLa as revealed by transmission and scanning electron microscopy. *Antimicrob Agents Chemother,* 54(8): 3132-3142.

Harvey RA, Champe PC & Fisher BD, 2013. *Microbiology,* Philadelphia, Pennsylvania, Lippincott Williams & Wilkins, p.49-51.

Hernández-Ledesma B, Davalos A, Bartolome B & Amigo L, 2005. Preparation of antioxidant enzymatic hydrolysates from α-lactalbumin and β-lactoglobulin. Identification of active peptides by HPLC-MS/MS. *J Agric Food Chem,* 53(3): 588-593.

Hirsh MI, Manov I, Cohen-Kaplan V & Iancu TC, 2007. Ultrastructural features of lymphocyte suppression induced by anthrax lethal toxin and treated with chloroquine. *Lab Invest,* 87(2): 182-188.

Hoffmann JA, 1995. Innate immunity of insects. *Curr Opin Immunol,* 7(1): 4-10.

Hoffmann JA & Hetru C, 1992. Insect defensins: Inducible antibacterial peptides. *Immunol Today,* 13(10): 411-415.

Holt P, Pal S, Catovsky D & Lewis S, 1972. Surface structure of normal and leukaemic lymphocytes. I. Effect of mitogens. *Clin Exp Immunol,* 10(4): 555-570.

Honzel D, Carter SG, Redman KA, Schauss AG, Endres JR & Jensen GS, 2008. Comparison of chemical and cell-based antioxidant methods for evaluation of foods and natural products: Generating multifaceted data by parallel testing using erythrocytes and polymorphonuclear cells. *J Agric Food Chem,* 56(18): 8319-8325.

Hotchkiss RD & Dubos RJ, 1941. The isolation of bactericidal substances from cultures of *Bacillus brevis*. *J Biol Chem,* 141(1): 155-162.

Hsu C-H, Chen C, Jou M-L, Lee AY-L, Lin Y-C, Yu Y-P, Huang W-T & Wu S-H, 2005. Structural and DNA-binding studies on the bovine antimicrobial peptide, indolicidin: Evidence for multiple conformations involved in binding to membranes and DNA. *Nucleic Acids Res,* 33(13): 4053-4064.

Huang D, Ou B & Ronald L, 2005. The chemistry behind antioxidant capacity assays. *J Agric Food Chem,* 53(6): 1841-1856.

Huang G-J, Deng J-S, Chen H-J, Huang S-S, Liao J-C, Hou W-C & Lin Y-H, 2012. Defensin protein from sweet potato (*Ipomoea batatas* [L.] Lam 'Tainong 57') storage roots exhibits antioxidant activities *in vitro* and *ex vivo*. *Food Chem,* 135(3): 861-867.

Hultmark D, Steiner H, Rasmuson T & Boman HG, 1980. Insect immunity. Purification and properties of three inducible bactericidal proteins from hemolymph of immunized pupae of *Hyalophora cecropia*. *Eur J Biochem,* 106(1): 7-16.

Iba T, Hashiguchi N, Nagaoka I, Tabe Y & Murai M, 2013. Neutrophil cell death in response to infection and its relation to coagulation. *J Intensive Care,* 1: 13-23.

Invitrogen. *Alamar blue assay* [Online]. USA. https://tools.thermofisher.com/content/sfs/manuals/PI-DAL1025-1100_TI%20alamarBlue%20Rev%201.1.pdf [Accesed 29 Feb 2016].

Issam A-A, Zimmermann S, Reichling J & Wink M, 2015. Pharmacological synergism of bee venom and melittin with antibiotics and plant secondary metabolites against multi-drug resistant microbial pathogens. *Phytomedicine*, 22(2): 245-255.

Izadpanah A & Gallo RL, 2005. Antimicrobial peptides. *J Am Acad Dermatol,* 52(3): 381-390.

Jenssen H, Hamill P & Hancock REW, 2006. Peptide antimicrobial agents. *Clin Microbiol Rev,* 19(3): 491-511.

Jeong CH, Jeong HR, Choi GN, Kim DO, Lee UK, & Heo HJ, 2011. Neuroprotective and anti-oxidant effects of caffeic acid isolated from *Erigeron annuus* leaf. *Chin Med*, 6(25): 1-9.

Johnston RB & Lehmeyer JE, 1976. Elaboration of toxic oxygen by-products by neutrophils in a model of immune complex disease. *J Clin Invest,* 57(4): 836-841.

Junqueira LCU & Mescher AL, 2010. *Junqueira's basic histology: Text & atlas*. 12th ed. New York, McGraw-Hill Medical, p. 2, 203-206.

Kalyanaraman B, Darley-Usmar V, Davies KJ, Dennery PA, Forman HJ, Grisham MB, Mann GE, Moore K, Roberts LJ & Ischiropoulos H, 2012. Measuring reactive oxygen and nitrogen species with fluorescent probes: Challenges and limitations. *Free Radic Biol Med,* 52(1): 1-6.

Kandasamy SK & Larson RG, 2006. Effect of salt on the interactions of antimicrobial peptides with zwitterionic lipid bilayers. *BBA Biomembranes,* 1758(9): 1274-1284.

Kapp A, Zeck-Kapp G, Danner M & Luger TA, 1988. Human granulocyte-macrophage colony stimulating factor: An effective direct activator of human polymorphonuclear neutrophilic granulocytes. *J Invest Dermatol,* 91(1): 49-55.

Katsu T, Kuroko M, Morikawa T, Sanchika K, Fujita Y, Yamamura H & Uda M, 1989. Mechanism of membrane damage induced by the amphipathic peptides Gramicidin S and melittin. 983(2): 135-141.

Kim H, Jang JH, Kim SC & Cho JH, 2014. *De novo* generation of short antimicrobial peptides with enhanced stability and cell specificity. *J Antimicrob Chemother,* 69(1): 121-132.

Kim S-K & Wijesekara I, 2010. Development and biological activities of marine-derived bioactive peptides: A review. *J Funct Foods,* 2(1): 1-9.

Kolter R, Siegele DA & Tormo A, 1993. The stationary phase of the bacterial life cycle. *Annu Rev Microbiol,* 47(1): 855-874.

Kong GM, Tao WH, Diao YL, Fang PH, Wang JJ, Bo P & Qian F, 2016. Melittin induces human gastric cancer cell apoptosis via activation of mitochondrial pathway. *World J Gastroenterol*, 22(11): 3186-3195.

Lamichhane TN, Abeydeera ND, Duc A-CE, Cunningham PR & Chow CS, 2011. Selection of peptides targeting helix 31 of bacterial 16S ribosomal RNA by screening M13 phage-display libraries. *Molecules,* 16(2): 1211-1239.

Laverty G & Gilmore B, 2014. Cationic antimicrobial peptide cytotoxicity. *SOJ Microbiol Infect Dis*, 2(1): 1-8.

Laverty G, Gorman SP & Gilmore BF, 2011. The potential of antimicrobial peptides as biocides. *Int J Mol Sci,* 12(10): 6566-6596.

Lazarev V & Govorun V, 2010. Antimicrobial peptides and their use in medicine. *Appl Biochem Microbiol,* 46(9): 803-814.

Lee J & Lee DG, 2015. Antimicrobial Peptides (AMPs) with dual mechanisms: Membrane disruption and apoptosis. *J Microbiol Biotechnol,* 25(6): 759-764.

Lehmann J, Retz M, Sidhu SS, Suttmann H, Sell M, Paulsen F, Harder J, Unteregger G & Stöckle M, 2006. Antitumor activity of the antimicrobial peptide magainin II against bladder cancer cell lines. *Eur Urol,* 50(1): 141-147.

Leptihn S, Har JY, Chen J, Ho B, Wohland T & Ding JL, 2009. Single molecule resolution of the antimicrobial action of quantum dot-labeled sushi peptide on live bacteria. *BMC Biol,* 7(1): 1-22.

Lewis J, Stewart W & Adams D, 1988. Role of oxygen radicals in induction of DNA damage by metabolites of benzene. *Cancer Res,* 48(17): 4762-4765.

López-Expósito I, Quirós A, Amigo L & Recio I, 2007. Casein hydrolysates as a source of antimicrobial, antioxidant and antihypertensive peptides. *Lait,* 87(4-5): 241-249.

Luzio JP, Pryor PR & Bright NA, 2007. Lysosomes: Fusion and function. *Nat Rev Mol Cell Biol,* 8(8): 622-632.

Lyu Y, Yang Y, Lyu X, Dong N & Shan A, 2016. Antimicrobial activity, improved cell selectivity and mode of action of short PMAP-36-derived peptides against bacteria and *Candida*. *Sci Rep,* 6:1-12.

Malan M, Serem JC, Bester MJ, Neitz AW & Gaspar AR, 2016. Anti-inflammatory and anti-endotoxin properties of peptides derived from the carboxy-terminal region of a defensin from the tick *Ornithodoros savignyi*. *J Pept Sci,* 22(1): 43-51.

Male D, Brostoff J, Roth DB & Roitt IM, 2013. Immunology. 8th ed, e-book. Phylidelphiaia, Pennsylvania, Elsevier/Saunders. https://www-clinicalkey-com.uplib.idm.oclc.org/#!/browse/book/3-s2.0-C20090605080 [Viewed 03 Aug 2016].

Malik A, Bissinger R, Liu G, Liu G & Lang F, 2015. Enhanced eryptosis following gramicidin exposure. *Toxins,* 7(5): 1396-1410.

Mandell LA, Ball P & Tillotson G, 2001. Antimicrobial safety and tolerability: Differences and dilemmas. *Clin Infect Dis*, 32(Supplement 1): S72-S79.

Mangoni ML, Papo N, Barra D, Simmaco M, Bozzi A, Di Giulio A & Rinaldi AC, 2004. Effects of the antimicrobial peptide temporin L on cell morphology, membrane permeability and viability of *Escherichia coli*. *Biochem J,* 380(3): 859-865.

Marzani B, Pinto D, Minervini F, Calasso M, Di Cagno R, Giuliani G, Gobbetti M & Angelis M, 2012. The antimicrobial peptide pheromone plantaricin A increases antioxidant defenses of human keratinocytes and modulates the expression of filaggrin, involucrin, β-defensin 2 and tumor necrosis factor-α genes. *Exp Dermatol,* 21(9): 665-671.

Mascio CT, Alder JD & Silverman JA, 2007. Bactericidal action of daptomycin against stationary-phase and nondividing *Staphylococcus aureus* cells. *Antimicrob Agents Chemother,* 51(12): 4255-4260.

Matsuzaki K, 1998. Magainins as paradigm for the mode of action of pore forming polypeptides. *BBA Reviews on Biomembranes*, 1376(3): 391-400.

Matsuzaki K, 2009. Control of cell selectivity of antimicrobial peptides. *Biochim Biophys Acta*, 1788(8): 1687-1692.

Mcleod IX & He Y, 2010. Roles of autophagy in lymphocytes: Reflections and directions. *Cell Mol Immunol,* 7(2): 104-107.

Meincken M, Holroyd D & Rautenbach M, 2005. Atomic force microscopy study of the effect of antimicrobial peptides on the cell envelope of *Escherichia coli*. *Antimicrob Agents Chemother,* 49(10): 4085-4092.

Melo RC, D'avila H, Wan H-C, Bozza PT, Dvorak AM & Weller PF, 2011. Lipid bodies in inflammatory cells structure, function, and current imaging techniques. *J Histochem Cytochem,* 59(5): 540-556.

Melo RC & Dvorak AM, 2012. Lipid body–phagosome interaction in macrophages during infectious diseases: Host defense or pathogen survival strategy? *PLoS Pathog,* 8(7): E1002729-E1002742.

Melo RC & Weller PF, 2016. Lipid droplets in leukocytes: Organelles linked to inflammatory responses. *Exp Cell Res,* 340(2): 193-197.

Memarpoor-Yazdi M, Asoodeh A & Chamani J, 2012. A novel antioxidant and antimicrobial peptide from hen egg white lysozyme hydrolysates. *J Funct Foods,* 4(1): 278-286.

Miller NJ, Rice-Evans C, Davies MJ, Gopinathan V & Milner A, 1993. A novel method for measuring antioxidant capacity and its application to monitoring the antioxidant status in premature neonates. *Clin Sci (Lond),* 84(4): 407-412.

Minkiewicz P, Dziuba J, Iwaniak A, Dziuba M, Darewicz M, 2008. Biopep database and other programs for processing bioactive peptide sequences. *J AOAC Int,* (91): 965-980.

Mohanram H & Bhattacharjya S, 2016. Salt resistant short antimicrobial peptides. *Biopolymers*, 103(3): 345-356.

Motobu M, Amer S, Yamada M, Nakamura K, Saido-Sakanaka H, Asaoka A, Yamakawa M & Hirota Y, 2004. Effects of antimicrobial peptides derived from the beetle *Allomyrina dichotoma* defensin on mouse peritoneal macrophages stimulated with lipopolysaccharide. *J Vet Med Sci,* 66(3): 319-322.

Murphy K, Travers P, Walport M & Janeway C, 2012. *Janeway's immunobiology,* New York, Garland Science, p. 37-45.

Nakajima Y, Ishibashi J, Yukuhiro F, Asaoka A, Taylor D & Yamakawa M, 2003. Antibacterial activity and mechanism of action of tick defensin against gram-positive bacteria. *Biochim Biophys Acta,* 1624(1-3): 125-130.

Nakao S, Komagoe K, Inoue T & Katsu T, 2011. Comparative study of the membrane-permeabilizing activities of mastoparans and related histamine-releasing agents in bacteria, erythrocytes, and mast cells. 1808(1): 490-497.

Nathan CF, 1987. Neutrophil activation on biological surfaces. Massive secretion of hydrogen peroxide in response to products of macrophages and lymphocytes. *J Clin Invest,* 80(6): 1550-1560.

Nguyen LT, Haney EF & Vogel HJ, 2011. The expanding scope of antimicrobial peptide structures and their modes of action. *Trends Biotechnol*, 29(9): 464-472.

Nguyen LT, Chau JK, Perry NA, De Boer L, Zaat SA & Vogel HJ, 2010. Serum stabilities of short tryptophan- and arginine-rich antimicrobial peptide analogs. *PLoS One*, 5: E12684-E12692.

Oliver J, 1978. Cell biology of leukocyte abnormalities-membrane and cytoskeletal function in normal and defective cells. A review. *Am J Pathol,* 93(1): 221-273.

Olivier N. 2002. Isolation and characterization of antibacterial peptides from hemolymph of the soft tick, *Ornithodoros savignyi.* MSc, University of Pretoria, p. 135.

Ou B, Huang D, Hampsch-Woodill M, Flanagan JA & Deemer EK, 2002. Analysis of antioxidant activities of common vegetables employing oxygen radical absorbance capacity (ORAC) and ferric reducing antioxidant power (FRAP) assays: A comparative study. *J Agric Food Chem,* 50(11): 3122-3128.

Pandey BK, Ahmad A, Asthana N, Azmi S, Srivastava RM, Srivastava S, Verma R, Vishwakarma AL & Ghosh JK, 2010. Cell-selective lysis by novel analogs of melittin against human red blood cells and *E. coli*. *Biochem,* 49: 7920-7929.

Parihar A, Eubank TD & Doseff AI, 2010. Monocytes and macrophages regulate immunity through dynamic networks of survival and cell death. *J Innate Immun,* 2(3): 204-215.

Park CB, Kim HS & Kim SC, 1998. Mechanism of action of the antimicrobial peptide buforin II: Buforin II kills microorganisms by penetrating the cell membrane and inhibiting cellular functions. *Biochem Biophys Res Commun* 244(1): 253-257.

Park CB, Yi K-S, Matsuzaki K, Kim MS & Kim SC, 2000. Structure–activity analysis of buforin II, a histone H2A-derived antimicrobial peptide: The proline hinge is responsible for the cell-penetrating ability of buforin II. *Proc Natl Acad Sci,* 97(15): 8245-8250.

Park YM & Bochner BS, 2010. Eosinophil survival and apoptosis in health and disease. *Allergy Asthma Immunol Res,* 2(2): 87-101.

Paiva CN & Bozza MT, 2014. Are reactive oxygen species always detrimental to pathogens? *Antioxid Redox Signal*, 20(6): 1000-1037.

Payne CM, Glasser L, Tischler ME, Wyckoff D, Cromey D, Fiederlein R & Bohnert O, 1994. Programmed cell death of the normal human neutrophil: An *in vitro* model of senescence. *Microsc Res Tech,* 28(4): 327-344.

Pham-Huy LA, He H & Pham-Huy C, 2008. Free radicals, antioxidants in disease and health. *Int J Biomed Sci,* 4(2): 89-96.

Phoenix DA, Dennison SR & Harris F, 2013. Antimicrobial peptides: Their history, evolution, and functional promiscuity. In: *Antimicrobial peptides.* Germany, Wiley-VCH Verlag, p.2.

Pilizota T & Shaevitz JW, 2013. Plasmolysis and cell shape depend on solute outer-membrane permeability during hyperosmotic shock in *E. coli*. *Biophys J,* 104(12): 2733-2742.

Pillay J, Den Braber I, Vrisekoop N, Kwast LM, De Boer RJ, Borghans JA, Tesselaar K & Koenderman L, 2010. *In vivo* labeling with $2H_2O$ reveals a human neutrophil lifespan of 5.4 days. *Blood,* 116(4): 625-627.

Pratchett T, Stewart I & Cohen JS, 2003. *The science of discworld*. United Kingdom, Random House, p.90.

Pratt JP, Ravnic DJ, Huss HT, Jiang X, Orozco BS & Mentzer SJ, 2005. Melittin-induced membrane permeability: A nonosmotic mechanism of cell death. *In Vitro Cell Dev Biol Anim,* 41(10): 349-355.

Prigent-Combaret C, Prensier G, Le Thi TT, Vidal O, Lejeune P & Dorel C, 2000. Developmental pathway for biofilm formation in curli-producing *Escherichia coli* strains: Role of flagella, curli and colanic acid. 2(4): 450-464.

Prinsloo L, 2013. *Structural and functional characterization of peptides derived from the carboxy-terminal region of a defensin from the tick Ornithodoros savignyi*. MSc, University of Pretoria, p. 41.

Prinsloo L, Naidoo A, Serem J, Taute H, Sayed Y, Bester M, Neitz A & Gaspar A, 2013. Structural and functional characterization of peptides derived from the carboxy-terminal region of a defensin from the tick *Ornithodoros savignyi*. *J Pept Sci,* 19:325-332.

Raghuraman H & Chattopadhyay A, 2005. Cholesterol inhibits the lytic activity of melittin in erythrocytes. *Chem Phys Lipids,* 134(2): 183-189.

Rai A, Pinto S, Velho TR, Ferreira AF, Moita C, Trivedi U, Evangelista M, Comune M, Rumbaugh KP & Simões PN, 2016. One-step synthesis of high-density peptide-conjugated gold nanoparticles with antimicrobial efficacy in a systemic infection model. *Biomaterials,* 85:99-110.

Ran Q, Xiang Y, Liu Y, Xiang L, Li F, Deng X, Xiao Y, Chen L, Chen L & Li Z, 2015. Eryptosis indices as a novel predictive parameter for biocompatibility of Fe_3O_4 magnetic nanoparticles on erythrocytes. *Sci Rep*, 5:1-15.

Rawlings ND, Waller M, Barrett AJ & Bateman A, 2014. MEROPS: the database of proteolytic enzymes, their substrates and inhibitors. *Nucleic Acids Res*, 42(D1): D503-D509.

Reuter S, Gupta SC, Chaturvedi MM & Aggarwal BB, 2010. Oxidative stress, inflammation, and cancer: How are they linked? *Free Radic Biol Med,* 49(11): 1603-1616.

Robinson JM, 2008. Reactive oxygen species in phagocytic leukocytes. *Histochem Cell Biol,* 130(2): 281-297.

Roth BL, Poot M, Yue ST & Millard PJ, 1997. Bacterial viability and antibiotic susceptibility testing with sytox green nucleic acid stain. *Appl Environ Microbiol,* 63(6): 2421-2431.

Salomon R & Farías RN, 1992. Microcin 25, a novel antimicrobial peptide produced by *Escherichia coli*. *J Bacteriol,* 174(22): 7428-7435.

Sarmadi BH & Ismail A, 2010. Antioxidative peptides from food proteins: A review. *Peptides,* 31(10): 1949-1956.

Sarmasik A, 2002. Antimicrobial peptides: A potential therapeutic alternative for the treatment of fish diseases. *Turk J Biol,* 26(1): 201-207.

Savill J, Wyllie A, Henson J, Walport M, Henson P & Haslett C, 1989. Macrophage phagocytosis of aging neutrophils in inflammation. Programmed cell death in the neutrophil leads to its recognition by macrophages. *J Clin Invest,* 83(3): 865-876.

Schaich K, Tian X & Xie J, 2015. Hurdles and pitfalls in measuring antioxidant efficacy: A critical evaluation of ABTS, DPPH, and ORAC assays. *J Funct Foods,* 14: 111-125.

Schall N, Page N, Macri C, Chaloin O, Briand J-P & Muller S, 2012. Peptide-based approaches to treat lupus and other autoimmune diseases. *J Autoimmun,* 39(3): 143-153.

Scocchi M, Mardirossian M, Runti G & Benincasa M, 2016. Non-membrane permeabilizing modes of action of antimicrobial peptides on bacteria. *Curr Top Med Chem,* 16(1): 76-88.

Serem J, 2012. *An exploratory investigation into the physicochemical, antioxidant and cellular effects of a selection of honey samples from the southern african region.* MSc, University of Pretoria, p. 43-44.

Serem JC & Bester MJ, 2012. Physicochemical properties, antioxidant activity and cellular protective effects of honeys from southern africa. *Food Chem,* 133(4): 1544-1550.

Sharma S & Khuller G, 2001. DNA as the intracellular secondary target for antibacterial action of human neutrophil peptide-I against *Mycobacterium tuberculosis* H_{37}Ra. *Curr Microbiol,* 43(1): 74-76.

Shen S, Chahal B, Majumder K, You S-J & Wu J, 2010. Identification of novel antioxidative peptides derived from a thermolytic hydrolysate of ovotransferrin by LC-MS/MS. *J Agric Food Chem,* 58(13): 7664-7672.

Shi J, Ross CR, Chengappa M, Sylte MJ, Mcvey DS & Blecha F, 1996[a]. Antibacterial activity of a synthetic peptide (PR-26) derived from PR-39, a proline-arginine-rich neutrophil antimicrobial peptide. *Antimicrob Agents Chemother,* 40(1): 115-121.

Shi J, Ross CR, Leto TL & Blecha F 1996[b]. PR-39, a proline-rich antibacterial peptide that inhibits phagocyte NADPH oxidase activity by binding to Src homology 3 domains of $p47^{phox}$. *Proc Natl Acad Sci,* 93(12): 6014-6018.

Sigma-Aldrich, 2010. Leukocyte seperation. *In:* Sigma-Aldrich *Procedure no. 1119.* United Kingdom, Runnymede Malthouse Egham.

Silhavy TJ, Kahne D & Walker S, 2010. The bacterial cell envelope. *Cold Spring Harb Perspect Biol,* 2(5): 1-16.

Siracusa MC, Comeau MR & Artis D, 2011. New insights into basophil biology: Initiators, regulators, and effectors of type 2 inflammation. *Ann N Y Acad Sci,* 1217(1): 166-177.

Sitterley G, 2008. Poly-lysine. *BioFiles*, 3(8): 1-12.

Sochacki KA, Barns KJ, Bucki R & Weisshaar JC, 2011. Real-time attack on single *Escherichia coli* cells by the human antimicrobial peptide lL-37. *Proc Natl Acad Sci,* 108(16): E77-E81.

Song J, Tan H, Perry AJ, Akutsu T, Webb GI, Whisstock JC & Pike RN, 2012. PROSPER: an integrated feature-based tool for predicting protease substrate cleavage sites. *PLoS One*, 7(11): E50300-E50323.

Stotz HU, James GH & Wang Y, 2009. Plant defensins: Defense, development and application. *Plant Signal Behav*, 4(11): 1010-1012.

Stromstedt AA, Pasupuleti M, Schmidtchen A & Malmsten M, 2009. Evaluation of strategies for improving proteolytic resistance of antimicrobial peptides by using variants of EFK17, an internal segment of LL-37. *Antimicrob. Agents Chemother.* 53: 593-602.

Subbalakshmi C & Sitaram N, 1998. Mechanism of antimicrobial action of indolicidin. *FEMS Microbiol Lett,* 160(1): 91-96.

Sun Y, Clinkenbeard KD, Ownby CL, Cudd L, Clarke CR & Highlander SK, 2000. Ultrastructural characterization of apoptosis in bovine lymphocytes exposed to *Pasteurella haemolytica* leukotoxin. *Am J Vet Res,* 61(1): 51-56.

Tabart J, Kevers C, Pincemail J, Defraigne J-O & Dommes J, 2009. Comparative antioxidant capacities of phenolic compounds measured by various tests. *Food Chem,* 113(4): 1226-1233.

Taylor DM, 2006. Innate immunity in ticks: A review. *Nihon Dani Gakkai Shi,* 15(2): 109-127.

Thakur S, Cattoni DI & Nöllmann M, 2015. The fluorescence properties and binding mechanism of sytox green, a bright, low photo-damage DNA intercalating agent. *Eur Biophys J*, 44: 337-348.

Tomita M, Fukuuchi Y, Tanahashi N, Kobari M, Terayama Y, Shinohara T, Konno S, Takeda H, Itoh D & Yokoyama M, 1995. Activated leukocytes, endothelial cells, and effects of

pentoxifylline: Observations by VEC-DEC microscopy. *J Cardiovasc Pharmacol,* 25(Suppl. 2): S34-S39.

Torrent M, Pulido D, Nogues MV & Boix E, 2012. Exploring new biological functions of amyloids: Bacteria cell agglutination mediated by host protein aggregation. *PLoS Pathog,* 8(11): 1-8.

Tse WC & Boger DL, 2004. A fluorescent intercalator displacement assay for establishing DNA binding selectivity and affinity. *Acc Chem Res,* 37(1): 61-69.

Tsoukas CD, Landgraf B, Bentin J, Valentine M, Lotz M, Vaughan JH & Carson DA, 1985. Activation of resting T lymphocytes by anti-CD3 (T3) antibodies in the absence of monocytes. *J Immunol,* 135(3): 1719-1723.

Tsuji N, Battsetseg B, Boldbaatar D, Miyoshi T, Xuan X, Oliver Jr JH & Fujisaki K, 2007. Babesial vector tick defensin against *Babesia* sp. parasites. *Infect Immun,* 75(7): 3633-3640.

Ueda K, Kobayashi S, Morita J & Komano T, 1985. Site-specific DNA damage caused by lipid peroxidation products. *BBA Gene structure and expression,* 824(4): 341-348.

US National Institutes of Health, 2015. *Clinicaltrials.Gov* [Online]. USA. https://www.clinicaltrials.gov/ct2/home [Viewed 25 Feb 2016].

Van Cruchten S & Van Den Broeck W, 2002. Morphological and biochemical aspects of apoptosis, oncosis and necrosis. *Anat Histol Embryol,* 31(4): 214-223.

Van Wetering S, Sterk PJ, Rabe KF & Hiemstra PS, 1999. Defensins: Key players or bystanders in infection, injury, and repair in the lung? *J Allergy Clin Immunol,* 104(6): 1131-1138.

Varkey J, Singh S & Nagaraj R, 2006. Antibacterial activity of linear peptides spanning the carboxy-terminal β-sheet domain of arthropod defensins. *Peptides,* 27(11): 2614-2623.

Venter C, Van Der Merwe CF, Oberholzer HM, Bester MJ & Taute H, 2013. Feasibility of high pressure freezing with freeze substitution after long-term storage in chemical fixatives. *Microsc Res Tech,* 76(9): 942-946.

Wang G, 2010. *Antimicrobial peptides: Discovery, design and novel therapeutic strategies,* Wallingford, Oxfordshire, UK, Cabi, p.3-14.

Wang G, Li X & Wang Z, 2009. APD2: The updated antimicrobial peptide database and its application in peptide design. *Nucleic Acids Res,* 37(Suppl. 1): D933-D937.

Wei Q-Y, Zhou B, Cai Y-J, Yang L & Liu Z-L, 2006. Synergistic effect of green tea polyphenols with trolox on free radical-induced oxidative DNA damage. *Food Chem,* 96(1): 90-95.

White SH, Wimley WC & Selsted ME, 1995. Structure, function, and membrane integration of defensins. *Curr Opin Struct Biol,* 5(4): 521-527.

Widmaier EP, Raff H & Strang KT, 2006. *Vander's human physiology: The mechanisms of body function,* Boston, McGraw-Hill, p.463-464.

Wolfe KL & Liu RH, 2007. Cellular antioxidant activity (CAA) assay for assessing antioxidants, foods, and dietary supplements. *J Agric Food Chem*, 55(22): 8896-8907.

Wright GD, 2013. Q&A: Antibiotic resistance: What more do we know and what more can we do? *BMC Biol,* 11(1): 51-55.

Ximenes VF, Lopes MG, PetrôNio MS, Regasini LO, Siqueira-Silva DH & Da Fonseca LM, 2010. Inhibitory effect of gallic acid and its esters on 2,2′-azobis(2-amidinopropane)hydrochloride (AAPH)-induced hemolysis and depletion of intracellular glutathione in erythrocytes. *J Agric Food Chem,* 58(9): 5355-5362.

Yan J-X, Wang K-R, Chen R, Song J-J, Zhang B-Z, Dang W, Zhang W & Wang R, 2012. Membrane active antitumor activity of NK-18, a mammalian NK-lysin-derived cationic antimicrobial peptide. *Biochimie,* 94(1): 184-191.

Yang H, Wang X, Liu X, Wu J, Liu C, Gong W, Zhao Z, Hong J, Lin D & Wang Y, 2009. Antioxidant peptidomics reveals novel skin antioxidant system. *Mol Cell Proteomics,* 8(3): 571-583.

Yang ZL, Ke YQ, Xu RX & Peng P, 2007. Melittin inhibits proliferation and induces apoptosis of malignant human glioma cells. *Nan Fang Yi Ke Da Xue Xue Bao*, 27(11): 1775-1777.

Yeaman MR, 2014. Platelets: At the nexus of antimicrobial defence. *Nat Rev Microbiol*, 12(6): 426-437.

Yeung ATY, Gellatly SL & Hancock REW, 2011. Multifunctional cationic host defence peptides and their clinical applications. *Cell Mol Life Sci,* 68(13): 2161-2176.

Yi T, Huang Y & Chen Y, 2015. Production of an antimicrobial peptide an5-1 in *Escherichia coli* and its dual mechanisms against bacteria. *Chem Biol Drug Des*, 85(5): 598-607.

You R-I, Ho C-L, Dai M-S, Hung H-M, Chen C-S & Chao T-Y, 2014. Autophagy regulation in heme-induced neutrophil activation is associated with microrna expression on transfusion-related acute lung injury. *Biomark Gen Med,* 6(4): 150-153.

Young AJ, Hay JB & Miyasaka M, 1995. Rapid turnover of the recirculating lymphocyte pool *in vivo*. *Int Immunol,* 7(10): 1607-1615.

Yu H-Y, Tu C-H, Yip B-S, Chen H-L, Cheng H-T, Huang K-C, Lo H-J & Cheng J-W, 2011. Easy strategy to increase salt resistance of antimicrobial peptides. *Antimicrob Agents Chemother,* 55(10): 4918-4921.

Zeya H & Spitznagel J, 1969. Cationic protein-bearing granules of polymorphonuclear leukocytes: Separation from enzyme-rich granules. *Science,* 163(3871): 1069-1071.

Zhang C, Li B, Lu SQ, Li Y, Su YH & Ling CQ, 2007. Effects of melittin on expressions of mitochondria membrane protein 7A6, cell apoptosis-related gene products Fas and Fas ligand in hepatocarcinoma cells. *Chin J Integr Med*, 5(5): 559-563.

Zhao H, 2003. *Mode of action of antimicrobial peptides*. PhD, University of Helsinki, p. 26.

Zheng L, Su G, Ren J, Gu L, You L & Zhao M, 2012. Isolation and characterization of an oxygen radical absorbance activity peptide from defatted peanut meal hydrolysate and its antioxidant properties. *J Agric Food Chem,* 60(21): 5431-5437.

Zucker-Franklin D, Greaves MF, Grossi CE & Marmont AM, 1981. *Atlas of blood cells: Function and pathology,* Milano, Ermes, p.158, 351.

Zughaier SM, Shafer WM & Stephens DS, 2005. Antimicrobial peptides and endotoxin inhibit cytokine and nitric oxide release but amplify respiratory burst response in human and murine macrophages. *Cell Microbiol,* 7(9): 1251-1262.

Appendix: Ethics approval certificate

The Research Ethics Committee, Faculty Health Sciences, University of Pretoria complies with ICH-GCP guidelines and has US Federal wide Assurance.
- FWA 00002567, Approved dd 22 May 2002 and Expires 20 Oct 2016.
- IRB 0000 2235 IORG0001762 Approved dd 22/04/2014 and Expires 22/04/2017.

UNIVERSITEIT VAN PRETORIA
UNIVERSITY OF PRETORIA
YUNIBESITHI YA PRETORIA

Faculty of Health Sciences Research Ethics Committee

27/11/2014

Approval Certificate
New Application

Ethics Reference No.: 452/2014

Title: The Mode of Action of the Synthetic Peptides Os and Os-C derived from the soft tick Ornithodoris Savignyi

Dear Mrs Helena Taute

The **New Application** as supported by documents specified in your cover letter for your research received on the 26/09/2014, was approved by the Faculty of Health Sciences Research Ethics Committee on the 26/11/2014.

Please note the following about your ethics approval:
- Ethics Approval is valid for 4 years.
- Please remember to use your protocol number (**452/2014**) on any documents or correspondence with the Research Ethics Committee regarding your research.
- Please note that the Research Ethics Committee may ask further questions, seek additional information, require further modification, or monitor the conduct of your research.

Ethics approval is subject to the following:
- The ethics approval is conditional on the receipt of 6 monthly written Progress Reports, and
- The ethics approval is conditional on the research being conducted as stipulated by the details of all documents submitted to the Committee. In the event that a further need arises to change who the investigators are, the methods or any other aspect, such changes must be submitted as an Amendment for approval by the Committee.

We wish you the best with your research.

Yours sincerely

Dr R Sommers; MBChB; MMed (Int); MPharMed.
Deputy Chairperson of the Faculty of Health Sciences Research Ethics Committee, University of Pretoria

The Faculty of Health Sciences Research Ethics Committee complies with the SA National Act 61 of 2003 as it pertains to health research and the United States Code of Federal Regulations Title 45 and 46. This committee abides by the ethical norms and principles for research, established by the Declaration of Helsinki, the South African Medical Research Council Guidelines as well as the Guidelines for Ethical Research: Principles Structures and Processes 2004 (Department of Health).

☎ 012 354 1677 🖷 0866516047 deepeka.behari@up.ac.za http://www.healthethics-up.co.za
✉ Private Bag X323, Arcadia, 0007 - 31 Bophelo Road, HW Snyman South Building, Level 2, Room 2.33, Gezina, Pretoria